



Norwegian University of
Science and Technology

Development of a Francis Turbine Test Rig at Kathmandu University

Morten Grefstad

Mechanical Engineering

Submission date: August 2017

Supervisor: Ole Gunnar Dahlhaug, EPT

Co-supervisor: Biraj Singh Thapa, Kathmandu University
Bjørn Winther Solemslie, EPT

Norwegian University of Science and Technology
Department of Energy and Process Engineering

MASTER THESIS

for
student Morten Grefstad
Spring 2017

*Development of a Francis Turbine Test Rig at Kathmandu University
Utvikling av en Francisturbin testrigg ved Kathmandu University*

Background

The Turbine Testing Laboratory at Kathmandu University was commissioned in 2011, and will be useful for future developments and improvements of hydraulic machinery necessary for the Nepali market and throughout the Himalaya region.

The laboratory is built up around a main pipe system, with the two main booster pumps located in the basement. Various running configurations are possible by utilizing different pipe loops, enabling both open and closed loop conditions. Kathmandu University are aiming to install test rigs equipped with high-precision measuring instruments in accordance with the IEC 60193 standard, enabling performance guarantee tests of Francis- and pump-turbines.

Recently, Kathmandu University received a grant from the Norwegian Government for a large research program named "Energize Nepal" where one activity is aiming to build a state of the art Francis turbine test rig. NTNU will support the development of this test rig by giving technical support from the Waterpower Laboratory.

The Francis turbine test rig is being used for research and development tests, along with model acceptance tests. The tests comprise determination of performances, such as efficiency, discharge, head and power. The operating behaviors are investigated, such as cavitation behavior and operation at runaway. The dynamic phenomena such as pressure fluctuations, torques and forces will also be investigated.

Objectives

Design a complete system for the efficiency measurement of Francis turbines in the Turbine Testing Laboratory at Kathmandu University with a special focus on the measurement and calibration for friction torque and axial load.

The following tasks are to be considered:

1. Literature study
 - a. Axial loads in Francis turbines
 - b. Friction torque in bearings
2. Software knowledge
 - a. CAD-drawing by CREO
3. Waterpower laboratory at NTNU
 - a. Get familiar with the measurement of axial load and friction torque
 - b. Get familiar with calibration of all instruments used in the test rig.
4. Turbine Testing Laboratory, Kathmandu University
 - a. Make detail 3D-drawings for the main components in the test rig.
 - b. Design a bearing block for the Francis turbine test rig
 - c. Design a measurement system for the axial load

Within 14 days of receiving the written text on the master thesis, the candidate shall submit a research plan for his project to the department.

When the thesis is evaluated, emphasis is put on processing of the results, and that they are presented in tabular and/or graphic form in a clear manner, and that they are analyzed carefully.

The thesis should be formulated as a research report with summary both in English and Norwegian, conclusion, literature references, table of contents etc. During the preparation of the text, the candidate should make an effort to produce a well-structured and easily readable report. In order to ease the evaluation of the thesis, it is important that the cross-references are correct. In the making of the report, strong emphasis should be placed on both a thorough discussion of the results and an orderly presentation.

The candidate is requested to initiate and keep close contact with his/her academic supervisor(s) throughout the working period. The candidate must follow the rules and regulations of NTNU as well as passive directions given by the Department of Energy and Process Engineering.

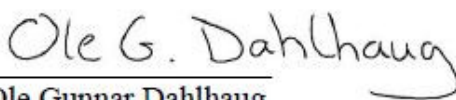
Risk assessment of the candidate's work shall be carried out according to the department's procedures. The risk assessment must be documented and included as part of the final report. Events related to the candidate's work adversely affecting the health, safety or security, must be documented and included as part of the final report. If the documentation on risk assessment represents a large number of pages, the full version is to be submitted electronically to the supervisor and an excerpt is included in the report.

Pursuant to "Regulations concerning the supplementary provisions to the technology study program/Master of Science" at NTNU §20, the Department reserves the permission to utilize all the results and data for teaching and research purposes as well as in future publications.

The final report is to be submitted digitally in DAIM. An executive summary of the thesis including title, student's name, supervisor's name, year, department name, and NTNU's logo and name, shall be submitted to the department as a separate pdf file. Based on an agreement with the supervisor, the final report and other material and documents may be given to the supervisor in digital format.

- Work to be done in the Waterpower laboratory
- Field work

Department for Energy and Process Engineering, *February 10th, 2017.*


Ole Gunnar Dahlhaug
Academic Supervisor

Co-Supervisors:

- Biraj Singh Thapa
- Bjørn Winther Solemslie

Abstract

The focus on hydropower development in Nepal has increased as consequence of the growing energy demand in the region. To render possible locally executed performance tests on model turbines, the Turbine Testing Laboratory (TTL) at Kathmandu University (KU) is under development.

The main objective of this master's thesis is to design a complete system for the efficiency measurement of Francis turbines at TTL. The test rig is to perform tests in accordance with *IEC60193* (1), the International Standard for model testing of hydraulic turbines.

The basis for the design of the Francis turbine test rig at TTL is the corresponding installation at the Waterpower Laboratory, NTNU. The rig is in comply with *IEC60193* (1) and has provided good experiences.

Piping and instrumentation diagrams for the Francis rig at TTL have been developed. Open and closed loop configurations are exemplified. Calibration of the instruments is limited to principal methods in compliance with *IEC60193* (1). Differential pressure transducers that are calibrated by a deadweight manometer measure the differential pressure between the turbine inlet and outlet. An electromagnetic flowmeter calibrated by the weighing method measures the volume flow rate. In conjunction with the main shaft is an arrangement for measuring the generator torque and the rotational speed. Strain gauges mounted in T-rosette on a customised stub shaft measure the forces acting in both axial directions. A calibration procedure that involves a jig utilising the lever principle is proposed for the axial force measurements. The mechanical torque applied to the shaft by the runner is measured by strain gauges mounted on the stub shaft at a 45° angle to the shaft centerline. Calibrated masses attached to a lever arm via a pulley applies the torque in the appurtenant calibration procedure.

3D-drawings of TTL have been made, with components for the Francis test rig integrated into the existing piping arrangement. A bearing-shaft-housing system comprising double-row roller bearings and a back-to-back arrangement of angular contact ball bearings has been designed.

The master thesis is done in relation to the NORAD-funded research program named *Energize Nepal*, aiming to facilitate Nepal in utilising their enormous hydropower resources.

Sammendrag

Fokuset på vannkraftutvikling i Nepal har vokst som følge av et voksende energibehov i regionen. For å kunne teste vannkraftturbiner lokalt, er Turbine Testing Laboratory (TTL) ved Kathmandu University (KU) under utvikling.

Hensikten med prosjektarbeidet er å designe et komplett system for effektivitetsmåling av Francis turbiner ved TTL. Francis testtriggen skal være i stand til å utføre tester i henhold til den internasjonale standarden *IEC60193 (1)*, som angir krav og anbefalinger for anvendte metoder under modelltesting av hydrauliske turbiner. Et utgangspunkt for designet er tilsvarende installasjon i tilknytning Vannkraftlaboratoriet på NTNU, en Francis testtrigg som er i henhold til *IEC60193 (1)* og som har gitt gode erfaringer.

Et prinsippskjema som viser plassering av måleinstrumenter ved TTL har blitt utarbeidet. Kalibrering av instrumentene er begrenset til prinsipielle metoder i henhold til *IEC60193 (1)*. Trykkforskjellen mellom turbinens innløp og utløp måles med differensialtrykksensorer som kalibreres med et manometer. Volumstrømmen måles av en elektromagnetisk strømningsmåler som kalibreres ved veiemetoden. Et system for måling av generatormoment og rotasjonshastighet er tilknyttet hovedakslingen. Strekkklapper orientert vinkelrett i akseretningen og montert på en spesialdesignet skjøteaksling måler aksielle krefter i begge retninger. En kalibreringsprosedyre innbefattende en jigg som benytter seg av vektarm-prinsippet er foreslått for kalibrering av aksiallast-målingen. Det mekaniske momentet påført akslingen av turbinen måles av strekkklapper som er montert på skjøteakslinger i 45° vinkel i forhold til akslingens senterlinje. Kalibrerte vekter som er tilkoblet en momentarm via en trinse påfører momentet i den tilhørende kalibreringsprosedyren.

3D-tegninger av TTL er utarbeidet i PTC Creo Parametric. Komponenter tilknyttet Francis testtriggen er integrert i det eksisterende rørsystemet. Design av et lager-aksling-deksel system som innebærer to vinkelkontaktlager montert side-mot-side og et toradig rullelager har blitt utviklet.

Denne masteroppgaven er tilknyttet forskningsprogrammet *Energize Nepal* som har mottatt støtte fra NORAD med det formål å bidra til å tilrettelegge for at Nepal får utnyttet de enorme ressursene innenfor vannkraft.

Preface

An interest in ecology and the environment has been growing in the author along with knowledge about the state of planet Earth. Electricity is an essential part of everyday life for a large share of the world's population, but there are still regions without a stable electrical grid. Considering the increase in living standards in developing countries, energy demand will continue to grow in the future. With fossil-based energy as a major contributor to climate change, the electricity must be produced in a sustainable matter to minimise the environmental impacts. In this context, working with renewable energy is highly attractive. In particular, doing practical work within the field of hydropower towards a developing country ticks all the boxes.

Thanks are directed to professor Ole Gunnar Dahlhaug for the opportunity to work on such an interesting subject, for always greeting everyone with a smile and for offering good advice. The engagement Dahlhaug shows in the development of TTL and Nepal, in general, is an inspiration.

Much appreciation also goes to the kind-hearted people at the Turbine Testing Laboratory. The cooperation has been rewarding, and the stay in Dhulikhel was an experience for a lifetime. I am looking forward to following the further progress of the Turbine Testing Laboratory and its influence on hydropower development in the Himalaya region.

It was an honour and a privilege to take part in the unique atmosphere at the Waterpower laboratory, from where the good memories even exceed the number of coffee cups ingested.

Table of Contents

Abstract	i
Sammendrag	ii
Preface	iii
List of Figures	vii
List of Tables	xi
Abbreviations	xii
Nomenclature	xiii
1. Introduction	1
1.1. Background.....	1
1.2. Objectives and Limitations	3
1.3. Reader’s Guidance.....	4
1.4. Previous Work	5
1.5. The Turbine Testing Laboratory at KU, Nepal	6
1.6. The Francis Turbine Test Rig at NTNU, Norway	9
1.7. Other Testing Laboratories.....	11
2. Theory	12
2.1. The Francis Turbine.....	12
2.2. Model Testing of Francis Turbines	13
2.2.1. Hydraulic Similitude.....	13
2.2.2. Hydraulic Efficiency.....	14
2.3. Measuring with Strain Gauges.....	16
3. Design of the Francis Turbine Test Rig at TTL	19
3.1. Instrumentation and Measurement Procedures.....	19

3.1.1.	VKL Overview: Piping and Instrumentation Diagram	21
3.1.2.	Oxygen Level	22
3.1.3.	Water Temperature	22
3.1.4.	Rotational Speed.....	23
3.1.5.	Pressure.....	23
3.1.6.	Volume Flow Rate.....	25
3.1.7.	Axial Force	27
3.1.8.	Generator Torque.....	34
3.1.9.	Friction/Mechanical Torque	36
3.1.10.	Uncertainty	38
3.2.	Components	39
3.2.1.	Guide Vane Regulating Mechanism and Head Covers	43
3.2.2.	Runner, Spiral Casing and Stay Vanes	45
3.2.3.	Bearing-Shaft-Housing System	46
3.2.4.	High- and Low-Pressure Tank.....	53
4.	Results and Discussion	55
4.1.	Instrumentation at TTL.....	55
4.1.1.	Piping and Instrumentation Diagram.....	56
4.1.2.	Oxygen Level	60
4.1.3.	Water Temperature	60
4.1.4.	Rotational Speed.....	60
4.1.5.	Pressure.....	61
4.1.6.	Volume Flow Rate.....	62
4.1.7.	Axial Force	66
4.1.8.	Generator Torque.....	76
4.1.9.	Friction/Mechanical Torque	79
4.1.10.	Uncertainty	90
4.2.	Components at TTL.....	93
4.2.1.	Guide Vane Regulating Mechanism and Head Covers	94
4.2.2.	Runner, Spiral Casing and Stay Vanes	99
4.2.3.	Bearing-Shaft-Housing System	100
4.2.4.	High- and Low-Pressure Tank.....	108
4.2.5.	Components Combined	111
5.	Conclusion	118

6. Further Work.....	119
Appendices.....	I
Appendix A: Piping & Instrumentation Diagrams, TTL	I
A.1. P&ID for the Francis Turbine Test Rig at TTL, KU	I
A.2. P&ID, Closed Loop Configuration, Pump B in Single Mode	I
A.3. P&ID, Open Loop Configuration with Both Reservoirs, Pumps in Series Mode	I
Appendix B: Measurement Procedures for the Francis Rig, VKL	I
Appendix C: Calibration Procedures for the Francis Rig, VKL	I
Appendix D: Product Data Sheets.....	I
D.1. HBM T40B Torque Flange Mounting Instructions	I
D.2. ROBA®-DS Coupling Installation Instructions to T40B	I
Appendix E: CRHT-VII, Paper no. CRHT17-12.....	I
Bibliography	V

List of Figures

Figure 1-1: Part of Kathmandu University campus and the Turbine Testing Laboratory (10). 6	6
Figure 1-2: See-through View of TTL (11)	7
Figure 1-3: The Turbine Testing Laboratory per May 2017	7
Figure 1-4: TTL Pump Room.....	8
Figure 1-5: Francis Turbine Test Rig at VKL; Closed Loop Configuration, mode 5 (12)	9
Figure 1-6: Francis Turbine Test Rig at VKL; Open Loop Configuration, Mode 8 (12)	10
Figure 2-1: Cross-sectional View of Francis Turbine (13)	12
Figure 2-2: a) Strain Gauges for Normal Stress, b) Wheatstone Full Bridge Circuit (14).....	16
Figure 3-1: Arrangement of the Measurements in the Waterpower Laboratory (17)	21
Figure 3-2: Model Francis Turbine Test Rig Installed at the Waterpower Laboratory (19)....	22
Figure 3-3: TTL Weighing Tank Placement	26
Figure 3-4: TTL Suggested Placement of Flow Meter and Weighing Facility.....	26
Figure 3-5: VKL Axial Load Measurement (17)	27
Figure 3-6: VKL Bearing Block.....	27
Figure 3-7: Lever Beam Concept with Rolling Support (8).....	28
Figure 3-8: Calibration Jig (Weights for Calibration of Upward Axial Force)	29
Figure 3-9: Moment Balance for Calibrating Upward Axial Thrust.....	30
Figure 3-10: Shaft Misalignment Types (21).....	34
Figure 3-11: Strain Gauges Measuring Torsion (14)	36

Figure 3-12: TTL 92kW Simplified Francis Test Rig; Components (5).....	40
Figure 3-13: VKL Francis Test Rig; Cross-sectional View.....	42
Figure 3-14: VKL Francis Test Rig Guide Vane Control; 3D Cross-section.....	43
Figure 3-15: TTL Existing Top Cover; 2D Drawing (5).....	44
Figure 3-16: TTL Existing Bottom Cover.....	44
Figure 3-17: a) TTL Spiral Casing and Runner (5) b) TTL Turbine.....	45
Figure 3-18: Cylindrical Coordinate System (26).....	46
Figure 3-19: Sealed Single Row Angular Contact Ball Bearings (28).....	48
Figure 3-20: Back-to-Back Arrangement of Angular Contact Ball Bearings (29).....	48
Figure 3-21: Radial Load (30).....	49
Figure 3-22: Cylindrical Roller Bearings, Single Row (31).....	49
Figure 3-23: Radial Shaft Seal (32).....	50
Figure 3-24: a) TTL Existing Shaft Key Slot, b) TTL Existing Hub/Shaft Interface (5).....	51
Figure 3-25: TTL Existing Detail Drawing for the Low-Pressure Tank (33).....	53
Figure 3-26: VKL High-Pressure Tank.....	54
Figure 4-1: TTL Piping & Instrumentation Diagram.....	56
Figure 4-2: TTL Pump Room; 3D Illustration.....	57
Figure 4-3: TTL P&ID Closed Loop Configuration, Pump B Running in Single Mode.....	58
Figure 4-4: TTL P&ID Open loop Configuration with both Reservoirs, Pumps in Series.....	59
Figure 4-5: Arrangement of Pressure Transducers in Circular Pipes (34).....	61
Figure 4-6: TTL Pipe Loop for Weighing Tank Calibration.....	62

Figure 4-7: TTL Flowmeter Arrangement; 3D View.....	63
Figure 4-8: TTL Axial Force Measurement by Strain Gauges	66
Figure 4-9: TTL Axial Force Measurement; Placement in P&ID	71
Figure 4-10: TTL Jig for Axial Load Calibration; Cross-sectional View.....	72
Figure 4-11: TTL Jig for Axial Load Calibration of Downward Force; 3D View	73
Figure 4-12: TTL Jig for Axial Load Calibration of Upward Force; 3D View	74
Figure 4-13: T40B Mechanical Construction (35).....	76
Figure 4-14: ROBA [®] -DS Shaft Coupling, “Preferred variant” (36).....	77
Figure 4-15: TTL Torque Transducer with Couplings.....	78
Figure 4-16: TTL Mechanical Torque at TTL	79
Figure 4-17: TTL Torque Arrangement.....	85
Figure 4-18: TTL Torque Calibration Jig Overview.....	86
Figure 4-19: TTL Torque Calibration Jig Attached to Bottom Cover	87
Figure 4-20: TTL Torque Calibration Jig with Axial Lever Arm.....	88
Figure 4-21: TTL Head Covers with Guide Vane Bushings and Covers.....	94
Figure 4-22: TTL GV Arrangement and Head Covers around Runner	95
Figure 4-23: TTL Guide Vane System; 3D View	96
Figure 4-24: TTL Suspension Cone; 3D View	97
Figure 4-25: TTL Runner; 3D View	99
Figure 4-26: TTL Spiral Casing with Stay Ring and Stay Vanes; 3D View	99
Figure 4-27: TTL Angular Contact Ball Bearings with Lock Nut and Washer.....	100

Figure 4-28: TTL V-ring Seal	102
Figure 4-29: TTL Seal Placement Overview	103
Figure 4-30: TTL Radial Shaft Seals	103
Figure 4-31: TTL Bearing-Shaft-Housing System.....	104
Figure 4-32: TTL Bearing Block Assembly	105
Figure 4-33: TTL Stub Shaft.....	106
Figure 4-34: VKL Hub to Stub Connection.....	107
Figure 4-35: TTL High-Pressure Tank; 3D View	108
Figure 4-36: TTL Low-pressure Tank; 3D View.....	109
Figure 4-37: TTL Low-pressure Tank; Front-, Side- and Top View	110
Figure 4-38: TTL Francis Turbine Test Rig; 3D View	111
Figure 4-39: TTL Back, Top and Front View.....	112
Figure 4-40: TTL Overview Without Lab Building, 3D View	113
Figure 4-41: TTL Loop Overview without Weighing Facility, 3D View.....	113
Figure 4-42: TTL Axial Force Calibration; 3D View	114
Figure 4-43: TTL Torque Calibration; 3D View	115
Figure 4-44: TTL Francis Rig; 3D View	116
Figure 4-45: Turbine Testing Laboratory; 3D View.....	117

List of Tables

Table 3.1: Measurands in Francis Turbine Testing.....	20
Table 3.2: Axial Force Calibration Calculation Input.....	31
Table 4.1: Definitions and Abbreviations for Axial Force Measurement.....	67
Table 4.2: Definitions and Abbreviations for Torque Measurement	81
Table 4.3: Systematic Uncertainties in Axial Load Measurement.....	90
Table 4.4: Systematic Uncertainties in Torque Measurement	91

Abbreviations

BEP	Best Efficiency Point
CAD	Computer-Aided Design
GV	Guide Vane
IEC	International Electrotechnical Commission
KU	Kathmandu University
mwc	meters water column
NORAD	Norwegian Agency for Development Cooperation
NTNU	Norwegian University of Science and Technology
rpm	revolutions per minute
P&ID	Piping and Instrumentation Diagram
TTL	Turbine Testing Laboratory
SG	Strain Gauge
VKL	Waterpower Laboratory (Norwegian: Vannkraftlaboratoriet)

Nomenclature

Symbol	Definition/Term	Unit
<i>A</i>	Area	<i>[m²]</i>
<i>D</i>	Diameter	<i>[m]</i>
<i>ε</i>	Strain	<i>[m/m]</i>
<i>g</i>	Gravity constant	<i>[m/s²]</i>
<i>H</i>	Head	<i>[m]</i>
<i>n</i>	Rotational speed	<i>[rpm]</i>
<i>k</i>	Gauge factor	
<i>σ</i>	Normal stress	<i>[N/m²]</i>
<i>p</i>	Pressure	<i>[Pa]</i>
<i>φ</i>	Latitude	<i>[°]</i>
<i>P_h</i>	Hydraulic power	<i>[W]</i>
<i>P_t</i>	Total power	<i>[W]</i>

P_m	Mechanical power of runner	$[W]$
P_{Lm}	Mechanical power losses	$[W]$
Q	Volume flow rate	$[m^3/s]$
T	Shaft torque	$[Nm]$
T_m	Runner torque	$[Nm]$
T_{Lm}	Friction torque	$[Nm]$
θ	Temperature	$[^{\circ}C]$
ρ_w	Density of water	$[kg/m^3]$
ω	Angular velocity	$[rad/s]$
z	Altitude	$[m]$

1. Introduction

1.1. Background

In the modern world, electricity plays a major part both for industrial purposes as well as in easing the everyday life of individuals. Even still, there are regions where people live without access to electricity or a steady supply thereof. To allow for a higher standard of life for a larger share of the world's population and to cover the increasing global energy demand, the utilisation of the natural resources available in a proper manner is growing in importance. The awareness of the social cost of providing electricity from conventional resources like coal and gas is increasing along with the knowledge of the impacts of climate change. The contribution from renewable resources is and will be, an important part in combatting these impacts. Technology for harvesting power from wind and solar has seen significant advances in recent years, and prognosis indicates the continuation of this trend in the future. Nevertheless, even with such technological advances, an efficient way of storing these intermittent sources are lacking. Regarding adjustability of electricity production dependent on the -demand, hydropower is a far better alternative in environments where this resource is readily available.

Snowmelt from the Himalayas, rainfall on mountainous terrain and a large number of rivers are among the reasons why Nepal's hydropower potential is enormous. The theoretical capacity for Nepalese hydropower production is estimated to be over 80 000 MW, of which 43 000 MW are techno-economically viable (2). As of 2016, installed hydropower capacity was 856 MW (3). The combination of a domestic demand-supply gap and a vast export potential through the Power Trade Agreement (PTA) with neighbouring India, suggests that substantial investments will be made towards realising projects for exploiting some of the large number of untapped resources that Nepal's topology and climate provide. The Nepalese government's plan to develop 38,000 MW in 25 years (from 2010) supports this.

The Turbine Testing Laboratory (TTL) at Kathmandu University (KU) was commissioned in 2011 and will be highly useful for the further development of the hydropower industry in Nepal and the Himalaya region. The laboratory is to be equipped with measuring instruments in accordance with *IEC60193* (1), the International Standard containing rules and methods for model acceptance tests and performance measurements of hydraulic turbines. Technical support in the development of the test rig at TTL will be provided from the NTNU Waterpower Laboratory (VKL). Experience from the Francis turbine test rig installed at VKL, where tests consistent with *IEC60193* (1) can be performed, will be employed to useful purpose.

1.2. Objectives and Limitations

The main objective of this thesis is to suggest a design for a complete system for the efficiency measurement of Francis turbines in the Turbine Testing Laboratory at Kathmandu University. Experience from the Francis test rig at the Waterpower Laboratory is to be utilised in the design. For all variables involved in the calculation of efficiency, a measuring method in compliance with the International standard *IEC60193* (1) is to be suggested. A special focus is to be placed on the measurement and calibration for axial load and torque.

3D-drawings for the main components in the test rig is to be produced in the computer program *PTC CREO Parametric*. A bearing block for the Francis turbine test rig is to be designed, with the capability of handling loads from the turbine when in operation. Principles for calibration of the suggested measuring instruments for axial load and torque is to be illustrated.

Scope and limitations of the design of the TTL Francis test rig:

- Strength analysis and details regarding bolted connections are not evaluated thoroughly.
- Cost estimates are not within the scope. However, the costs are taken into consideration when choosing methods. The budget of TTL is a limitation in the instrumentation.
- Selection of specific equipment is limited to bearings and seals in conjunction with the bearing block.
- The measuring of guide vane torque and the linear actuator system for controlling the guide vanes are not described.
- Electrical engineering, including generator connection and signal handling for instruments, is beyond the scope of this thesis.
- The space available in TTL for pipe systems, pump room and test rigs is the basement and the laboratory floor.

A successful design compliant with the *IEC60193* (1) standard will contribute towards the goal of enabling performance guarantee tests at TTL.

1.3. Reader's Guidance

The thesis is structured by first listing relevant previous work, before presenting the Turbine Testing Laboratory (TTL) at Kathmandu University (KU), Nepal. Subchapter 1.6 introduces the Francis test rig at the Waterpower Laboratory (VKL) at the Norwegian University of Science and Technology (NTNU). The introduction is concluded by an overview of other turbine testing laboratories.

Chapter 2 starts by introducing the Francis turbine and its main components. The prerequisites for model testing of Francis turbines are then presented along with the mathematical equations for calculating the efficiency of a Francis turbine.

The background for the selection of measuring methods and instrument calibration at TTL is presented in subchapters under 3.1. General guidelines for measurements according to *IEC60193* (1) are mentioned. For each of the variables involved in the efficiency measurement, the method used at the VKL Francis test rig is described with reference to the belonging measuring and calibration procedures. Measurements of oxygen level, water temperature, rotational speed and pressure are briefly described as they are less complex than acquiring the remaining quantities subjected to measurement. Volume flow rate, axial force and torque measurements are described in more detail. The chapter aims not to list all measuring and calibration methods complying with *IEC60193* (1), but rather to describe how and why the compliant method that is assessed as best suited for each measurand will work.

The suggested method for all measurements are presented in the subchapters under 4.1. Oxygen level, water temperature, rotational speed and pressure is explained briefly. Flow rate, axial force and torques are presented in detail. Calibration procedures for axial force and mechanical torque are suggested. Discussions, where applicable, are found at the end of each subchapter.

3D-drawings for the main components in the Francis turbine test rig at TTL are provided in subchapters under 4.2. Discussions, where applicable, are found at the end of each subchapter.

A conclusion for main elements in the suggested design of the Francis turbine test rig is made in chapter 5. Some of the remaining tasks towards fulfilling the design of the Francis model test rig at TTL are mentioned in chapter 6.

1.4. Previous Work

The two universities NTNU and KU have cooperated on several projects regarding TTL.

The design of a Francis turbine test rig at TTL, with proposed options for the placement of the pipes, the turbine and the measuring instruments, was done by B. R. Halwai for his project thesis in 2012 (4). Some modifications to the design were done by TTL employees, with the installation of a simplified Francis test rig as a result (5).

In 2013, J. Seierstad made suggestions for the calibration of the flow measurement at the simplified Francis test rig for her master's thesis (6). The evaluation done by Seierstad was the basis for the suggestion of flow meter, dimensions and calibration system when I. J. Rasmussen did a complete design of the Francis test rig at TTL for her master's thesis in 2014 (7). The design by Rasmussen is based on the methods and requirements stated in *IEC60193* (1), and the setup at the Francis turbine test rig at NTNU. Rough cost estimates for several instruments that are applicable to the suggested methods found in this thesis can be found in Rasmussen (7).

For his master's thesis, M. Selmurzaev designed a system for measurement and calibration of axial load and friction torque on the Francis Turbine test rig at TTL and at VKL (8). Selmurzaev designed a calibration jig for axial load calibration at VKL. The jig is used as the basis for the setup of axial load calibration at the TTL Francis rig. Rough cost estimates for strain gauges and telemetry system along with of a method for estimating axial loads in Francis turbines are among the content in Selmurzaev's thesis that makes it useful as a supplement to this thesis.

To get familiar with TTL, model testing of turbines and applicable standards, the author worked on a pre-project to this master thesis. Calibration of the instruments at the Waterpower Laboratory's Francis turbine test rig was performed along with efficiency tests, resulting in a hill chart diagram. Field work was conducted at Kathmandu University in April 2017 together with fellow master student A. Kjerschow, who in August 2017 is handing in his master's thesis treating the signal handling in the TTL Francis turbine test rig (9).

Based on the pre-project and field work at TTL, a description of the VKL and TTL labs are given in subchapters 1.5 and 1.6.

1.5. The Turbine Testing Laboratory at KU, Nepal

With the aim to support hydropower development in Nepal, KU conceived the idea of building a turbine testing facility in 1997. Detailed preliminary designs were made in 2000/2001, and KU was by an independent feasibility study identified as an appropriate Institute for the placement of a turbine testing facility. In 2009, an agreement regarding financial support for the construction of the Turbine Testing Laboratory was signed between KU and Norwegian Agency for Development Corporation (NORAD). Faculties of KU proceeded with the design of TTL and NTNU, having a similar lab with the Waterpower Laboratory, provided guidance. After 2.5 years of construction, TTL was inaugurated in 2011 and on November 24th, 2016, TTL marked its fifth anniversary. The facade of TTL and the placement of the upper and lower reservoir are shown in Figure 1-1.

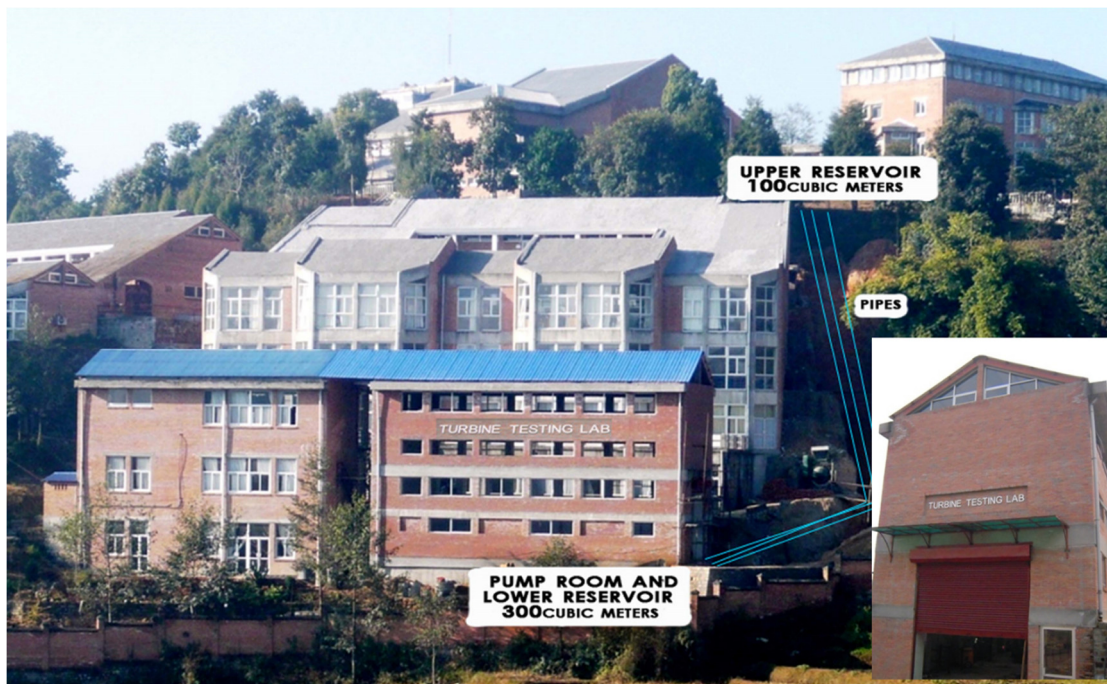


Figure 1-1: Part of Kathmandu University campus and the Turbine Testing Laboratory (10)

The upper reservoir of 100 m³ capacity is situated at the top of KU premises and allows for tests with a natural head of 30 m to be performed. The underground lower reservoir holds a capacity of 300 m³.

In Figure 1-2, providing an overview of the main lab building, a camera symbol denotes the position from which the picture in Figure 1-3 is taken. The picture was taken during the author's field work at TTL and shows the Turbine Testing Laboratory per May 2017. It includes rig setups not shown in Figure 1-2, among other what's left of the simplified student test rig where a 92 kW Francis turbine was tested.

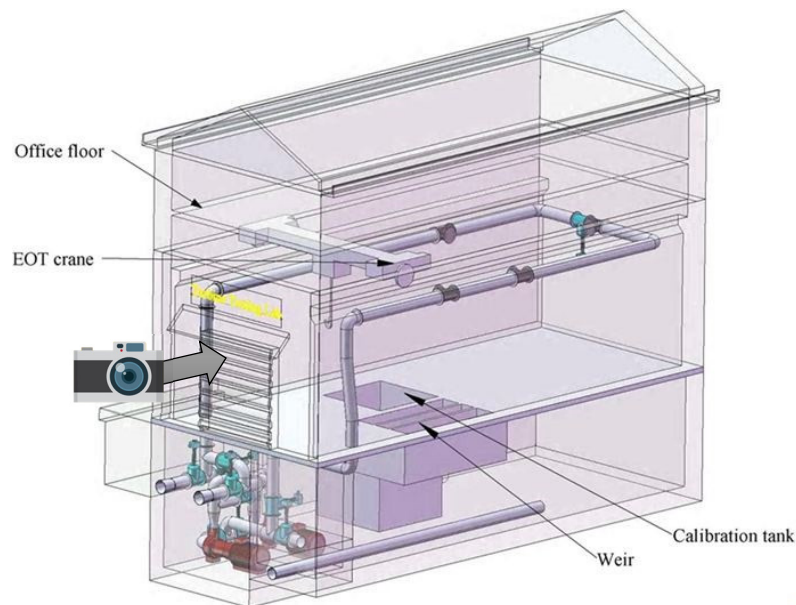


Figure 1-2: See-through View of TTL (11)



Figure 1-3: The Turbine Testing Laboratory per May 2017



Figure 1-4 shows the TTL pump room in two ways: picture and 3D-model from approximately the same perspective for comparison.



In the pump room are two centrifugal pumps of 250 kW, each capable of producing a maximum flow of $0.25 \text{ m}^3/\text{s}$ and a maximum head of 75 m.

Series or parallel combination of the pumps enable a closed system head of 150 m or flow of $0.50 \text{ m}^3/\text{s}$ respectively (11).

Figure 1-4: TTL Pump Room

1.6. The Francis Turbine Test Rig at NTNU, Norway

A basis for the design of the Francis turbine test rig at TTL is the corresponding rig installed at the Waterpower Laboratory, a Francis turbine test rig which is according to the International standard *IEC60193* (1). A brief description of the rig and the laboratory, based on (12) follows.

Established in 1917 and later refurbished in 2001, the Waterpower Laboratory at NTNU has contributed significantly to the Norwegian hydropower industry. Supplying the main pipe system around which the laboratory is built, are two main pumps enabled to operate individually, in series as well as in parallel. These configurations, along with varying the pump rotational speed, renders possible an extensive range of flow and head. In series configuration, the pumps can provide a pressure of up to 100 mwc. By the utilisation of different pipe-loops in the laboratory, various operational modes are possible.

Figure 1-5 shows mode 5, an example of a closed loop configuration (no free surfaces). In this mode, the water is pumped by a single pump to the high-pressure tank, which acts as the imaginary reservoir of the system. The water is then led through the Francis turbine rig and the draft tube, into the low-pressure tank and finally through pipes back to the pump before the cycle is repeated. The high-pressure tank of stainless steel has a diameter of 2.25 m and a volume of 18 m³. The low-pressure tank has a holding capacity of 7 m³ and serves as the tail water in the loop. It has a water-to-air surface when the rig is running, and air can be evacuated by the use of a vacuum pump to obtain the desired pressure.

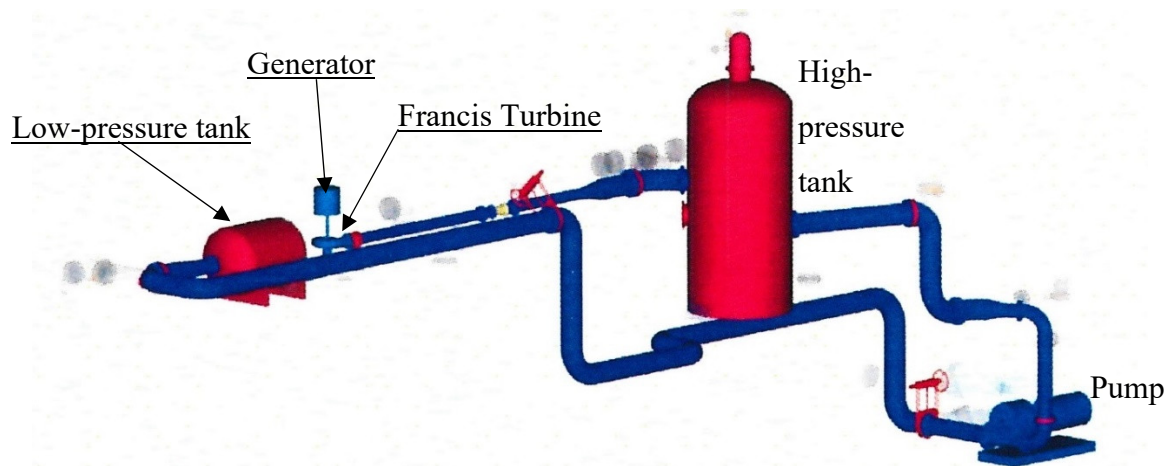


Figure 1-5: Francis Turbine Test Rig at VKL; Closed Loop Configuration, mode 5 (12)

On the fifth floor of the Waterpower Laboratory building, there is a u-shaped, free surface storage channel with an elevation of 16.25 m relative to the laboratory floor. This upper reservoir enables tests being run in an open loop configuration, as mode eight shown in Figure 1-6. In this mode, water is pumped from the lower to the upper reservoir. By a dead head of up to about 16 m, the water goes to the high-pressure tank, through the turbine and draft tube, and via the low-pressure tank before released back into the lower reservoir.

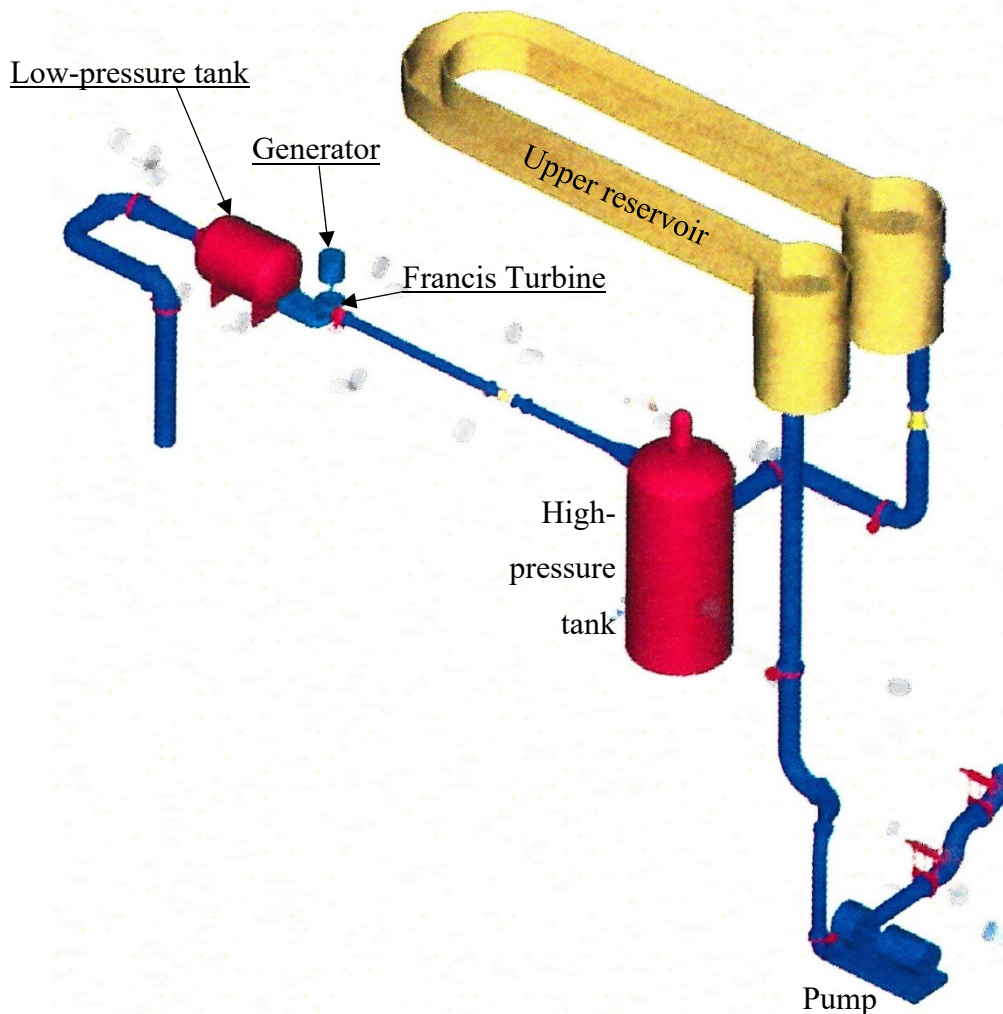


Figure 1-6: Francis Turbine Test Rig at VKL; Open Loop Configuration, Mode 8 (12)

1.7. Other Testing Laboratories

In addition to the laboratories at NTNU and VKL, other independent or university owned turbine laboratories include:

- **Alternative Hydro Energy Centre**, Roorkee, India
- **Central Water and Power Research Station**, Poona, India
- **Mini-Hydraulics Laboratory (MHyLab)**, Montcherand, Switzerland
- **Laboratory for Hydraulic Machinery (LHM)**, Lausanne, Switzerland
- **Turboinstitut**, Ljubljana, Slovenia

In addition, **Andritz Hydro** and **Rainpower** are examples of turbine laboratories owned by turbine companies.

2. Theory

2.1. The Francis Turbine

The Francis turbine is a reaction type turbine, a category of turbine in which conversion of specific to mechanical energy comes from pressure energy as well as from impulse forces. Figure 2-1 shows the cross-sectional view of a Francis turbine and its main components.

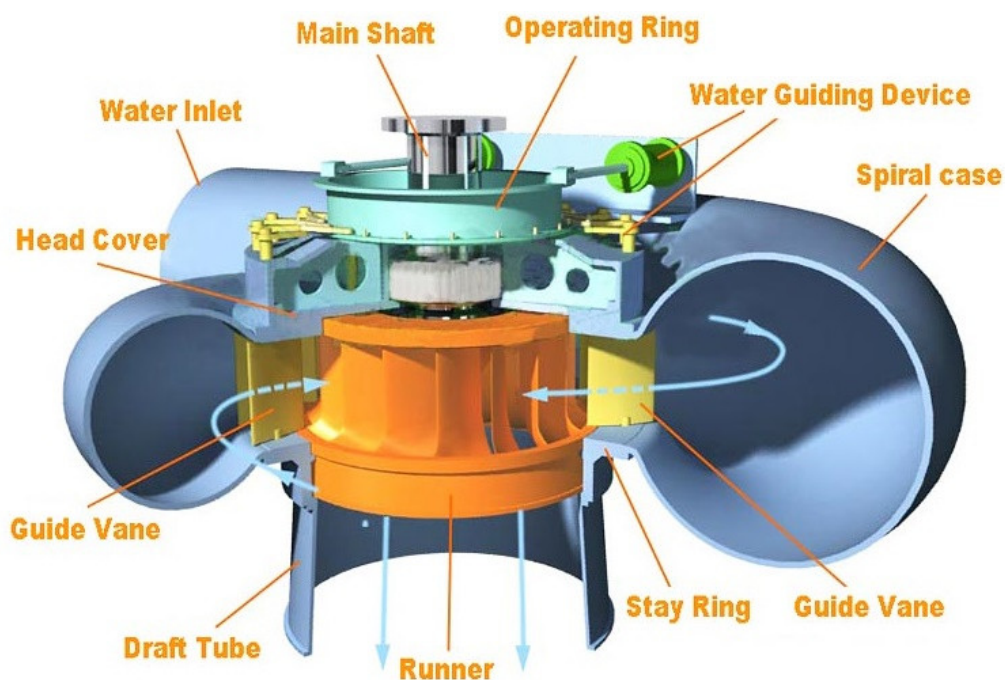


Figure 2-1: Cross-sectional View of Francis Turbine (13)

The water enters the spiral casing (which has numerous openings at regular intervals, and a uniformly decreasing cross-sectional along the circumference) at the inlet and is distributed onto the guide vanes through the stay vanes. By adjusting the guide vane angle, the flow and its rotation can be regulated to direct the flow onto the runner blades at optimum angles of attack. Full submergence of the turbine causes the water to approach the turbine at high pressure that is utilised into mechanical energy by the carefully designed runner. With low rotational components and velocity, the water enters the draft tube. The draft tube has an increasing cross-section so to lower the flow rate further, allowing for recovery of pressure energy and minimising the loss of kinetic energy at the outlet. The runner is connected to the main shaft, which in turn is connected to a generator.

2.2. Model Testing of Francis Turbines

A hydroelectric power plant is in most cases an enormous structure, and the components too large to be tested in a laboratory. Conducting performance tests in the field is costly and arduous. However, testing a scaled down turbine model in a laboratory is significantly easier, and the costs are often repaid in a fraction of the turbine lifetime by the increased efficiency of the power plant turbine (the prototype).

2.2.1. Hydraulic Similitude

To predict the performance of a power plant turbine by measuring and testing a smaller model turbine in a laboratory, the two must be hydraulically similar. Hydraulic similitude is achieved when the prototype and the model are geometrically similar and identical ratios of forces act between the fluid and the turbine components. The ratios of forces are Reynolds ($Re = \frac{\text{inertia}}{\text{viscosity}}$), Euler ($Eu = \frac{\text{pressure}}{\text{inertia}}$), Froude ($Fr = \frac{\text{inertia}}{\text{gravity}}$), and Weber ($Wb = \frac{\text{inertia}}{\text{surface tension}}$). Similitude of all these ratios in the same test is extremely difficult so for model efficiency tests, one considers the model to be representative of the prototype when the dimensionless factors for discharge Q_{ED} , speed n_{ED} and Thoma's cavitation factor σ , are identical.

$$(Q_{ED})_{Prototype} = (Q_{ED})_{Model} = \frac{Q}{D^2 \cdot \sqrt{g \cdot H}} \quad \text{Equation 2.1}$$

$$(n_{ED})_{Prototype} = (n_{ED})_{Model} = \frac{n \cdot D}{60 \cdot \sqrt{g \cdot H}} \quad \text{Equation 2.2}$$

$$(\sigma)_{Prototype} = (\sigma)_{Model} = \frac{NPSH}{H} \quad \text{Equation 2.3}$$

Here, $Q [m^3/s]$ is the discharge, $D [m]$ is the outlet diameter of the turbine, and $n [rpm]$ is the rotational speed. H is the model net head in unit $[m]$, and $NPSH$ is the Net Positive Suction Head.

g [m/s] is the acceleration due to gravity. The gravity constant varies with location¹, and is given as a function of latitude ϕ [°] and altitude z [m] in *IEC60193* (1) *Subclause 2.5.2*:

$$g = 9.7803 \cdot (1 + 0,0053 \sin^2 \phi) - 3 \cdot 10^{-6} \cdot z \quad \text{Equation 2.4}$$

It is stated that measured values of g shall be used if available. Additional details on similitude requirements for performance tests are covered in *IEC60193* (1), chapter 2.3.

By varying the discharge and speed factor one can map the turbine efficiency at different operational points, which is what is done when performing an efficiency test.

2.2.2. Hydraulic Efficiency

The expressions and variables for calculating the hydraulic efficiency of a Francis turbine are presented. The model net head E in unit [m²/s²] = [J/kg] is the head available for performing work on the turbine:

$$E = g \cdot H = \frac{\Delta p \cdot 1000}{\rho_w} + \frac{Q^2 \cdot \left(\frac{1}{A_1^2} - \frac{1}{A_2^2}\right)}{2} \quad \text{Equation 2.5}$$

The second term of Equation 2.5 represents the difference in specific kinetic energy between the high- pressure reference section A_1 [m²] and the low-pressure reference section A_2 [m²]. The first term represents the difference in pressure energy between the same sections. In other words, the model net head E is the specific energy of water between A_1 and A_2 . Δp is the pressure differential, and ρ_w [kg/m³] is the density of water. Accounting for compressibility, ρ_w is dependent on the water temperature θ [°C] and the pressure p . For temperatures up to 35°C and pressures up to $150 \cdot 10^5$ Pa, ρ_w can be calculated from Equation 2.6:

¹ Coordinates for TTL were extracted by *mapcoordinates* (44), verification of the values is recommended. Latitude 27.6197338° and altitude 1 485m are used to calculate the local gravity at TTL:

$$g = 9.7803 \cdot (1 + 0.0053 \sin^2(27.6197338)) - 3 \cdot 10^{-6} \cdot 1485 \approx 9.79506 \text{ m/s}^2$$

$$\rho_w = \frac{10^3}{((1 - A \cdot p) + 8 \cdot 10^6 \cdot (\theta - B + C \cdot p)^2 - 6 \cdot 10^{-8} \cdot (\theta - B + C \cdot p)^3)} \quad \text{Equation 2.6}$$

$$A = 4.6699 \cdot 10^{-10}; \quad B = 4.0; \quad C = 2.1318913 \cdot 10^{-7}$$

The pressures and temperatures at section A_1 and A_2 give the water density in each section, and the density in the turbine is estimated to be the average of these. When applied to model test heads $H \leq 40$ m, the compressibility of water is negligible and it is assumed that $\overline{\rho_w} = \rho_1 = \rho_2$.

Rearranging Equation 2.5 provides the way of expressing the model net head in unit $[m]$, symbolised by H as shown in Equation 2.7:

$$H = \frac{E}{g} \quad \text{Equation 2.7}$$

The total available power or the hydraulic power $P_h [W]$ is expressed in as the mass flow rate $\dot{m} = \rho_w \cdot Q$ multiplied by the model net head $E = gH$:

$$P_h = \rho_w \cdot Q \cdot g \cdot H \quad \text{Equation 2.8}$$

As seen from Equation 2.9, the mechanical power of the runner $P_m [W]$ is found by multiplying the torque applied to the runner $T_m [Nm]$ by the angular speed ω :

$$P_m = T_m \cdot \omega = T_m \cdot \frac{2 \cdot \pi \cdot n}{60} \quad \text{Equation 2.9}$$

With T_m being equal to the sum of the shaft torque, $T [Nm]$, and the friction torque due to seal and bearing arrangement, $T_{Lm} [Nm]$ as expressed mathematically in Equation 2.10:

$$T_m = T + T_{Lm} \quad \text{Equation 2.10}$$

The ratio of power transferred in the runner to the total available power is termed the hydraulic efficiency, $\eta_h [\%]$. The hydraulic efficiency can be calculated by the use of Equation 2.11:

$$\eta_h = \frac{P_m}{P_h} = \frac{T_m \cdot \omega}{\rho_w \cdot Q \cdot g \cdot H} \quad \text{Equation 2.11}$$

2.3. Measuring with Strain Gauges

Strain \mathcal{E} describes the elongation or the compression of a section, defined as the quotient of change in length ΔL and a reference length L_0 . An example of measuring with strain gauges is such as the shaft of a turbine which is subjected to axial forces in both directions. The downward axial load acts as a tension force on the measurement section, while the upward axial thrust acts as a compression force. Strain gauges mounted on the surface of the section will experience a change in electrical resistance when subjected to strain. By smart mounting of several strain gauges connected in bridge circuits, unwanted influences on the result can be compensated for. The arrangement in Figure 2-2 with mirror-imaged cross-sections connected in a Wheatstone full bridge circuit will compensate for electrical resistance changes due to thermal strain as well as superimposed bending strains, and is very well suited for measuring the axial strain on a shaft (14).

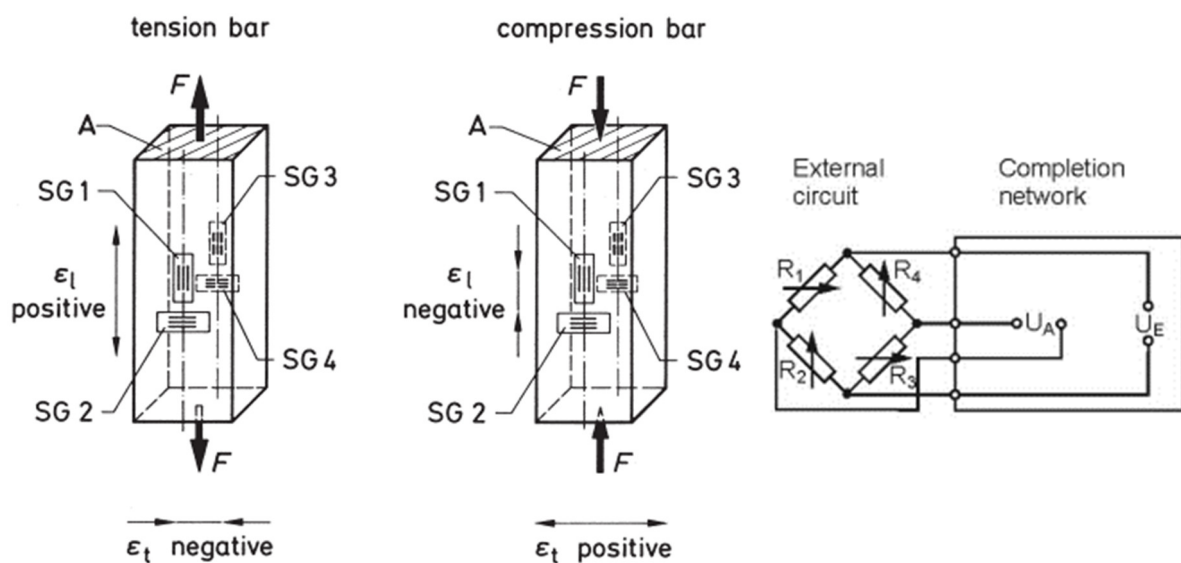


Figure 2-2: a) Strain Gauges for Normal Stress, b) Wheatstone Full Bridge Circuit (14)

The change in length of the measurement section is dependent on the material-specific properties. The modulus of elasticity or Young's modulus, E , is a measure of the strain of the material in relationship to the applied force F . The quotient of the axial force and the cross-

sectional area of the stressed material is the normal stress σ . Consequently, the modulus of elasticity can be expressed as $E = \frac{\sigma}{\varepsilon}$ (For steel, $E \sim 200 \text{ kN/mm}^2$). When a material is subjected to a tension force, it extends longitudinally by $\varepsilon_l = \frac{\sigma}{E}$, but at the same time compresses transversely by $\varepsilon_T = -\nu \cdot \varepsilon_l$. Poisson's ratio ν expresses the ratio between the two: $\nu = -\frac{\varepsilon_t}{\varepsilon_l}$. (For steel, $\nu \sim 0.3$). Introducing the gauge factor k as an experimentally checked characteristic of the strain gauge, a change of resistance $\Delta R_1 = \varepsilon_1 \cdot k \cdot R_1$ is experienced in SG1, and $\Delta R_2 = -\nu \cdot \varepsilon_1 \cdot k \cdot R_2$ in SG2. Accordingly, this is also true for SG3 and SG4 respectively (15).

Excitation of the Wheatstone bridge circuitry is required to convert the tiny change in resistance into a measurable voltage. Recommendations for excitation and signal handling is found in National Instruments' *Engineer's Guide to Accurate Sensor Measurements* (16). The measured voltage U_A as a function of the supplied voltage U_E is found as:

$$\frac{U_A}{U_E} (= \frac{U_{out}}{U_{in}}) = \frac{k}{4} \cdot (\varepsilon_1 - \varepsilon_2 + \varepsilon_3 - \varepsilon_4) \quad \text{Equation 2.12}$$

By applying $\varepsilon_2 = \varepsilon_4 = -\nu\varepsilon_1$ and $\varepsilon_3 = \varepsilon_1 = \varepsilon$, the measured voltage signal is

$$U_A = \frac{k}{4} \cdot (2 \cdot (1 + \nu) \cdot \varepsilon) \cdot U_E \quad \text{Equation 2.13}$$

Alternatively, expressing the strain as a function of voltage, gauge and material properties

$$\varepsilon = \frac{4}{k \cdot (2 \cdot (1 + \nu))} \cdot \frac{U_A}{U_E} \quad \text{Equation 2.14}$$

The equation for the axial stress

$$\sigma = \frac{\varepsilon \cdot E}{2 \cdot (1 + \nu)} \quad \text{Equation 2.15}$$

Which multiplied by the cross-sectional area gives the axial force. By applying the area of a hollow circular section as the stress area, the axial force as function of the strain is

$$A = \frac{E}{2 \cdot (1 + \nu)} \cdot \pi \cdot (r_{outer}^2 - r_{inner}^2) \cdot \varepsilon \quad \text{Equation 2.16}$$

Where r_{outer} and r_{inner} is the radius of the outer and inner surface of the section, respectively.

3. Design of the Francis Turbine Test Rig at TTL

3.1. Instrumentation and Measurement Procedures

A system for evaluating efficiency and performance of Francis turbines at TTL needs measuring of certain quantities. Through a measuring chain of components such as transducers, computers, signal converters or conditioners, the needed data is acquired and processed. The measured signals are converted into appropriate engineering units with meaningful performance data as the end output.

In general, the following guidelines are followed for the measurement instruments:

- Measurement instruments in accordance with *IEC60193* (1).
- Calibration of instruments on-site.
- Cavitation bubble effects on measurements must be avoided.
- The output from the system for data acquisition and processing shall be a true reflection of the quantities subjected to measurement (the measurands).
- Uncertainty in the measurement instruments must be accounted for.
- All instruments in use should have documented calibration procedures.

IEC60193 (1) distinguishes between two types of measuring methods:

1. Primary methods are the most accurate and need only measurements of fundamental quantities like length, mass and time.
2. Secondary methods are founded on various principles. To comply with the high accuracy required for the purpose of *IEC60193* (1), secondary methods must be calibrated against a primary method.

The quantities subjected to measurement are presented in Table 3.1:

Table 3.1: Measurands in Francis Turbine Testing

Symbol	Description	Unit
D.O.	Dissolved oxygen	<i>mg/l</i>
θ	Water temperature	$^{\circ}\text{C}$
n	Rotational speed	<i>rpm</i>
p_{measured}	Inlet Pressure	<i>Pa</i>
Δp	Differential pressure over turbine	<i>Pa</i>
Q	Volume flow rate	m^3/s
T_m	Mechanical torque on runner	<i>Nm</i>
T	Generator torque	<i>Nm</i>
T_{Lm}	Friction torque (calculated, $T_{Lm} = T_m - T$)	<i>Nm</i>
A	Axial load	<i>N</i>

Averages of each of the measurands shall be obtained for measurements performed in the same time interval.

The design of the system for efficiency measurement at the Francis turbine test rig at the Turbine Testing Laboratory is based on:

- Requirements/recommendations/methods as stated in *IEC60193* (1), other relevant standards or best practices from turbomachinery instrument/component providers.
- Instruments/components installed at the Francis turbine test rig at the NTNU Waterpower Laboratory, which have proven to work well.

Relevant information regarding the design, primarily *IEC60193* (1) guidelines and VKL procedures, are presented for each of the measurands in the appurtenant subchapter. Rather than listing all measuring and calibration alternatives in comply with *IEC60193* (1), the purpose of each subchapter is to describe the function of the compliant method that is assessed as best suited for TTL.

3.1.1. VKL Overview: Piping and Instrumentation Diagram

The arrangement of measurements that are used for performance calculations of the model turbine at the Francis turbine test rig at the Waterpower Laboratory, NTNU, are presented in Figure 3-1. Red lines indicate the closed loop used during the performance test of the turbine.

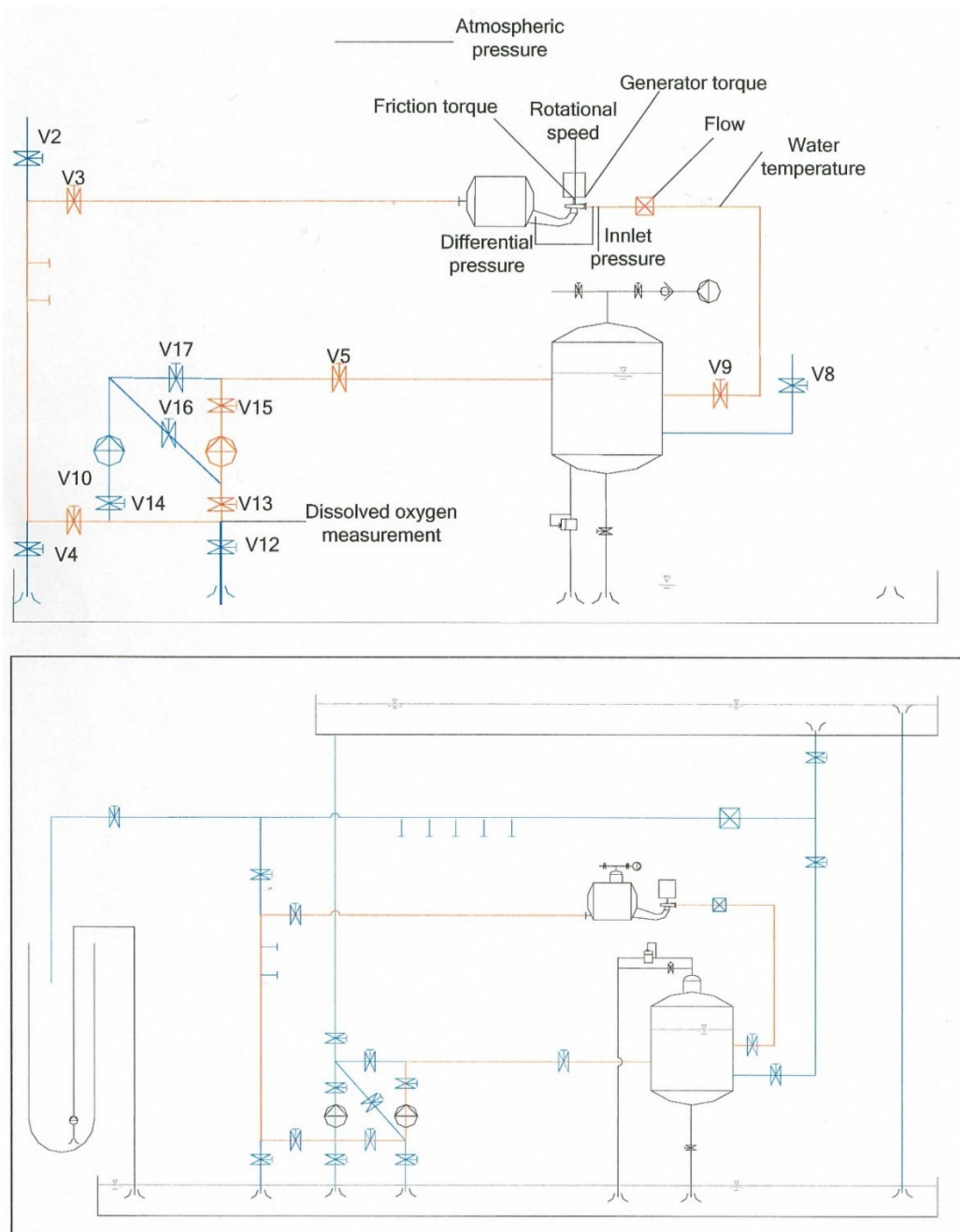


Figure 3-1: Arrangement of the Measurements in the Waterpower Laboratory (17)

By the use of a data acquisition unit connected to a computer program written in the software *LabView*, data from the instruments are collected and post-processed with calibration data if applicable. Calculations are performed in *LabView* using the collected data and relevant constants like the outlet area A_2 where outlet pressure is measured, diameter d_1 at the point of inlet pressure measurement, and the model gravity g_m .

The main components from the high-pressure tank upstream of the turbine to the downstream low-pressure tank is shown in Figure 3-2. Running of the test rig, and the component specification are described in detail in (18) and (7).

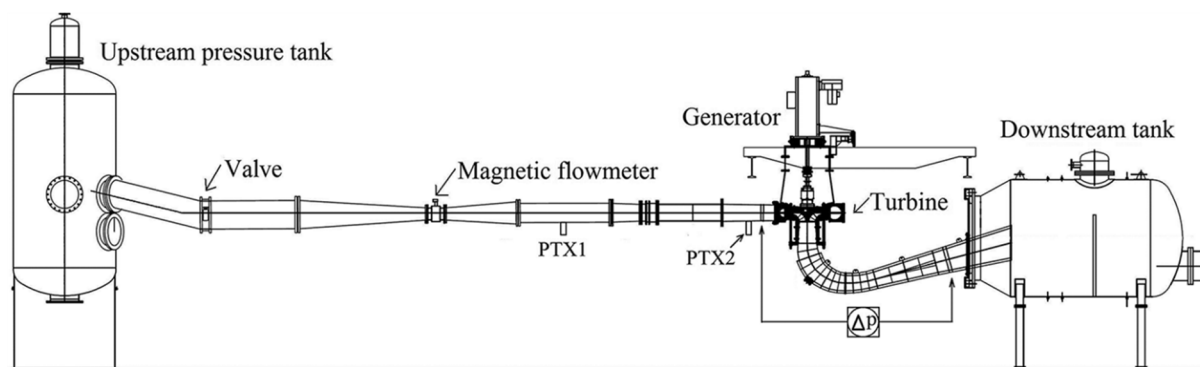


Figure 3-2: Model Francis Turbine Test Rig Installed at the Waterpower Laboratory (19)

The piping and instrumentation diagram for TTL is found in chapter 4.1.1.

3.1.2. Oxygen Level

The purpose of measuring the dissolved oxygen level in the water is to control that the values are within acceptable limits. In *IEC60193 (1) Subclause 2.1.2.3*, which handles the condition of the water, that air bubbles should be removed to a reasonable extent before performing model tests. The water's content of mixed and dissolved oxygen should be measured close to the model intake, as at VKL where an oxygen probe is located at the main pump inlet. The measurement procedure is found in Appendix B, doc. No. *LM-4551-1*. The oxygen probe is calibrated externally according to calibration procedure *LC-4551-1* in Appendix C.

The suggested method for oxygen level measurement at TTL is found in chapter 4.1.2.

3.1.3. Water Temperature

The density of water is corrected from the measured water temperature θ . Additionally, the water temperature should be monitored as water temperature should not exceed 35°C, and large

temperature variations should be avoided during test (1). A temperature probe located downstream the high-pressure tank measures the water temperature at VKL Francis turbine test rig as described in measuring procedure *FM-4514-3* in Appendix B. VKL has no option for calibrating the water temperature measuring system by a primary method; another temperature probe is used as a reference as described in procedure *FC-4514-3* in Appendix C.

The suggested method for water temperature measurement at TTL is found in chapter 4.1.3.

3.1.4. Rotational Speed

The rotational speed of the runner and shaft, n , is needed to calculate the mechanical power of the runner. The measuring procedure at the VKL Francis turbine test rig is described in measuring procedure *FM-4431-1* in Appendix B. A photocell sends infrared light towards a disc with a cut that is connected to the generator shaft. Each time the cut passes, the logging computer receives a signal. The rotational speed is calculated from the number of times the slot is passing per unit time. This is a primary method as stated in *IEC60193 (1) Subclause 3.7*, an absolute measurement that does not need calibration but is checked using a tachometer or a high accuracy stroboscope.

The suggested method for rotational speed measurement at TTL is found in chapter 4.1.4.

3.1.5. Pressure

In relation to the hydraulic performance of the turbine, the pressure is measured to determine the specific energy in the water (pressure component). The differential pressure across the turbine inlet and draft tube outlet at VKL, Δp , is measured by a differential pressure transducer, as described in Appendix B, doc. No. *FM-4536-2*.

In addition, the pressure in, p_1 , is measured by a differential pressure transducer that is fed water pressure on the high-pressure side and where the low-pressure side is open to atmosphere. Appendix B, doc. No. *FM-4536-4* describes the procedure. A digital barometer located inside the control room measures the atmospheric pressure p_{amb} in the laboratory. By knowing p_1 , p_{amb} and Δp , the pressure after the turbine p_2 can be calculated.

The differential pressure transducers at VKL are calibrated by a deadweight manometer that uses a piston with a known area to pressurise a fluid. Calibrated weights are loaded onto the piston, inducing a certain pressure for which the pressure transducer gives an output Volt signal that varies linearly with the load. Appendix C, doc. No. *LC-4536* describes the calibration procedure.

IEC60193 (1) *Subclause 3.3* handles the guidelines for pressure measurement.

The suggested method for pressure measurements at TTL is found in chapter 4.1.5.

3.1.6. Volume Flow Rate

The volume flow rate or the discharge, Q , is used to calculate the specific energy in the water (kinetic component). An electromagnetic flowmeter measures the discharge at the VKL Francis turbine test rig, as described in measuring procedure *FM-4624-4* in Appendix B. A voltage, which magnitude is directly proportional to the water speed, is induced in the flowmeter as the water moves across the magnetic field. By multiplying the speed with the known cross-section, the volume flow rate is found.

An electromagnetic flowmeter is to measure the flow rate at the Francis turbine test rig at TTL. Electromagnetic flowmeters are not very sensitive to wear, have no pressure losses and generate little disturbance in the flow. A DN200 flowmeter, dimensioned to accurately measure flow rates between $0.16 \text{ m}^3/\text{s}$ and the maximum discharge of $0.5 \text{ m}^3/\text{s}$, was suggested for the Francis rig by Rasmussen (7). The accuracy of the flowmeter is dependent on the velocity of the flow subject to measure. Consequently, a DN100 flowmeter is recommended for other test rigs in the laboratory running with $Q \leq 0.16 \text{ m}^3/\text{s}$.

Calibration

As advised in *IEC60193 (1) Subclause 3.2*, TTL will have one primary and one secondary method for measuring the flow rate. The flowmeters, which is a secondary method, will be calibrated by the primary method; a weighing tank facility. The specific instruments and placement thereof are different for VKL and TTL, but the measuring principles and calibration procedures at VKL have transfer value to the TTL test rig.

Appendix C, calibration procedure *FC-4624-4* describes how the flowmeter at VKL is calibrated by the weighing method. The weighing tank load cells also need calibration; procedure is found in Appendix C, Doc. No. *LC-4331-5/6/7*.

ISO 4185 – Measurement of liquid flow in closed conduits – Weighing method (20) states requirements concerning the measuring apparatus, procedure, discharge calculation method and uncertainties for the weighing method.

An existing rectangular cavity in the TTL floor, beneath the steel plates shown in Figure 3-3 is a suitable placement for the weighing tank. The sides were measured to $2.5\text{m} \cdot 2.1\text{m}$.

According to R. Koirala (personal communication, April 2017), the depth is 5m. Due to water in the hole, this depth was not verified by measurement.



Figure 3-3: TTL Weighing Tank Placement

With the suggested weighing tank placement and the flowmeter installed upstream of the tank, the existing pipe arrangement makes it difficult to fit all parts affiliated the volume flow rate measurement while simultaneously accomplishing optimal flow conditions through the flowmeter. Consequently, the design requires modifications to the pipes shown in Figure 3-4.



Figure 3-4: TTL Suggested Placement of Flow Meter and Weighing Facility

The suggested design affiliated the calibration and measurement of volume flow rate at TTL is described in chapter 4.1.6.

3.1.7. Axial Force

When the Francis turbine is in operation, forces in the axial direction occur due to a combination of hydrostatic and hydrodynamic effects, the weight and buoyancy of the runner and rotating parts, impulses from the flow, as well as water pressure. The axial forces acting on bearings and embedded parts are important design parameters, and should be measured as a function of the various operating conditions of the Francis turbine (1).

A system consisting of a hydraulic thrust bearing and a differential pressure transducer measures the axial load at the VKL Francis turbine test rig, as described in measuring procedure *FM-4536-8* in Appendix B. Figure 3-5 shows the arrangement, where oil is fed to the differential pressure transducer from the two sections of the hydraulic thrust bearing. The system involves the VKL bearing block shown in Figure 3-6.

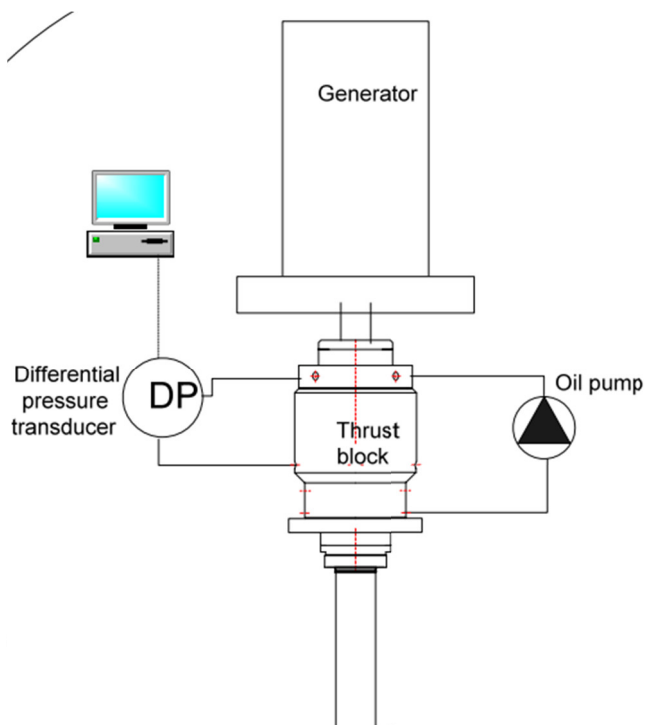


Figure 3-5: VKL Axial Load Measurement (17)



Figure 3-6: VKL Bearing Block

Hydraulic bearings are highly sensitive to contaminants which may lead to unit failure, an unfortunate characteristic considering TTL's location and the Nepal climate. Agriculture fields are right outside the laboratory, and especially the dry season holds a substantial amount of dust

in the air. Furthermore, the VKL bearing block is complex and a result of high precision machining. Axial force measurements based on strain gauges (SG) as an IEC60193-compliant alternative of less complexity and lower cost is recommended for the TTL Francis test rig. The setup of the strain gauges to be as explained in subchapter 2.3 - *Measuring with Strain Gauges*.

Calibration

The axial load must be calibrated both in the positive and negative axial direction. Procedure *FC-4536-8* in Appendix C describes the current calibration of the differential pressure transducer that measures the axial force at VKL. The procedure assumes calibrated weights on a fixture hanging coaxially to the shaft, a method that limits the calibration to downward acting axial force. A new design for calibrating the axial load measurement at VKL, which also added upward directed axial thrust calibration, was developed by Selmurzaev (8). The suggested method is built upon the same base principle in compliance with *IEC60193* (1); using certified masses to apply force perpendicular to the runner. The basic concept is presented in Figure 3-7, where the lever principle is utilised. A load at point A is transferred to an upward force in point B through a rolling support. Two single row ball bearings reduce the friction in the rolling support, which is fixed to a circular plate that is bolted to the turbine housing.

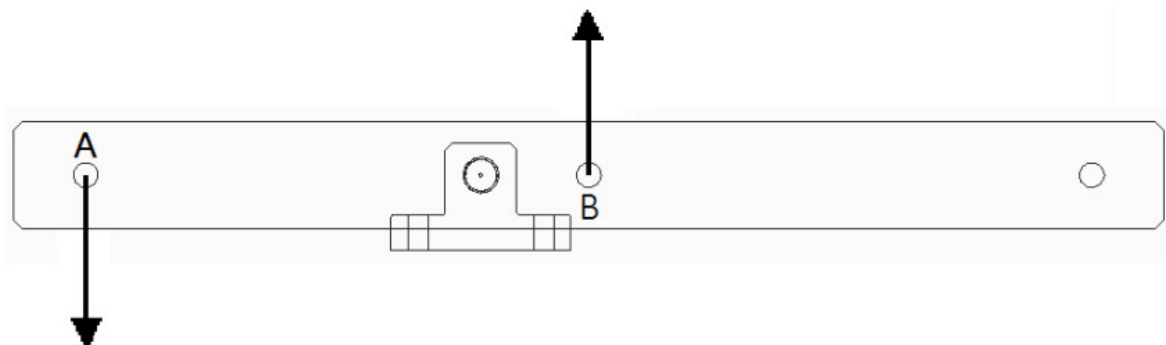


Figure 3-7: Lever Beam Concept with Rolling Support (8)

The VKL calibration procedure is adapted to Selmurzaev's design and used as the basis for the TTL calibration arrangement, as the method also holds valid for calibrating axial strain measuring gauges.

The axial force calibration jig is shown in Figure 3-8, where a circular plate is bolted to the bottom cover. Two holes in the circular plate allow for weight holders hanging from point A and C. A bar is attached to point B with basic screw joints on one end. Via an arrangement of adjustable length, the bar distributes force to the shaft (not shown in figure) along the center line.



Figure 3-8: Calibration Jig (Weights for Calibration of Upward Axial Force)

The mass for calibrating the full range of axial load is estimated by assessing the forces and moments at work on the beam. The first assumption made is that the load from the beam's mass is uniformly distributed. The second is that two weight beds of equal mass hang from point A and C. For calibration of an upward axial force, calibrated weights are loaded onto the weight holder attached to A as shown in Figure 3-8. When applying a moment balance at the rolling support as shown in

Figure 3-9, it is apparent that a force works downward on the beam in point B to keep it static. An equal and opposite force acts on the shaft above point B, creating tension in the material that is measurable by strain gauges; this is the upward axial force.

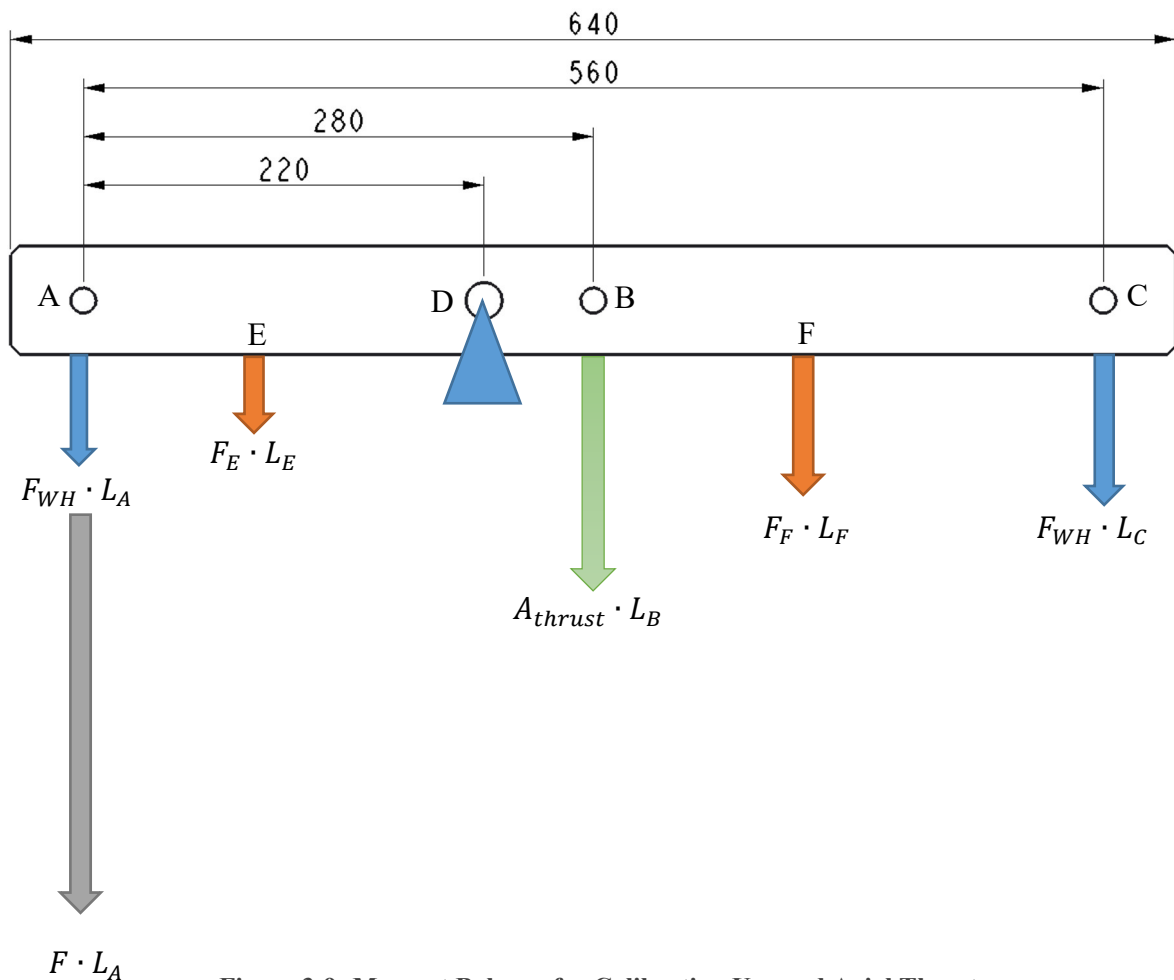


Figure 3-9: Moment Balance for Calibrating Upward Axial Thrust

All arm lengths $L_{@}$ are given with references to the rolling support (fixed point D). Points E and F are the centres of the moment contribution left and right of D due to the mass of the beam. A description of the symbols are given in Table 3.2.

Table 3.2: Axial Force Calibration Calculation Input

Symbol	Description	Formula	Value	Unit
L_A	Arm for weight holder UP		0.22	m
L_B	Arm for balancing load	$0.28 - 0.22$	0.06	m
L_C	Arm for weight holder DOWN	$0.56 - 0.22$	0.34	m
L_E	Arm for load of beam left of D	$\frac{0.22 + (l_{beam} - 0.56)/2}{2}$	0.13	m
L_F	Arm for load of beam right of D	$\frac{l_{beam}}{2} - L_E$	0.19	m
g	Local gravity constant	See chapter 2.2.1	9.79506	m/s^2
F_{WH}	Load, weight holder	$m_{WH} \cdot g$		N
F	Load, calibrated weights	$\sum m \cdot g$		N
F_E	Load, beam left of D	$m_{beam} \cdot \frac{2 \cdot L_E}{l_{beam}} \cdot g$		N
F_F	Load, beam right of D	$m_{beam} \cdot \frac{2 \cdot L_F}{l_{beam}} \cdot g$		N
A_{thrust}	Axial load (Downward on beam, Upward on shaft)			N
A_{load}	Axial load (Upward on beam, Downward on shaft)			N

Now follows the calculation of the necessary sum of mass of calibrated weights to be loaded onto the weight holder at point A for calibrating the upward axial load.

The moment balance is given as

$$F \cdot L_A + F_{WH} \cdot L_A + F_E \cdot L_E = F_F \cdot L_F + F_{WH} \cdot L_C + A_{thrust} \cdot L_B$$

Rearranged into

$$F \cdot L_A = A_{thrust} \cdot L_B + F_F \cdot L_F - F_E \cdot L_E + F_{WH} \cdot (L_C - L_A)$$

The mass of calibrated weights in *weight holder UP* as function of the other variables is

$$m = \frac{\frac{A_{thrust} \cdot L_B}{g} + \frac{2 \cdot m_{beam}}{l_{beam}} \cdot (L_F^2 - L_E^2) + m_{WH} \cdot (L_C - L_A)}{L_A}$$

By input of the known values, the mass is given as

$$m = \frac{3}{11} \cdot \left(\frac{A_{thrust}}{g} + m_{beam} + 2 \cdot m_{WH} \right)$$

With upward axial force $A_{thrust}=20\text{kN}$ to be calibrated, the sum of calibrated weights is

$$m = \frac{3}{11} \cdot \left(\frac{20\,000\text{N}}{9.79506\text{N/kg}} + m_{beam} + 2 \cdot m_{WH} \right) \approx 557\text{kg} + \frac{3}{11} \cdot (m_{beam} + 2 \cdot m_{WH})$$

The mass of the beam and weight holders can be cancelled out in the calibration by adding weights in one of the weight holders until the point of zero axial load is found, and start the calibration from that point. Calibration of the upward axial thrust using calibrated weights $\Sigma m = 560\text{kg}$ is sufficient.

The relation between the upward-acting axial force A_{thrust} and the mass in *weight holder up* should then be

$$A_{thrust} = \frac{11}{3} m \cdot g \quad \text{Equation 3.1}$$

For calibration of downward axial force, weights are placed in the weight holder at point C. Consequently, the moment balance is

$$F \cdot L_C = F_E \cdot L_E - F_F \cdot L_F + F_{WH} \cdot (L_A - L_C) - (-A^- \cdot L_B)$$

The mass of calibrated weights in *weight holder DOWN* as function of the other variables is

$$m = \frac{\frac{A_{load} \cdot L_B}{g} - \left(\frac{2 \cdot m_{beam}}{l_{beam}} \cdot (L_F^2 - L_E^2) + m_{WH} \cdot (L_C - L_A) \right)}{L_C}$$

With downward axial force $A_{load}=20\text{kN}$ to be calibrated, the sum of calibrated weights is

$$m = \frac{3}{17} \cdot \left(\frac{20\,000\text{N}}{9.79506\text{N/kg}} - m_{beam} - 2 \cdot m_{WH} \right) \approx 360\text{kg} - \frac{3}{17} \cdot (m_{beam} + 2 \cdot m_{WH})$$

Similarly, as for upward axial thrust calibration, the mass of the beam and weight holders can be cancelled out, thus the necessary mass m for calibration of the downward axial load using calibrated weights $\Sigma m = 360\text{kg}$ is sufficient.

The relation between the downward-acting axial load A_{load} and the mass in *weight holder DOWN* should then be

$$A_{load} = \frac{17}{3} m \cdot g \quad \text{Equation 3.2}$$

The measurement and calibration of axial force at TTL are handled in chapter 4.1.7.

3.1.8. Generator Torque

The generator torque is the torque absorbed by the generator, and equals the mechanical torque of the runner subtracted the friction torque in the bearing and seal arrangement.

A load cell connected to an arm mounted on the VKL Francis rig generator measures the torque absorbed. The measuring procedure is described in doc. No. *FM-4331-5* in Appendix B. The generator rests on a hydrostatic bearing that requires a hydraulic pumping unit for oil feeding, making the bearing approximately friction-free.

A less complex method with a lower cost is recommended for the TTL Francis test rig, and a torque transducer has been ordered by the TTL staff.

Shaft Couplings

Alignment errors in the drivetrain are among the sources of parasitic loads affecting the transducer accuracy. In addition, misaligned shafts without proper coupling are subject to severe stresses that damage bearings and seals. The shaft ends installed on the measurement flange will have one, more or all of the misalignment types shown in Figure 3-10.

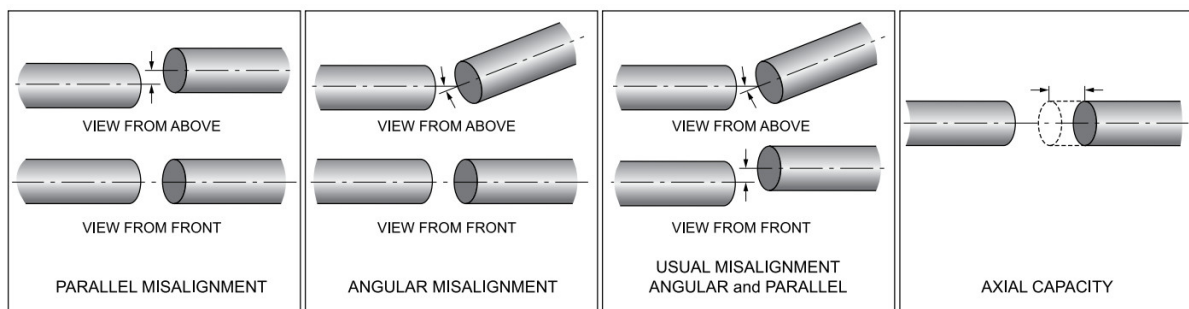


Figure 3-10: Shaft Misalignment Types² (21)

² The figure shows alignment types for horizontal shaft arrangement, but is also applicable to vertical shafts.

Parallel misalignment of the shafts generates a bending moment and a radial force affecting the transducer. Angular misalignment results in a bending moment, while an axial offset will result in both a bending moment and an axial force (22).

To avoid costly damage to equipment and improve the transducer's accuracy, installing flexible shaft couplings that are able to compensate for shaft misalignment in a torsionally rigid way is imperative.

Calibration

To comply with *IEC60193 subclause 3.6 for shaft torque measurement* (1), the torque transducer at TTL must be calibrated by the basic primary method: calibrated weighing masses on a calibrated lever arm. The same approach is used to calibrate the generator torque measuring load cells at VKL, as described in Appendix C, doc. No. *FC-4331-4* (+supplement for calibrating torque arm length). A calibration procedure for the TTL Francis generator torque measurement is developed based on the corresponding procedure at VKL.

The force applied to a lever arm is measured and multiplied by the radius at which it is applied: $T = F \cdot r$. Using calibrated weights to apply the force via a pulley yields $F = m \cdot g$. Torque is related to power by Equation 2.9. The Francis turbine test rig at TTL shall be capable of performing tests on turbines up to $P=150\text{kW}$, and the full range of torque to be measured must be calibrated. By applying minimum rotational speed $n=500\text{rpm}$, the necessary mass for calibration can be found per meter arm:

$$m = T \cdot \frac{1}{r \cdot g} = \frac{P}{2 \cdot \pi \cdot n} \cdot \frac{1}{r \cdot g} = \frac{150\,000 \frac{\text{Nm}}{\text{s}}}{2 \cdot \pi \cdot 500 \frac{\text{rpm}}{60\text{s}} \cdot r \cdot 9.81 \frac{\text{N}}{\text{kg}}} \cong \frac{292\text{kg}}{r}$$

The suggested setup for applying the force to the arm and method for calibrating the torque is described in chapter 4.1.8.

3.1.9. Friction/Mechanical Torque

The friction torque is the losses in torque from the runner to the generator due to friction in bearings and seals in the bearing block. A load cell connected to a hydraulic bearing unit and a mechanical stop measures the friction torque at the VKL Francis turbine test rig, as described in measuring procedure *FM-4331-2* in Appendix B. Two mechanical bearings, connected to the shaft and placed inside the hydraulic bearing unit, absorb all radial and axial movement in the turbine. The load cell absorbs all friction present in the two mechanical bearings. As with the measuring system for axial load and generator torque, the hydraulic unit is complex, and thus an alternative method for measurement is recommended for the TTL Francis turbine test rig.

The friction torque equals the difference between the mechanical torque and the generator torque. By developing a method for measuring the mechanical torque in addition to the generator torque measurement; the friction torque can be calculated. Measurement by strain gauges between the runner and the bearings is a secondary method complying with *IEC60193* (1).

Measuring axial force with strain gauges is described in subchapter 2.3. The basic principle behind strain gauge measurement of torque is the same, but a different force distribution necessitates a different of the strain gauges. The strain maxima on a twisted shaft occur at $\pm 45^\circ$ with reference to the shaft axis. By mounting the strain gauges at a 45° angle to the central axis of the shaft as shown in Figure 3-11, the torsion load can be measured. The left part shows the application of 4 separate strain gauges. Proper alignment of the strain gauges can be quite difficult, especially on a curved surface. Application of special X rosettes, as shown on the right, offers an equally valid measurement and simplifies alignment.

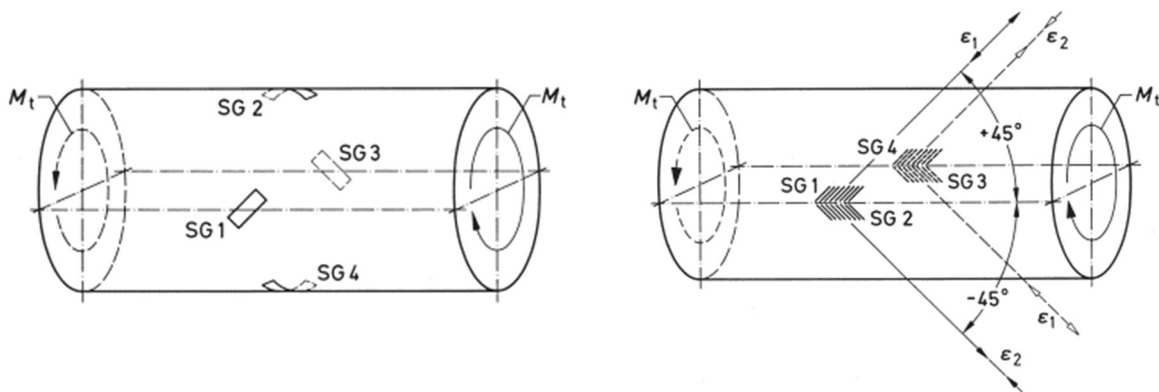


Figure 3-11: Strain Gauges Measuring Torsion (14)

As with the axial force, connection of the strain gauges in a full bridge circuit is favourable. SG1 and SG3 will experience positive strain, SG2 and SG4 will experience negative strain, and Equation 2.12 holds valid also for this case.

Calibration

The mechanical torque at TTL can be calibrated by the same method as the generator torque. The suggested measuring and calibration procedure is handled in chapter 4.1.9.1.

3.1.10. Uncertainty

In experimental setups involving measurements, the difference between the measured value of a quantity and the true value of the quantity is termed an error. The uncertainty in a measurement is the range within which the true value of the measured quantity can be expected to lie. In accordance with *IEC60193* (1), three types of errors shall be considered:

- **Spurious errors** invalidate a measurement, examples of which are instrument malfunction or human errors.
- **Random errors** arise due to unpredictable fluctuations in the experiment and may occur in the measuring instruments or due to the environmental conditions. Repetition of measurements can reduce the impact of random errors on the results as the random error of n independent measurements is \sqrt{n} smaller than the random error of an individual measurement (1). In the Francis rig at VKL, a 1000 Hz logging frequency and a logging time of minimum 30 second for each measurement lower the random uncertainty.
- **Systematic errors** arise from the characteristics of the measuring apparatus, the installation and the operating conditions, and thus cannot be reduced by repeating measurements.

The total uncertainty in the measurement of the hydraulic efficiency of the test point, $(f_{\eta_h})_t$ is calculated by the root sum of the squares for random errors $(f_{\eta_h})_r$ and systematic errors $(f_{\eta_h})_s$

$$(f_{\eta_h})_t = \sqrt{(f_{\eta_h})_s^2 + (f_{\eta_h})_r^2} \quad \text{Equation 3.3}$$

A full evaluation of the uncertainty in measurements at TTL is beyond the scope of this report. An analysis of the uncertainties at the VKL Francis test rig was done by Storli (23), and can, along with *IEC60193*, serve as guidance for a future uncertainty analysis at TTL. An overview of expected uncertainty sources in torque and axial loads measurements at the Francis test rig at TTL are presented in subchapters 4.1.10.1 and 4.1.10.2.

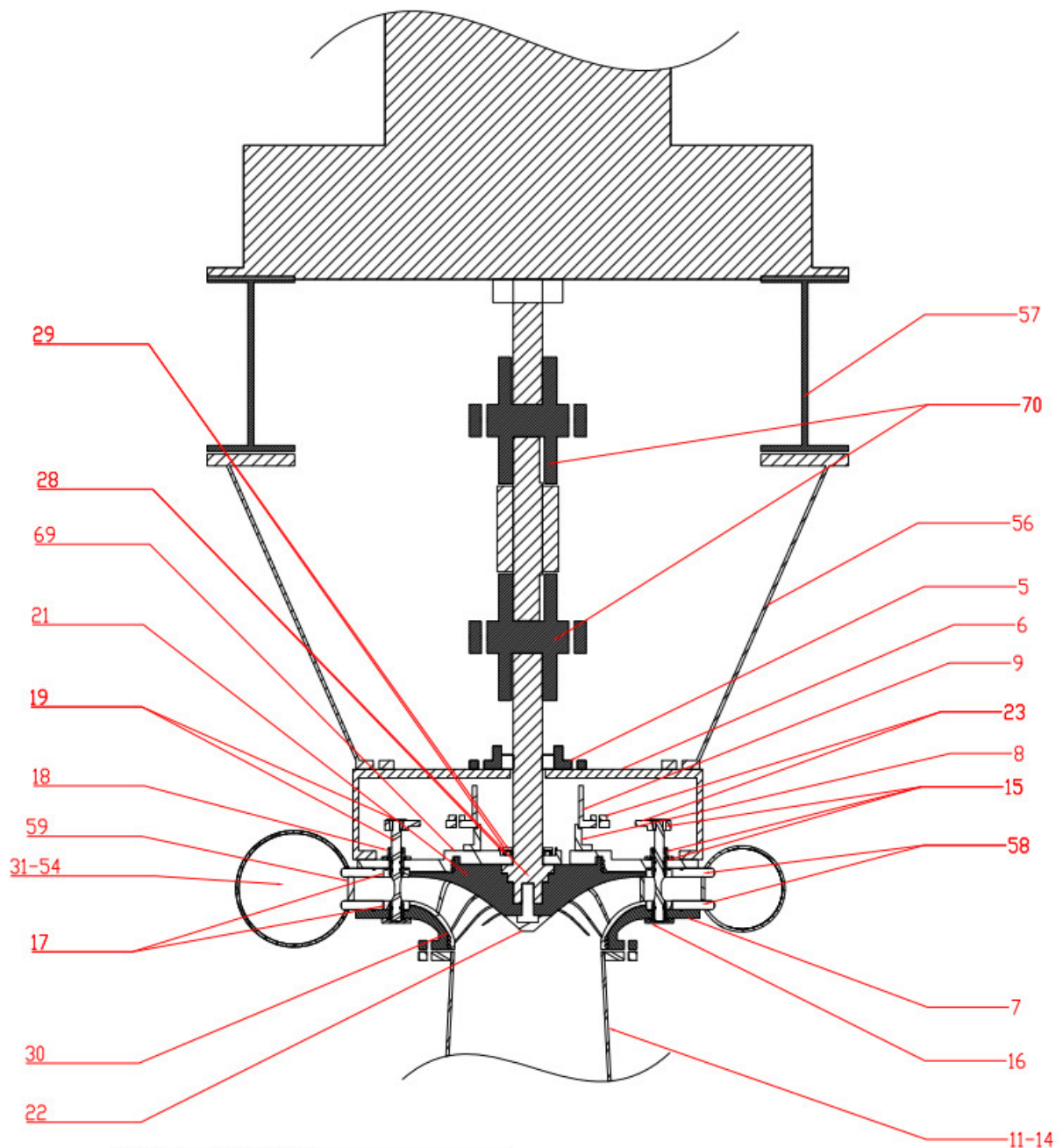
3.2. Components

The 3D-drawings of the Francis turbine test rig at the Turbine Testing Laboratory at Kathmandu University are made by the use of the computer-aided design software PTC CREO Parametric. The design premises presented in the subchapters that follow serve to explain the function and background for the features that are shown in the 3D-drawings in chapter 4.

The design is based on:

- Requirements and recommendations as stated in *IEC60193* (1), other relevant standards or best practice.
- The Francis turbine test rig at the Waterpower Laboratory at NTNU.
- Previous work by Rasmussen (7), Selmurzaev (8) and Seierstad (6).
- Work by academic staff at the Turbine Testing Laboratory (24).

Adaptation of the design to the existing pipe system at the Turbine Testing Laboratory is attempted. Without compromising the quality of the test rig, the parts from the simplified Francis test rig at TTL are reused to the extent possible. An overview of the components in the simplified 92 kW Francis test rig is shown in Figure 3-12.



S.NO.	COMPONENTS
5	BEARING HUB
6	BEARING SUPPORT
7	BOTTOM COVER
8	CONTROL RING SUPPORT
9	CONTROL RING
11-14	DRAFT TUBE AND SECTIONS
15	TAPER BUSH, PLAIN BEARING, FLANGE BUSH
16	FLANGE BUSH COVER
17	GUIDE RING
18	GUIDE VANE COVER
19	GUIDEVANE AND TAPER BUSH COVER
21	HUB

S.NO.	COMPONENTS
22	HUB CAP
23	LINKS FOR GUIDE VANE OPERATION
28	SHAFT SEAL METAL STRIP-BA & SHAFT
29	SHAFT SEAL COVER AND SHAFT SEAL- BA
30	SHROUD
31-54	SPIRAL CASING SECTION (SURFACE DEVELOPMENTS)
56	SPIRAL CASING SUPPORT SURFACE DEVELOPEMENT
57	SPIRAL CASING SUPPORT
58	STAY RING
59	STAY VANE
69	TOP COVER
70	TRANSDUCER COUPLING

Figure 3-12: TTL 92kW Simplified Francis Test Rig; Components (5)

A description of the main components and their functions can be found in Chapter 7.4 of *Mechanical Equipment* (25). The existing parts from the simplified test rig at TTL that are implemented into the design of the new Francis turbine test rig include:

- Guide ring and guide vanes with covers. Further discussed in subchapter 3.2.1.
- Hub, runner blades and shroud. (Hub cap is not included in the 3D-illustrations.)
- Spiral casing sections, stay vanes and stay ring.
- Bottom cover.

The state of the parts must be assessed in place; corrosion, bruising, buckling and other damages to the material will alter the premise for reuse. Where redesign of parts is necessary, connection to existing parts is taken into consideration.

Main components between Francis turbines and the generator were introduced in Figure 2-1, a general overview that may be useful when viewing Figure 3-12 and the next figure. A cross-sectional view of the components surrounding the VKL Francis turbine, including the bearing block from Figure 3-6, is shown in Figure 3-13.

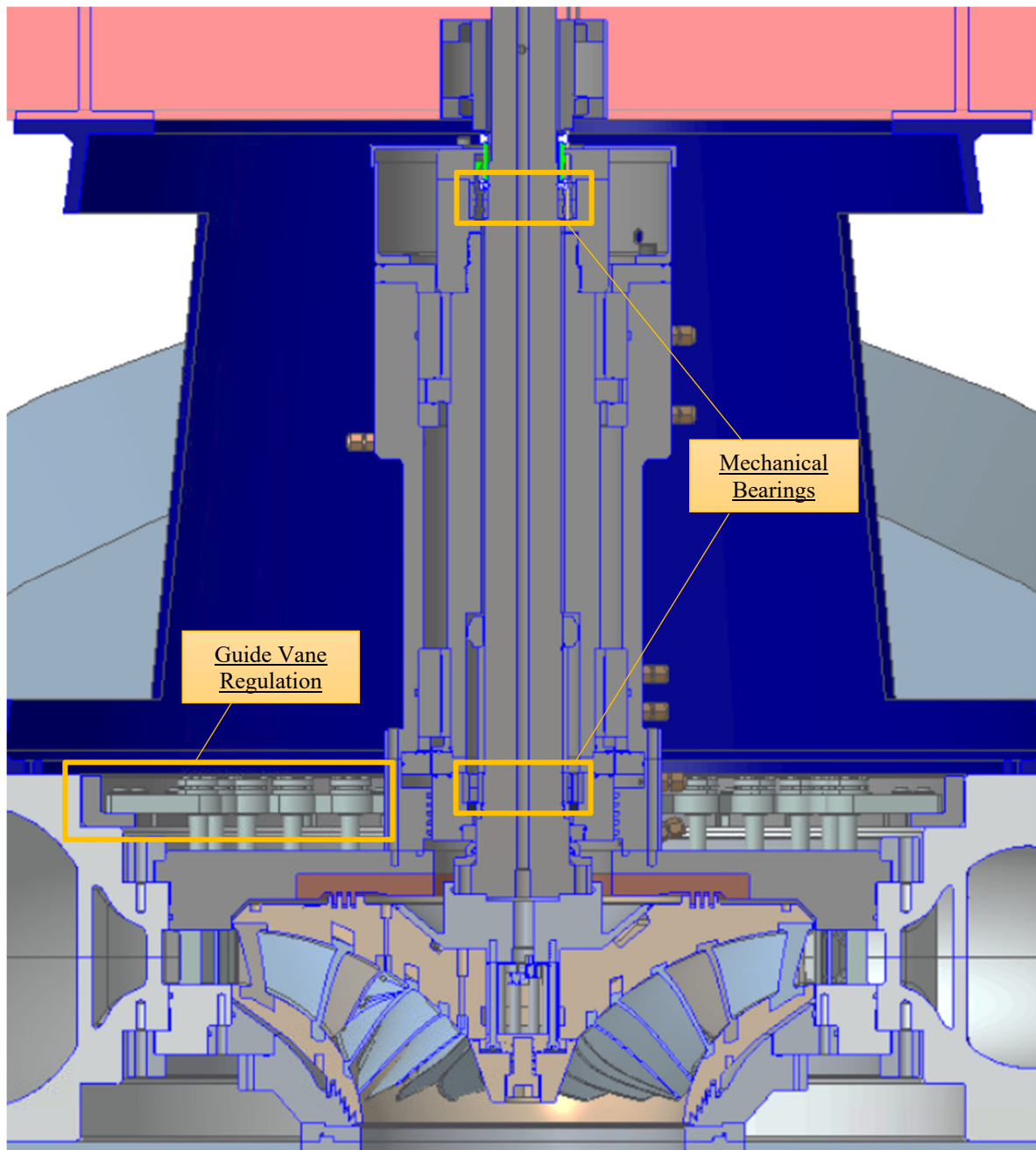


Figure 3-13: VKL Francis Test Rig; Cross-sectional View

Even if the complexity of the VKL bearing block including a system for hydraulic bearings is apparent, the setup shown in Figure 3-13 is taken into consideration when designing the TTL bearing block and surrounding parts. The background for selection of bearings are discussed in subchapter 3.2.3 and the design for TTL is presented in subchapter 4.2.3.

Background for the 3D-drawings of the main components in the TTL Francis test rig is presented in subchapters under 3.2, starting with the guide vane regulation and head covers.

3.2.1. Guide Vane Regulating Mechanism and Head Covers

By adjusting the guide vane angle, the flow and its rotation can be regulated to direct the flow onto the runner blades at optimum angles of attack. The system for adjusting the guide vanes at the VKL Francis test rig makes use of a regulating ring mounted on the spiral casing side of the guide vanes, as seen in Figure 3-14. A linear actuator pushes the regulating ring to revolve, with that also rotating the guide vanes through the lever arm that connects them.

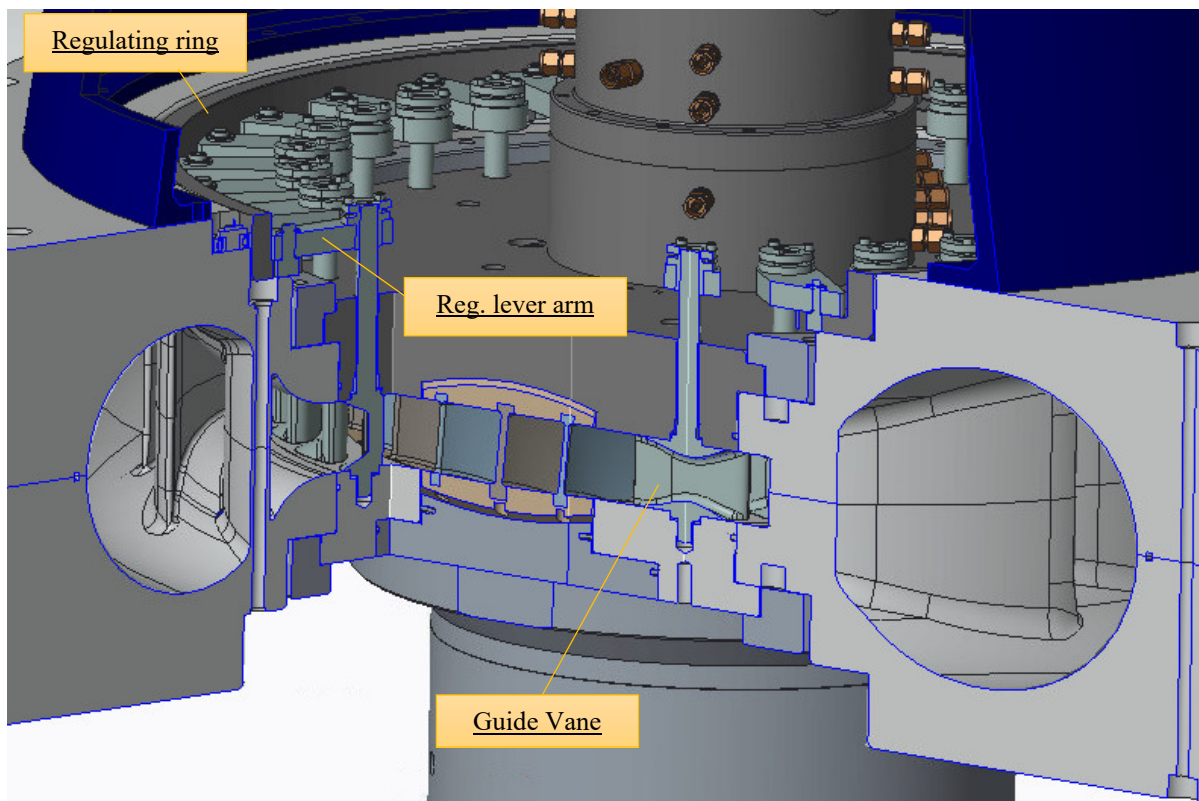


Figure 3-14: VKL Francis Test Rig Guide Vane Control; 3D Cross-section

The corresponding system that was used at the TTL simplified Francis rig supposes a regulating ring mounted on the inner diameter of the guide vanes. As seen in Figure 3-12, it is a solution that leaves little space for a bearing block. The control mechanism is redesigned with the setup installed at VKL as a basis. The existing guide vanes from the simplified Francis test rig is implemented into the design of the new Francis turbine test rig.

The top cover must allow space for a functional bearing block solution. In addition, damage to the hub side of the upper labyrinth seal must be avoided in the case of parts colliding due to e.g. misalignment. The existing top cover does not satisfy these requirements. Consequently, the

top cover is redesigned. Reuse of connecting parts is desirable, hence some features from the existing top cover in Figure 3-15 are brought along to the new design.

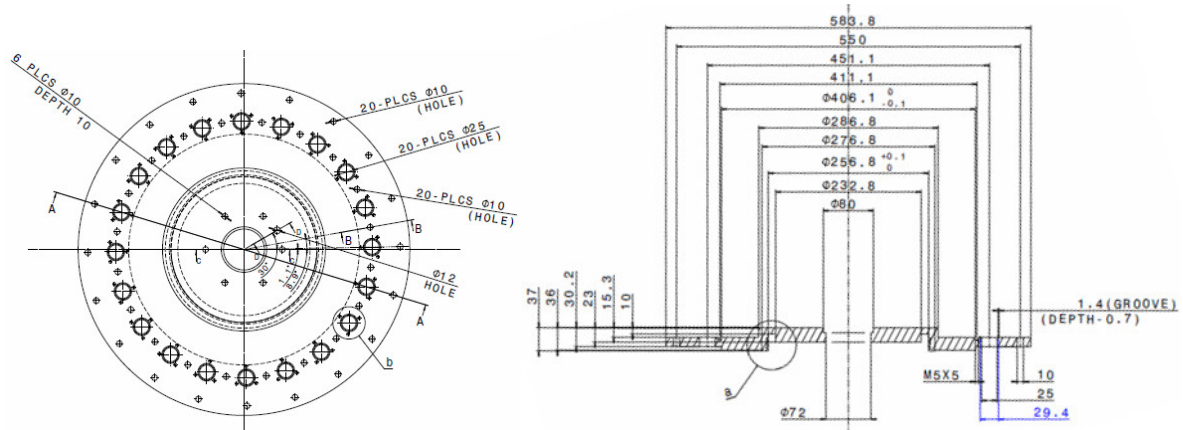


Figure 3-15: TTL Existing Top Cover; 2D Drawing (5)

The 20 holes through which the guide vanes will be mounted have the same placement and diameter on the new top cover as the existing one. The existing bottom cover shown in Figure 3-16 is implemented into the design of the new Francis turbine test rig.

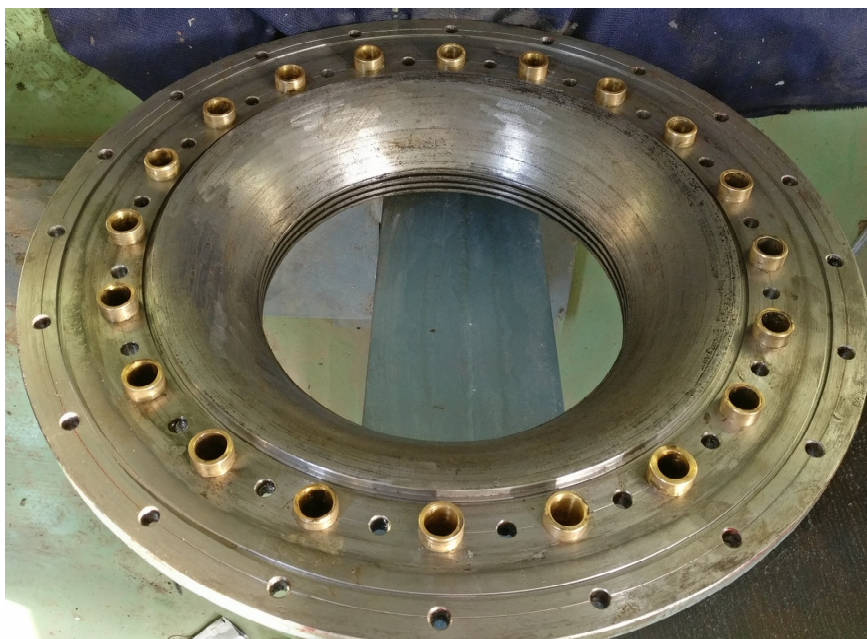


Figure 3-16: TTL Existing Bottom Cover

3.2.2. Runner, Spiral Casing and Stay Vanes

The 92 kW turbine used in the simplified test rig at TTL is refurbished and will be the first to be tested at the new Francis turbine test rig. It is a model of a turbine installed at Jhimrukh hydropower plant, Nepal. Figure 3-17 shows the turbine with 17 runner blades (RB), 20 spiral casing sections (SC), 20 stay vanes (SV) and 20 guide vanes (GV).

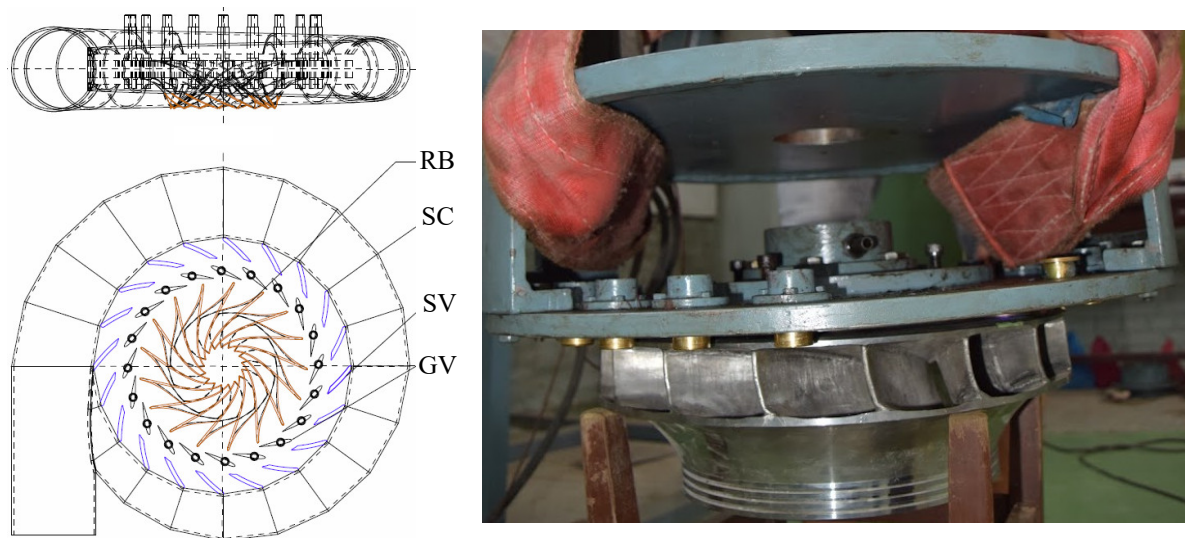


Figure 3-17: a) TTL Spiral Casing and Runner (5) b) TTL Turbine

3D-drawings of the runner, spiral casing and stay vanes exist and are implemented into the model without modification. They are presented in chapter 4.2.2 and also partake in other drawings in subchapters under 4.

3.2.3. Bearing-Shaft-Housing System

The component setup in and around the bearing block at the TTL Francis rig is redesigned to facilitate the measurement and calibration of friction torque and axial load.

3.2.3.1. Bearing Arrangement

For designing the bearing arrangement, the functions of bearings are investigated. These are reducing friction, carrying loads and guiding moving parts. Load can be applied to bearings in either of two basic directions:

- **Radial loads**, F_r , act in right angles to the shaft.
- **Axial loads**, F_z in Figure 3-18, act parallel to the axis of rotation.

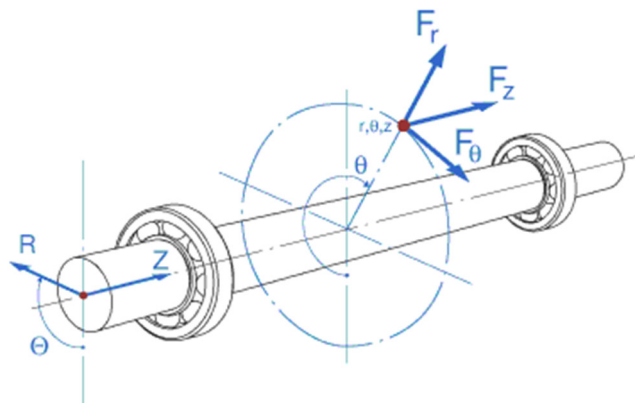


Figure 3-18: Cylindrical Coordinate System (26)

The offset of these loads from either the bearing axis or radial plane axis creates a resulting moment load.

For handling the loads present at the TTL Francis turbine test rig, a cost-effective solution with low maintenance-requirements is sought-after. Bearings consisting components that are in mechanical contact are considered, among which the most commonly used in turbomachinery are (27):

- **Ball bearings** contain balls rolling between outer and inner surface tracks, and can handle both axial and radial loads.
- **Roller bearings** contain cylindrical or spherical elements rolling between two circular surfaces. They have an elongated contact area compared to ball bearings, meaning they

can take higher radial loads albeit creating a larger frictional force. The axial load handling capability is limited.

Both ball and roller bearings have a simple basic design, but with a wide variety of types and materials suited for different applications.

High-precision bearings are to be installed at TTL, and further selection factors (26) to take into consideration are:

- **Available space:** The shaft at the TTL Francis rig is redesigned to facilitate the measurement and calibration of friction torque and axial load. The limitations are to fit the connecting parts in the assembly while facilitating room for the guide vane links and control ring.
- **Load:** The direction and magnitude of loads for which the bearings are designed to carry. Both radial loads and axial loads in both directions need to be handled. According to O.G. Dahlhaug (personal communication, March 2017), the maximum axial load for the design is 20 kN, while the maximum radial load is 1 000 N.
- **Misalignment:** The shaft and connecting parts are designed for proper alignment in and after mounting. The required distance between the bearings is at least five times the diameter to help guide the shaft and minimise misalignment.
- **Axial displacement:** The shaft is to be supported by a locating bearing and a non-locating bearing. The locating bearing keeps the shaft in position and does not allow the shaft to move axially relative to the bearing. The non-locating bearing supports the shaft and allows axial movement of the shaft to avoid stress on the bearings.
- **Noise level:** No particular requirements.
- **Speed:** The maximum rotational speed of the TTL shaft is 1 500 rpm.
- **Stiffness:** The elastic deformation under load is small and can be ignored.

The expected loads the bearings at the TTL Francis rig will be carrying are in the same order of magnitude as the loads carried by the VKL Francis rig bearings, and the design prerequisites are similar. The bearings installed at VKL have yielded good experience:

1. Sealed angular contact ball bearings, single row, installed in pair, designation *NSK 7015CTYDBMP5*.

2. Sealed cylindrical roller bearings, double row, designation *NSK NN3017TKRCC1P5*.

Similar bearings are suitable for the TTL Francis test rig. Single row angular contact ball bearings, Figure 3-19, are designed to accommodate radial and axial loads in one direction. The raceways of the inner and outer rings are displaced relative to each other in the direction of the bearing axis, allowing for load transmission from contact points between the raceways and the balls. Mounting a matched pair of single row angular contact ball bearings back-to-back as shown in Figure 3-20 can support combined radial loads and axial loads in both directions, and a larger contact angle means a higher axial load can be supported. The **load lines** diverge towards the bearing axis. It is a relatively stiff arrangement that also can provide accurate positioning of the shaft.



Figure 3-19: Sealed Single Row Angular Contact Ball Bearings (28)

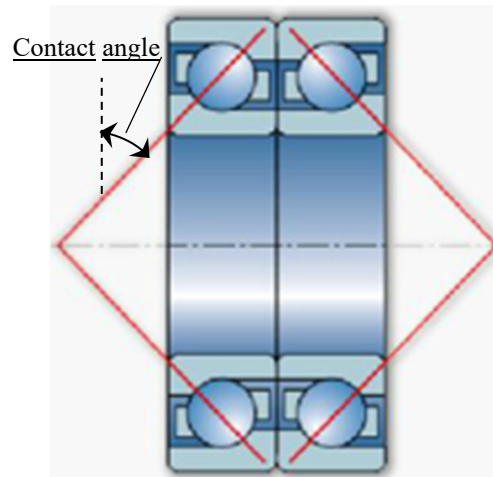


Figure 3-20: Back-to-Back Arrangement of Angular Contact Ball Bearings (29)

Ball bearings make a point contact with the inner and outer rings, while the cylindrical roller elements of a cylindrical roller bearing make a line contact with the rings. This gives cylindrical roller bearings a high radial load capacity, since radial loads act perpendicularly to the axis of rotation as illustrated in Figure 3-21. The number of roller rows in the bearings can vary, in Figure 3-22 is shown a single row variant.

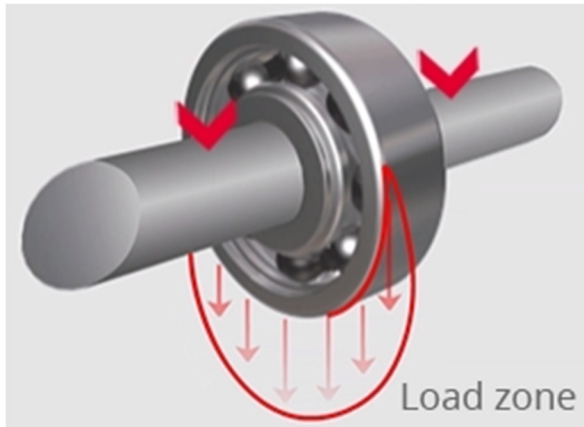


Figure 3-21: Radial Load (30)

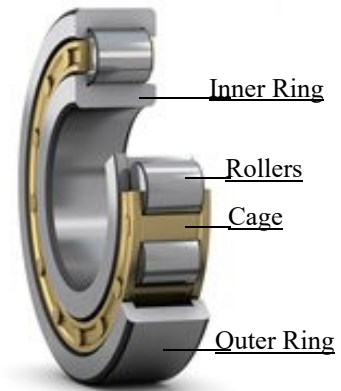


Figure 3-22: Cylindrical Roller Bearings, Single Row (31)

Contamination can lead to many different problems in bearings such as scratches or denting of the balls and raceways. Moisture or water cause oxidation and corrosion of the raceways and rolling elements, and it may also compromise the bearing lubrication by degradation of the lubricant. All of these will likely lead to premature bearing failure and necessitates sealing of the opening between the rotating shaft and the stationary housing.

3.2.3.2. Seals

All seals are designed according to selection criteria in SKF's *Shaft Seal Catalogue* (32), assuming negligible pressure differences across the seals. The operating temperature for the materials used in the seals requires a maximum permissible speed over 1500rpm for the selected seal ((32) Diagram 1, p. 22).

Even though the bearings that are installed on the TTL Francis rig are sealed, additional seals is an easily installed and non-costly insurance in case of leakages. Two radial shaft seals of the type shown in figure 3-23 are installed for this purpose.

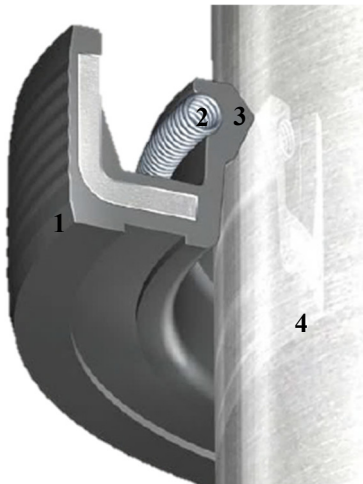


Figure 3-23: Radial Shaft Seal (32)

The rubber outside diameter [1] seals statically against the housing bore.

A stainless-steel garter spring [2] with a defined radial load presses the sealing lip edge [3] against the counterface surface of the shaft [4], sealing dynamically and statically against the shaft.

The seals and bearings are mounted between the shaft and the housing, parts that are to be discussed in the following subchapter.

3.2.3.3. Shaft and Housing

The shaft from the simplified test rig at TTL does not fit the requirements that will be described in this subchapter. The lower section of the existing shaft with key slot, left on Figure 3-15, is used as basis for the connection to the existing runner hub for the new shaft to be designed.

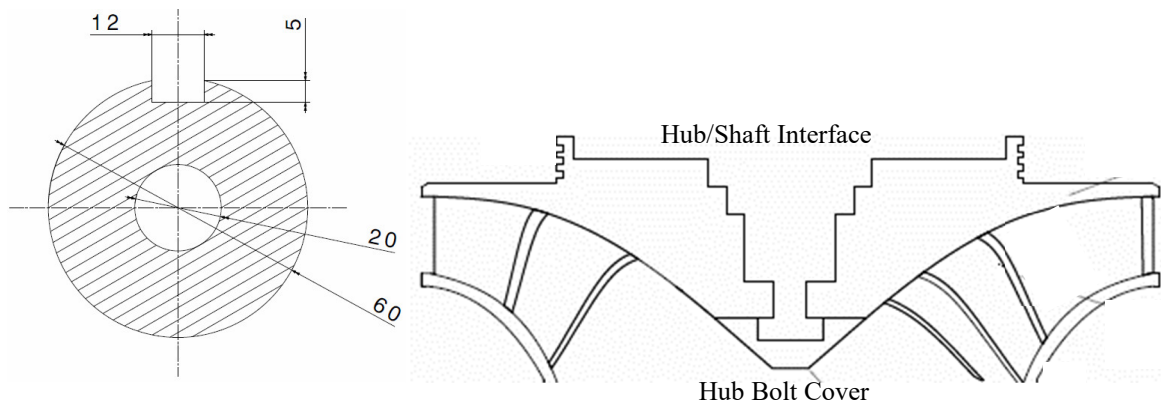


Figure 3-24: a) TTL Existing Shaft Key Slot, b) TTL Existing Hub/Shaft Interface (5)

Some of the requirements that influence the features that are found along the length of the shaft, are:

- The shaft must facilitate the measurement of both axial load and torque by strain gauges as suggested in subchapters 3.1.7, 3.1.8 and 09. Because the measurements are to take place where the maximum occurrence of tension/compression/torsion load is found, a region of lower cross-sectional area is integrated into the design.
- Due to the load carried and friction losses that occur in the bearings and seals, the measurements must take place between the runner and the lowest mounted seal in contact with the shaft. The seal is positioned as close to the strain gauges as possible without disturbing the measurement; this is where the shaft cross-sectional area increases. The shaft and housing seat tolerances are defined by the seal requirements.

- The interface with the lower bearing is above the radial shaft seals. Roller bearings, for uptake of radial forces, are to be placed as close to the runner as possible. The shaft and housing seat tolerances are defined by the bearings product data.
- Adequate distance between the bearings is critical for carrying loads as well as centring and alignment of the moving parts. The shaft and housing seats are designed to accommodate five diameters distance between the bearings. For lower cost of machining, the requirements for precision and surface roughness are lower in the region between the bearings.
- The upper bearings are to be located on the shaft by the use of a lock nut and washer. Threads on the shaft are required for screwing the lock nut into place, and a keyway in the shaft is needed to engage the washer that secures the lock nut.
- The connection between the calibration jig and the shaft is designed to for application of axial force in both directions as well as torque.
- Ease of installation and interface with surrounding parts are taken into consideration in the shaft and housing design. The same goes for maintenance and simplicity of extracting and replacing damaged parts in the bearing block.
- By designing a separate stub shaft for strain gauges to perform the measurements on, redesign iterations are rendered possible for finding the optimal solution. After evaluation of test results, other designs can be assessed without remanufacturing of the entire shaft.
- The avoidance and monitoring of water in unwanted areas are taken care of by O-rings, labyrinth seals and inspection holes where leakages may occur.

The suggested design for shaft and housing-arrangement in the Francis turbine test rig at TTL is presented in chapter 4.2.3.

3.2.4. High- and Low-Pressure Tank

Detail drawings for the pressure tanks at TTL were completed by TTL staff in April 2016, as shown for the low-pressure tank in Figure 3-25.

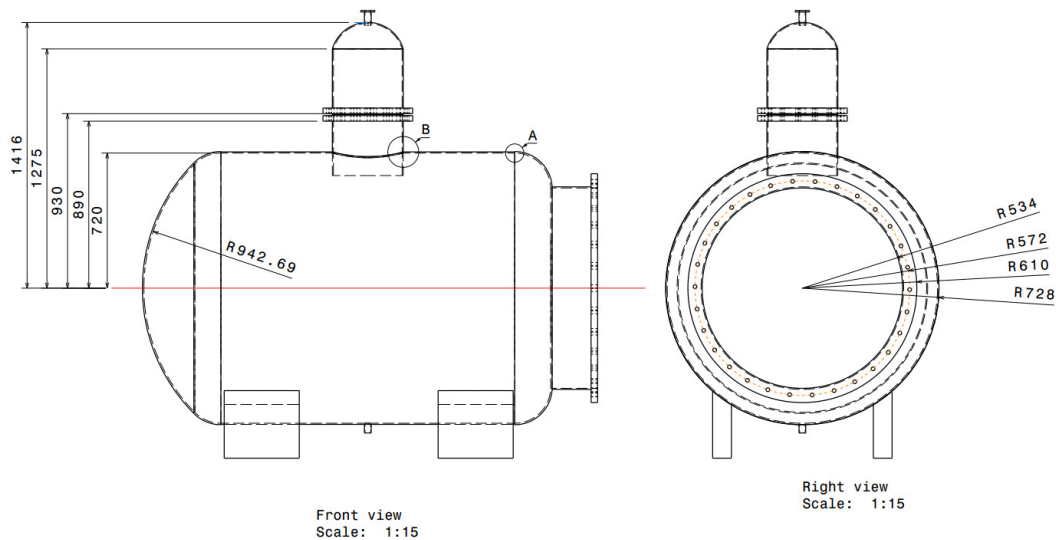


Figure 3-25: TTL Existing Detail Drawing for the Low-Pressure Tank (33)

3D-models existed as built in the CAD-program *CATIA*. When importing these files to CREO, much information was lost. Adding further details to parts in affiliation with the tanks proved difficult. For these reasons, dimensions from the detail-drawings along with measured values from the *CATIA*-models are used to redraw the tanks in CREO.

The pressure tanks at VKL have affiliated water level and pressure measurement, as shown for the high-pressure tank in Figure 3-26.



Figure 3-26: VKL High-Pressure Tank

Components attached to the pressure tanks at VKL are considered for the pressure tanks at TTL, and necessary details added to the CREO model and piping and instrumentation diagrams. The resulting 3D-models of the high- and low-pressure tanks are found in chapter 4.2.4.

4. Results and Discussion

4.1. Instrumentation at TTL

The instrumentation of the Francis turbine test rig at TTL is based mainly on the requirements of *IEC60193* (1), and the experiences from the corresponding test rig at the Waterpower Laboratory, NTNU. In the following subchapters, the suggested design and methods for measuring all variables involved in efficiency calculation are presented. The function of and background for the chosen methods for each of the measurements, and calibration thereof are found in the appurtenant subchapters under chapter 3.1.

4.1.1. Piping and Instrumentation Diagram

The piping and instrumentation diagram (P&ID) in Figure 4-1 shows the principal design of the system for the efficiency measurement of Francis turbines in the Turbine Testing Laboratory at Kathmandu University. A larger version of the diagram, providing better detail, can be found in Appendix A.

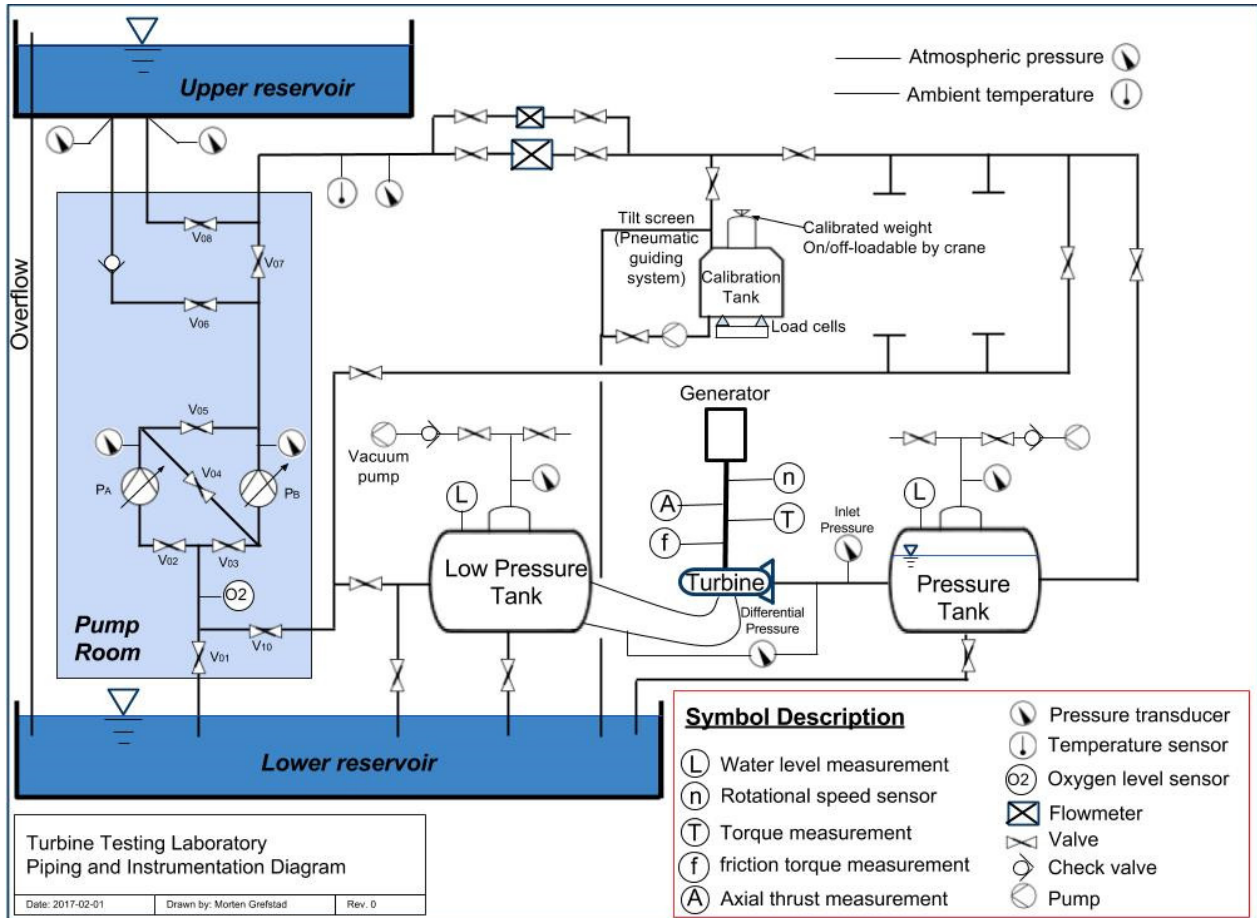
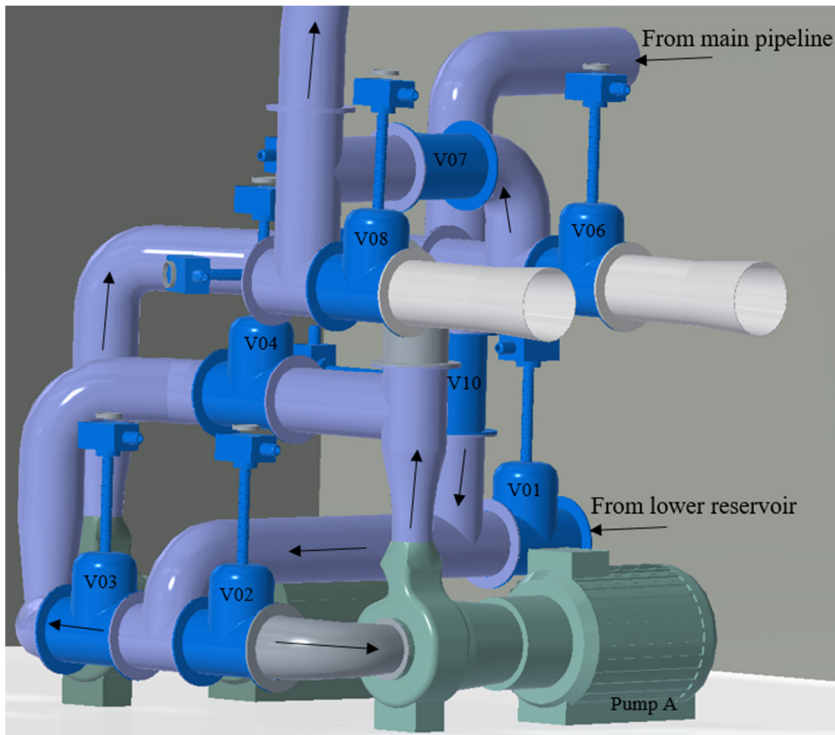


Figure 4-1: TTL Piping & Instrumentation Diagram

The diagram³ serves as a summary and reference for the measurement principles presented in the following subchapters and should be regarded as the main output for the system for efficiency measurement.

³ Power outages are quite common in the Nepalese electrical grid due to load shedding. The check valve on the pipe going up to the upper reservoir serves the purpose of preventing water from flowing in “the wrong direction” (to the pumps from the upper reservoir) in the case of a loss of power.



Different configurations are made possible by opening and closing various valves.

Figure 4-2 is a reference for the piping and instrumentation diagrams, illustrating the numbered valves and pipe setup in the pump room. The arrows show the direction of flow; this can however vary depending on the state of the different valves.

The pumps, with adjustable rotational speed, can be run in single, series or parallel mode.

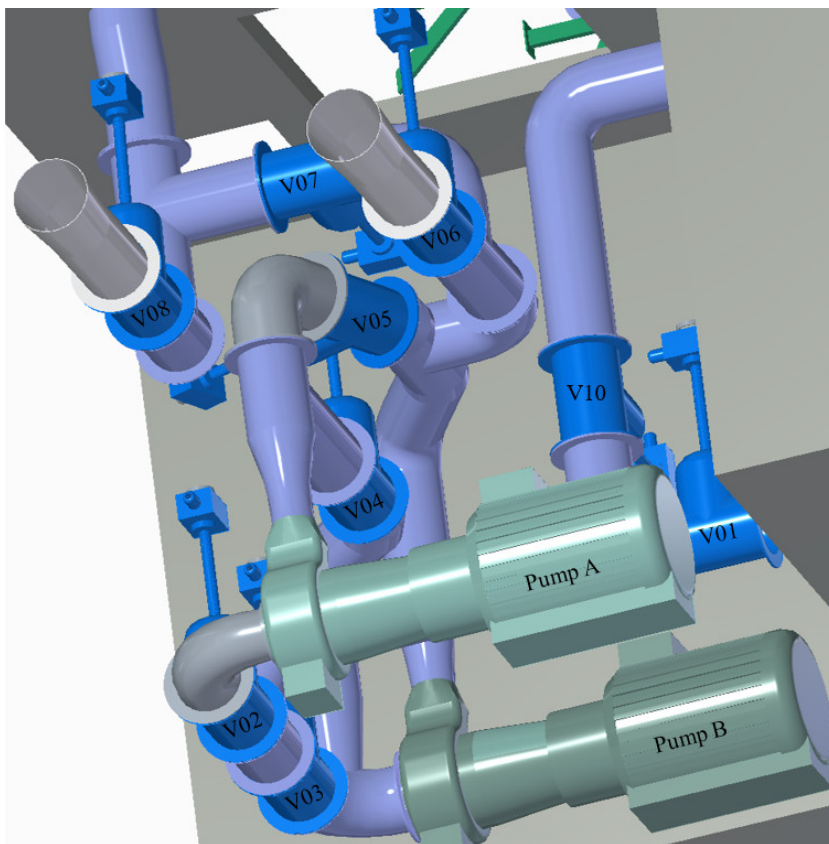


Figure 4-2: TTL Pump Room; 3D Illustration

Figure 4-3 shows one of the possible running setups, a closed loop configuration with pump B running in single mode. The flow follows the pipe loop shown in colour green, which denotes that V_{03} , V_{07} , V_{10} in the pump room are open. The valves sitting on the lines of black colour are in a closed state.

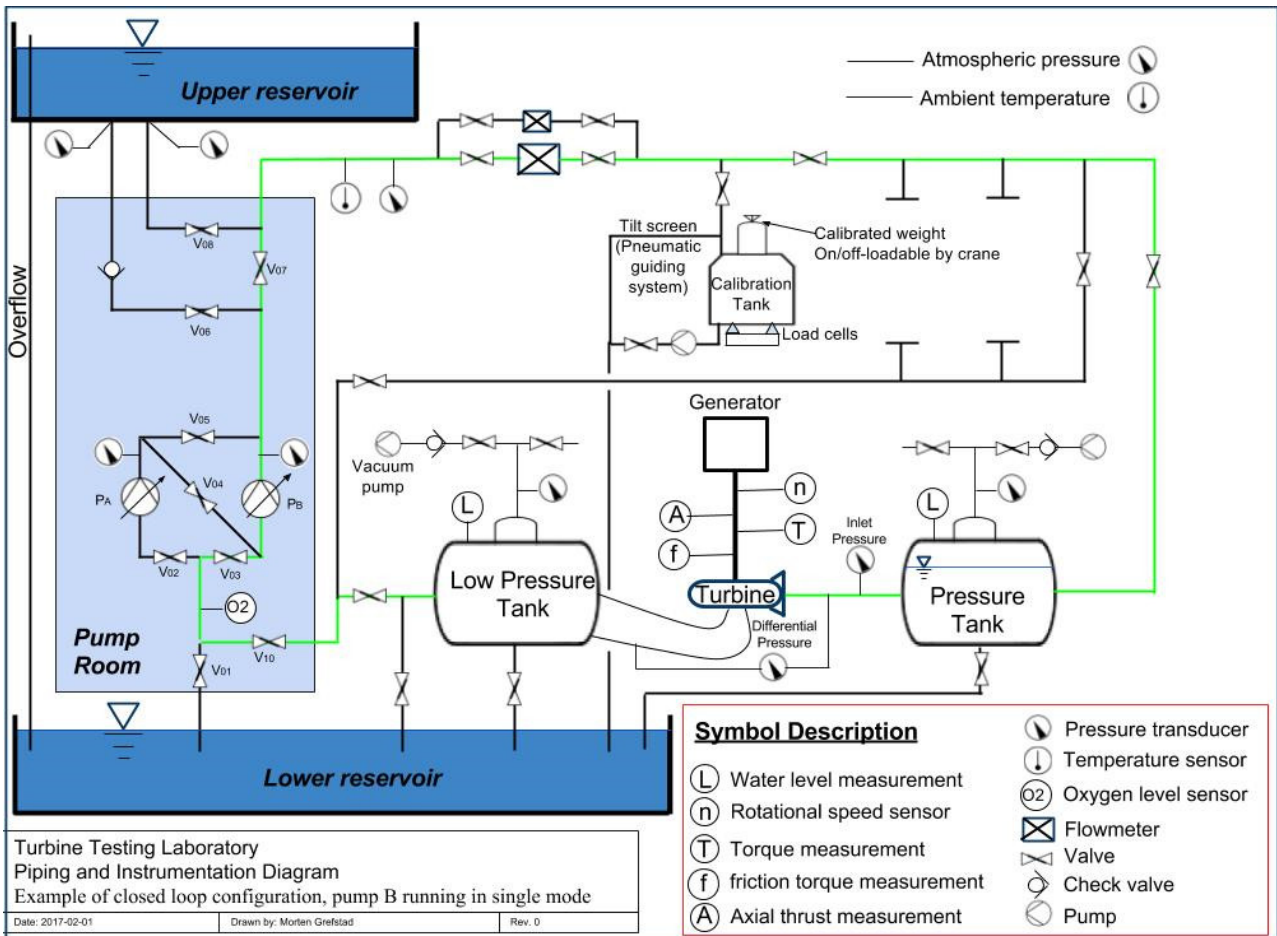


Figure 4-3: TTL P&ID Closed Loop Configuration, Pump B Running in Single Mode

Figure 4-4 shows an example of open loop configuration with the pumps running in series. The direction of flow and valves in open state as indicated by red line colour.

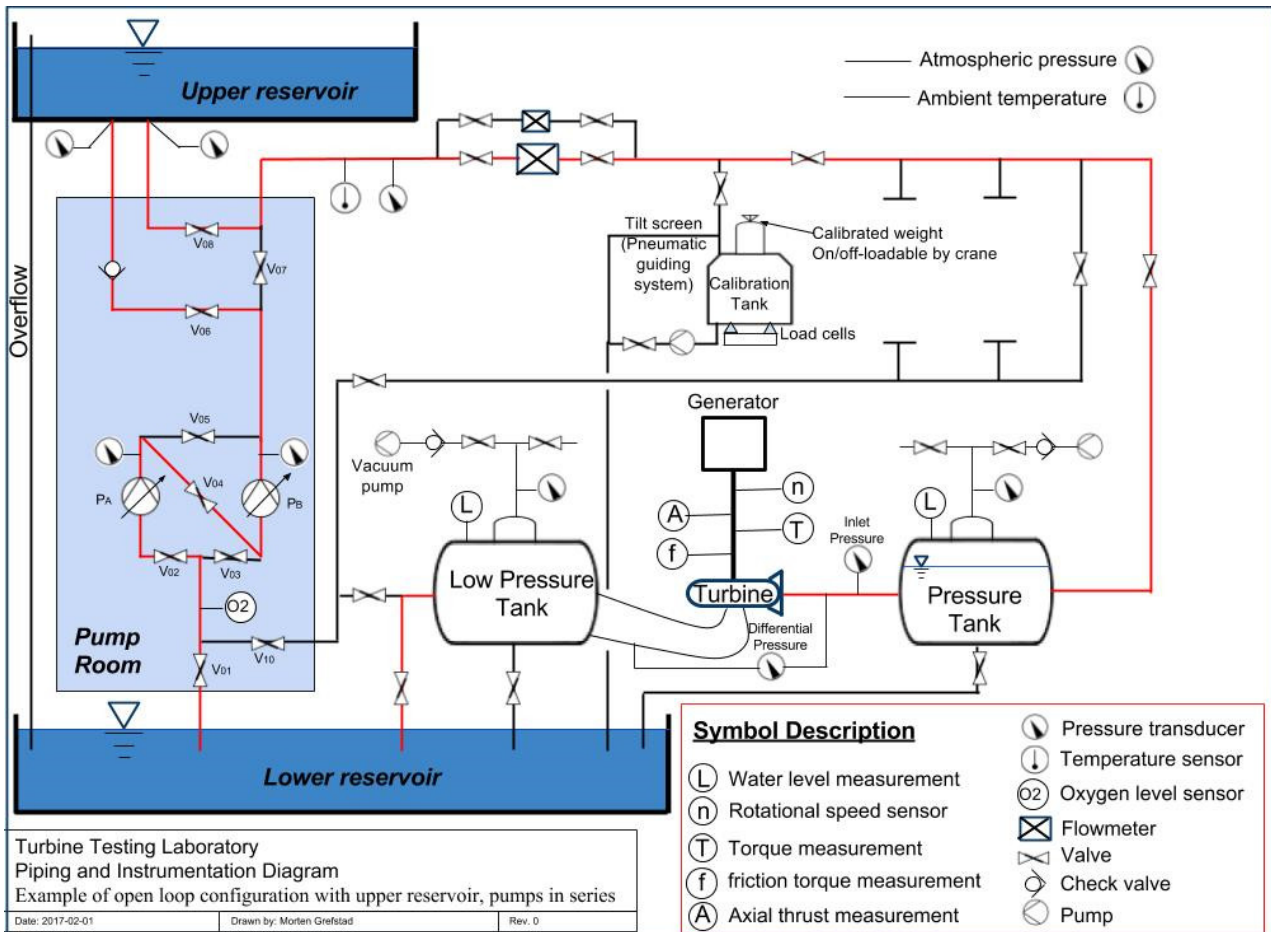


Figure 4-4: TTL P&ID Open loop Configuration with both Reservoirs, Pumps in Series

The T-junctions lead to other rigs and laboratory equipment that are not shown in the diagrams.

4.1.2. Oxygen Level

An externally calibrated oxygen probe installed near the main pump inlet measures the dissolved oxygen, *D.O.* or O_2 , at the TTL Francis turbine test rig.

4.1.3. Water Temperature

An externally calibrated temperature probe installed just downstream of the pump room measures the water temperature θ at the TTL Francis turbine test rig.

4.1.4. Rotational Speed

The rotational speed n is measured magnetically by an AMR sensor and a magnetic ring which is welded to the flange of the torque transducer. See chapter 4.1.8. - Generator Torque.

4.1.5. Pressure

A differential pressure transducer measures the differential pressure Δp across the turbine at the TTL Francis turbine test rig. Pressure taps installed at the turbine inlet pipe and the draft tube are connected to a manifold leading into the differential pressure transducer. When installing the pressure taps in the circular sections, two pairs of opposed pressure taps shall be arranged on two diameters at right angles to each other. To avoid air pockets, the taps should not be located at or near the highest point of the measuring section. Because of the risk of dirt obstructing the taps, they should not be placed at or near the lowest point of the measuring section. An illustration of the arrangement is seen in Figure 4-5:

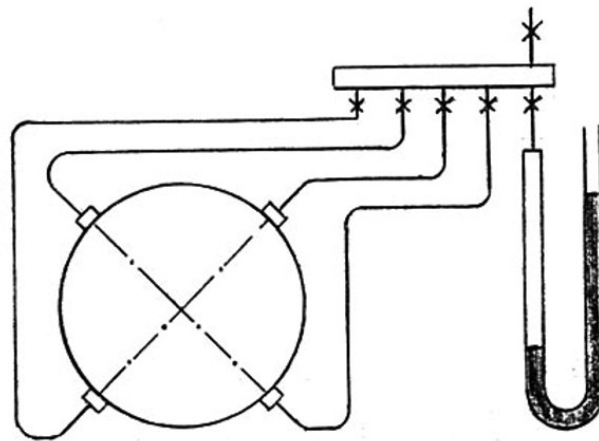


Figure 4-5: Arrangement of Pressure Transducers in Circular Pipes (34)

Avoiding air trapping must be kept in mind when installing the tap piping, and transparent plastic pipes for high pressure is recommended so that air bubbles may be detected. No leaks are permitted in the pressure taps and pipes.

In addition, a differential transducer open to atmosphere on the low-pressure side and connected to the turbine inlet pipe on the high-pressure side measures the turbine inlet pressure p_1 . Calibration of both transducers can be done by following the same procedures as used at VKL. The deadweight manometer utilised in the calibration is very sensitive and should be stored in a well-sealed and preferably pressurised room. A digital barometer measures the ambient/atmospheric pressure p_{amb} in the lab and is installed as low as possible on the wall next to the turbine along with the transducers.

4.1.6. Volume Flow Rate

An electromagnetic flowmeter of DN200 installed just downstream of the pump room measures the volume flow rate Q at the TTL Francis turbine test rig.

The weighing method is suggested for calibrating the flowmeter. The water, preferably from the upper reservoir, is discharged through the flowmeter to be calibrated and to the weighing tank system as indicated by pipes shown in purple in Figure 4-6.

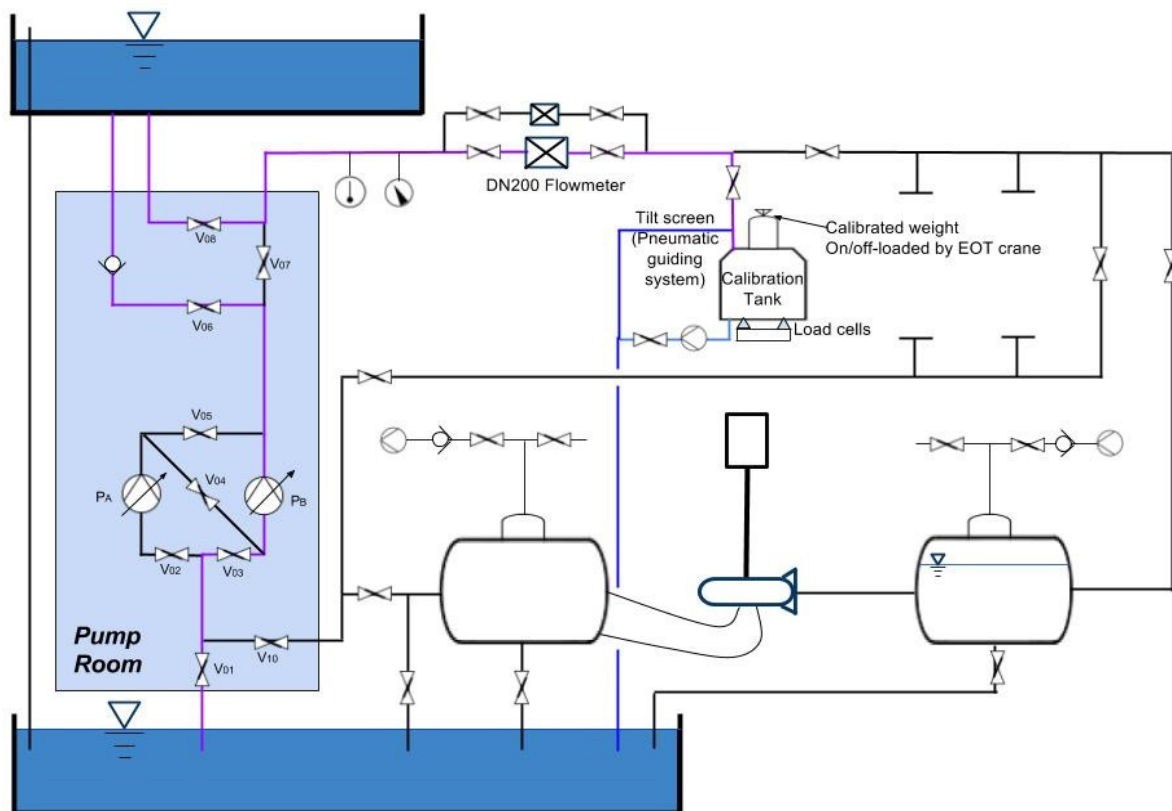


Figure 4-6: TTL Pipe Loop for Weighing Tank Calibration

The pneumatic guiding system, or tilt screen, is first set as to lead the water to the lower reservoir (blue colour). The calibration tank, which rests on load cells, is empty and the valve on the pipe leading from it is closed. For a given time interval of minimum 30 seconds, the tilt screen state is changed such that the water partly fills the tank. By recording the filling time along with the tank weight before and after filling, the flow rate through the flowmeter is found. Filling intervals are repeated until the tank is full, each time allowing the water and tank to stabilise before recording the weight.

Supplementing Figure 4-6, a 3D-representation of the setup with the calibration facility is shown in Figure 4-7. Partitions underneath the floor, load cells and pump under the calibration tank is not shown.

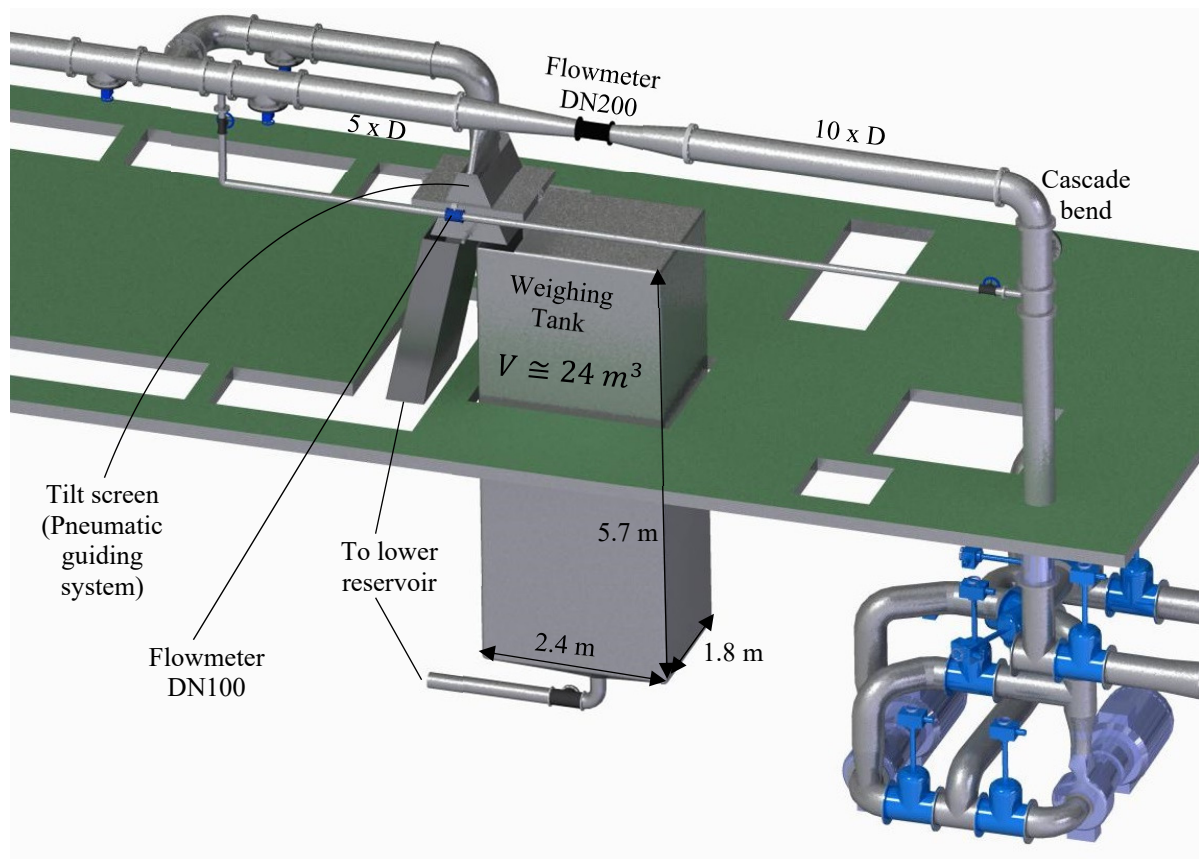


Figure 4-7: TTL Flowmeter Arrangement; 3D View

The flow velocity through the flowmeter is increased by a converging pipe section upstream of the flowmeter. A cascade bend and ten pipe diameters straight run of pipe upstream the flowmeter contribute towards steadying the flow to ensure more precise measurement results.

The calibration equation for the load cells weighing the tank is found by substituting a calibrated weight on top of the tank. Water of approximately the same weight as the calibrated weight is filled into the tank. After stabilisation, the measured value of the amplifier connected to the load cells is recorded. The calibrated weight is loaded onto the tank using the EOT crane, and the weight is again recorded. By repeating this until full tank capacity is reached, a function for the relationship between the measured weight and the true value can be found for the weight range of the calibration tank.

Discussion

At VKL, the flowmeter is mounted just upstream of the turbine. At TTL, the water passes several branches and connected pipes from the flowmeter to the turbine. Leakages in any of the connections would make the measurements erroneous, as loss or gain of water between the flowmeter and the turbine must be avoided. Alternative setups that would allow for mounting the flowmeter closer to the turbine may be assessed, provided that stable flow conditions through the flowmeter are achieved.

The setup for the pipe leading from the main loop to the calibration tank is not ideal. Assessing under which conditions the flowmeter can provide accurate measurements may facilitate a different setup. If a flow straightener can shorten the upstream straight run of pipe requirement, this may allow for a more “direct” route to the calibration tank.

The weighing tank is rectangular with a blend feature to a circular hole in the lowest point, which connects to a pipe with a pump for emptying the tank. An alternative is a flat bottom surface which would yield lower production costs and an improved interface to the load cells. A prerequisite is that the tank can be emptied completely by the use of the pump affiliated the arrangement. Strength analysis of the tank must be done, with special focus on the load from the calibrated weight.

Space for on- and offloading of the calibrated weight is attempted in the design, but the shape and size of the calibrated weight are not yet decided. The calibrated weight must be within the EOT crane capacity of 5 tons, and a certificate for the verified weight of the object with uncertainty must be obtained from a certified instance.

Redesign of the complete weighing facility arrangement is advised when more factors are known. All connected details from the CAD-model must be verified in situ by laser, in particular, the cavity suggested for calibration tank placement. The suggested design aims to fit in a calibration tank with an as high volume as possible, resulting in a suggested tank volume $V \approx 24\text{m}^3$. The tank volume can be decreased if space under/over the tank proves to be inadequate. Rasmussen (7) calculated the minimum tank volume $V_{\min} = 15\text{m}^3$, and suggested $V = 20\text{m}^3$ with a safety factor added.

The arrangement for water transportation from tilt screen to lower reservoir is highly adjustable. The final design must take laboratory space, floor openings, and ease of manufacture into consideration. The support structure for the tilt screen arrangement is not in the 3D-drawings and should be designed when final decisions have been made regarding guiding system, tank height and other affiliated setups.

4.1.7. Axial Force

Strain gauges with four measuring grids offset by 90° relative to each other and connected in full bridge are suited for measuring the axial force A at the TTL Francis test rig with high accuracy (15). The bipartite stub shaft designed for TTL is described in chapter 4.2.3.3. The strain gauges are placed on the inside surface of the stub shaft as shown in the cross-sectional front view in Figure 4-8. The mirrored-image setup of the remaining two strain gauges is found revolved 180° around the shaft centerline.

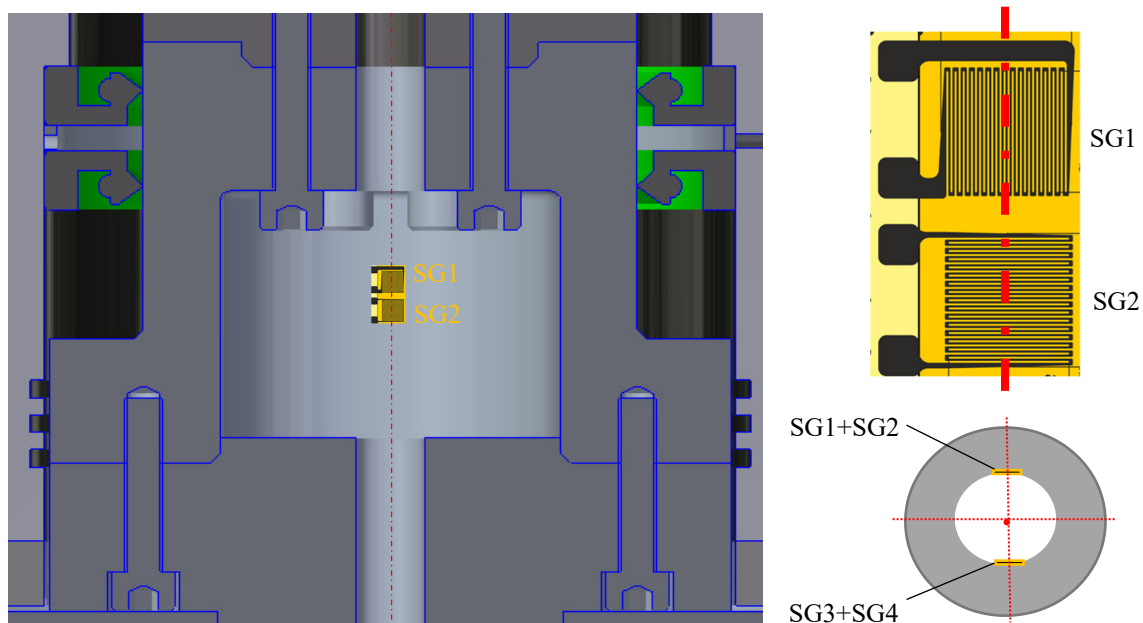


Figure 4-8: TTL Axial Force Measurement by Strain Gauges

Since the shaft is rotating, the measurement data is transmitted wirelessly. A telemetry system and necessary equipment affiliated the strain gauges can be installed in the stub shaft, provided that the cavity is kept dry.

The principle behind the calibration of axial force in both directions was described in subchapter 3.1.7, along with a presentation of a calibration jig and calculation of the necessary weight range for the calibration. The axial force measuring system is described further in the preliminary proposal for calibration procedure that follows.

4.1.7.1. Axial Force Measuring System and Calibration

I. General

The following subchapters present a procedure for calibration of the axial force measuring system at the Francis Turbine Test Rig at the Turbine Testing Laboratory.

Table 4.1: Definitions and Abbreviations for Axial Force Measurement

Symbol	Description	Unit
m	Mass of weights	<i>kg</i>
m.v.	Measured value	<i>V</i>
a	Slope in calibration equation	<i>N/V</i>
b	Intersection constant in calibration equation	<i>N</i>
g	Gravity	<i>m/s²</i>
L_A	Arm from the fixed point D to point A	<i>m</i>
L_B	Arm from the fixed point D to point B	<i>m</i>
L_C	Arm from the fixed point D to point C	<i>m</i>
A_{load}	Downward-acting axial load	<i>N</i>
A_{thrust}	Upward-acting axial load	<i>N</i>
A	Axial force	<i>N</i>

Gravity *g* is 9.79506m/s².

L_A is 0.22m, L_B is 0.06m and L_C is 0.34m.

II. The System

a. Description

The measuring system consists of strain gauges installed on the inside of the top section of a two-part stub shaft. Through an external amplifier, the output signal from the strain gauge system is transformed into a 0-10V signal that varies linearly with the axial force/weights applied, and sent to the data acquisition unit for post-processing.

The axial force for calibration is applied by placing known weights in weight holders that are connected to the stub shaft through a lever arm. *Weight holder DOWN* in Figure 4-10 is used for applying a downward-acting force. By applying weights to the other weight holder, an upward-acting axial thrust is applied to the stub shaft.

b. Equipment used in measuring and calibration

- Strain gauges
- Measuring amplifier
- Telemetry system
- Data acquisition unit
 - National Instruments data acquisition unit
 - LabView for computation and presentation of data
 - External power supply
- Calibrated weights
- Calibration jig

III. Calibration

a. Preparations

1. Unfasten and detach the draft tube, runner and lower part of the two-part stub shaft.
2. Make sure the display for visualisation of the measured volt signal is present on the data acquisition system.
3. Record the volt signal with no axial load. This is the zero point.
4. Connect the equipment necessary to apply axial force:

- a. Reattach the lower part of the stub shaft to the other stub shaft part where the strain gauges are mounted.
 - b. Fasten the connecting arm to the exposed lower part of the two-part stub shaft. Bolts are to be fastened in a cross-pattern.
 - c. Fasten the calibration jig with plate, support and lever arm to the bottom cover. Fasten the weight holders.
 - d. Connect the bottom end of the connecting arm to the lever arm via the double-ended female screw connection. Adjust the screw connection such that the lever system is horizontally levelled. A cross-sectional view of the setup is shown in Figure 4-10.
5. Because of the difference in moment arms on the sides of the fixed point D with the roller bearings, a tension load is applied to the shaft even without weights in the weight holders. Load weights onto *weight holder UP* until the imbalance is evened out and the zero point is retrieved.

b. Calibration of Downward-acting Axial Load

The weights that were added in preparations are left in *weight holder UP*, so the calibration starts with no axial load. Remaining calibrated weights are to be loaded onto *weight holder DOWN* as seen in Figure 4-11.

1. Starting with the setup as prepared, record the volt signal at zero point. This will be the first point in a graph with the volt signal on the x-axis and the axial load on the y-axis.
2. Load on the weights one by one and record the total mass (not counting the weights added in preparations) and corresponding measured volt signal (m.v.) for each weight in *weight holder DOWN*. The volt signal should be stable before the reading is taken. A minimum of 10 points are needed to find a satisfying calibration equation, and the whole measuring range (0-20kN or 0-360kg) has to be covered.
3. Load off the weights one by one and record the volt signals for each weight again.
4. Repeat 1 to 3 to obtain a minimum three sets of data.

c. Calibration of Upward-acting Axial Thrust

Continuing from the weights that were added to *weight holder UP* in the preparations, the remaining calibrated weights are to be loaded onto the same weight holder as seen in Figure 4-12.

1. Record the volt signal at zero point.
2. Load on the weights one by one and record the total mass (not counting the weights added in preparations) and corresponding measured volt signal (m.v.) for each weight in *weight holder UP*. The volt signal should be stable before the reading is taken. A minimum of 10 points are needed to find a satisfying calibration equation and the whole measuring range (0-20kN or 0-600kg) has to be covered.
3. Load off the weights one by one and record the volt signals for each weight again.
4. Repeat 1 to 3 to obtain a minimum of three sets of data.

IV. Computations

The downward-acting axial force A_{load} is defined as negative. The relation between the axial load and the mass added to *weight holder DOWN* for calibration is

$$A_{load} = -\frac{L_C}{L_B} \cdot m \cdot g = -\frac{17}{3} \cdot m \cdot g$$

The upward-acting axial force A_{thrust} is defined as positive. The relation between the axial thrust and the mass added to *weight holder UP* for calibration is

$$A_{thrust} = \frac{L_A}{L_B} \cdot m \cdot g = \frac{11}{3} \cdot m \cdot g$$

The axial force for the calibration is the combination of the two

$$A = A_{load} + A_{thrust}$$

The strain gauge circuit gives an output signal in Volts that varies linearly with the axial force/weights applied. For each load applied, the average voltage values from the data sets should be averaged. The calibration equation is a linear function for A

$$A = a \cdot (m \cdot v.) + b$$

b is the intersection constant for the calibration equation,

a is the slope

$$a = \frac{\Delta A}{\Delta m \cdot v.} \equiv g \cdot \frac{\Delta m}{\Delta m \cdot v.}$$

V. Figures

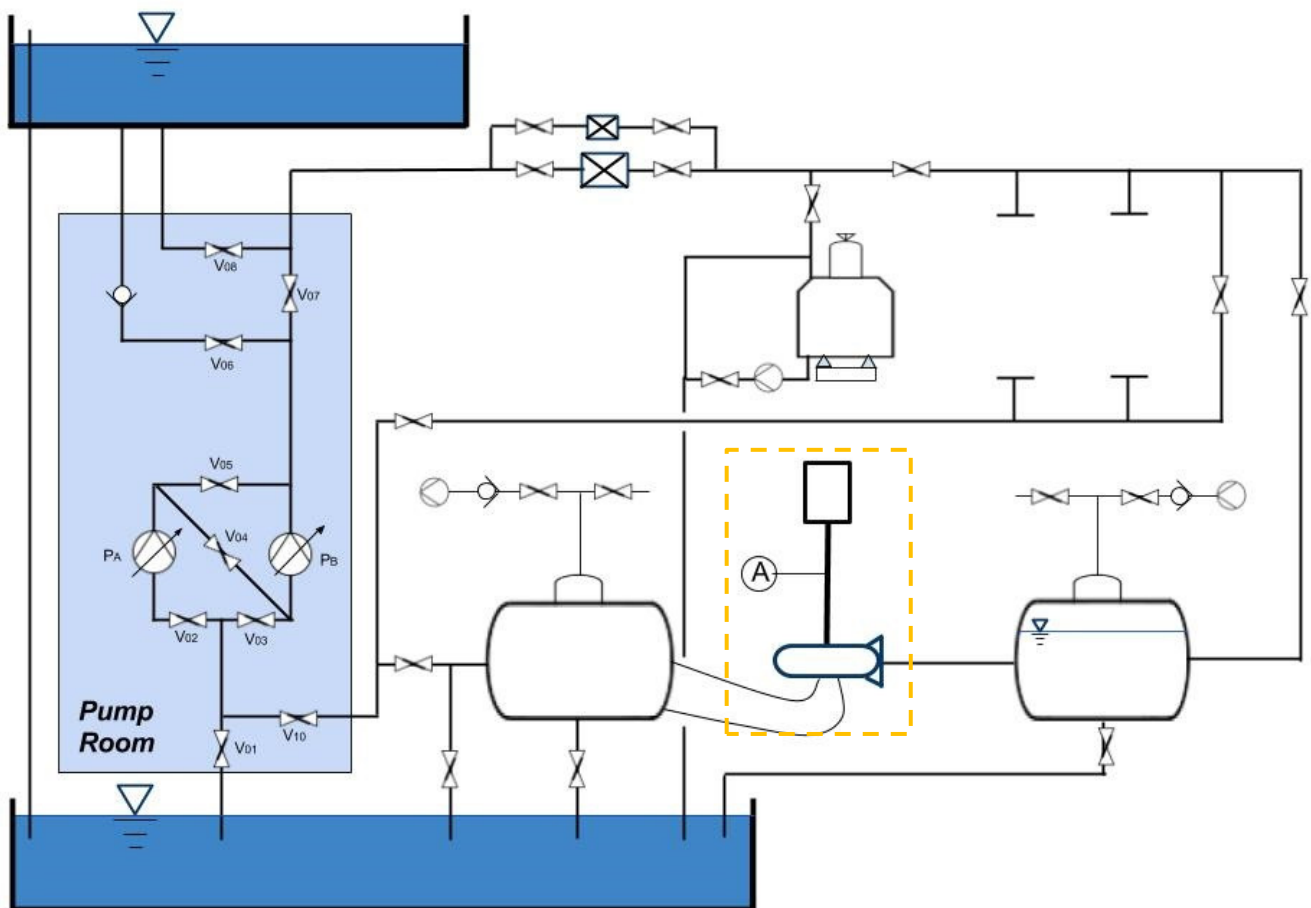


Figure 4-9: TTL Axial Force Measurement; Placement in P&ID

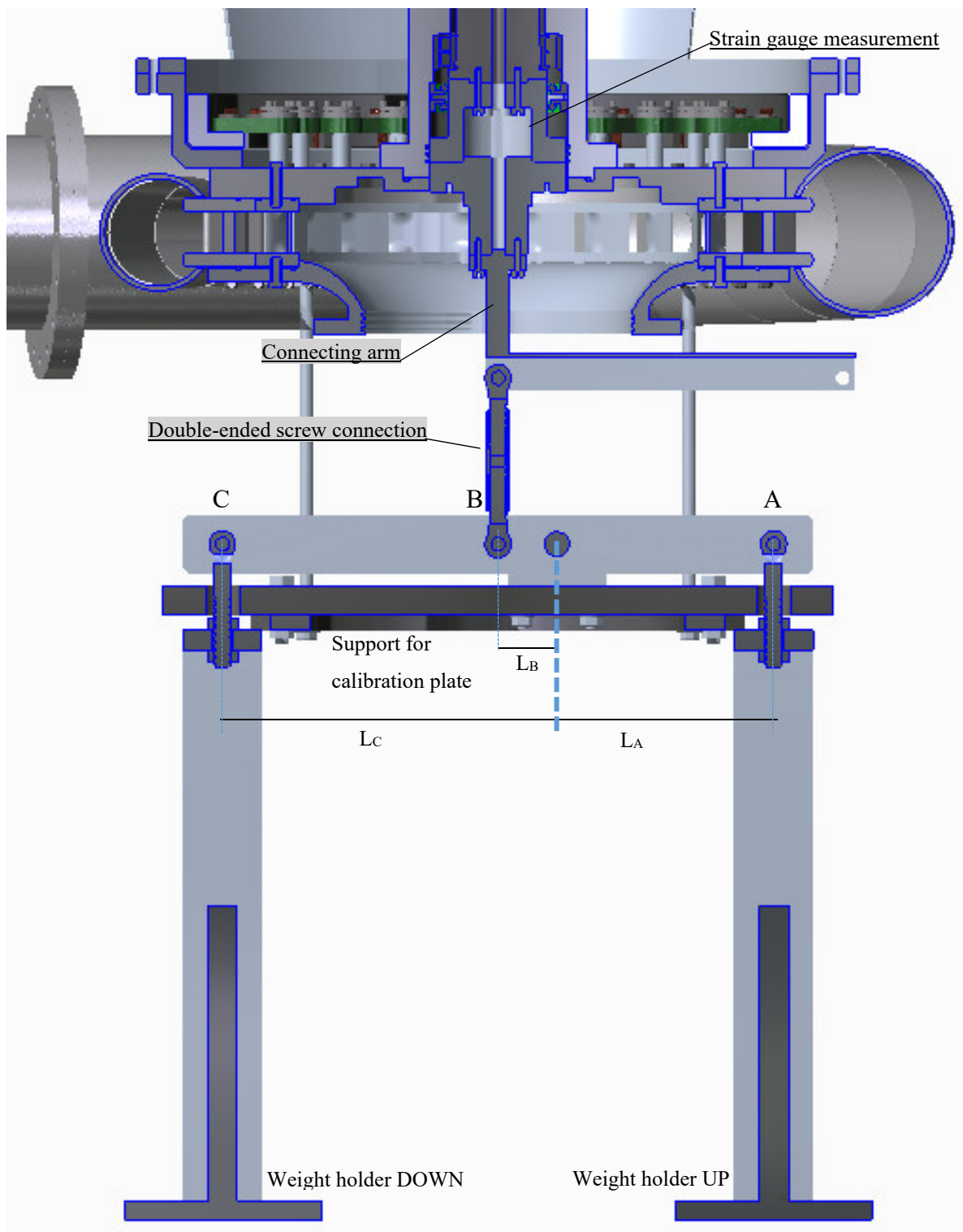


Figure 4-10: TTL Jig for Axial Load Calibration; Cross-sectional View

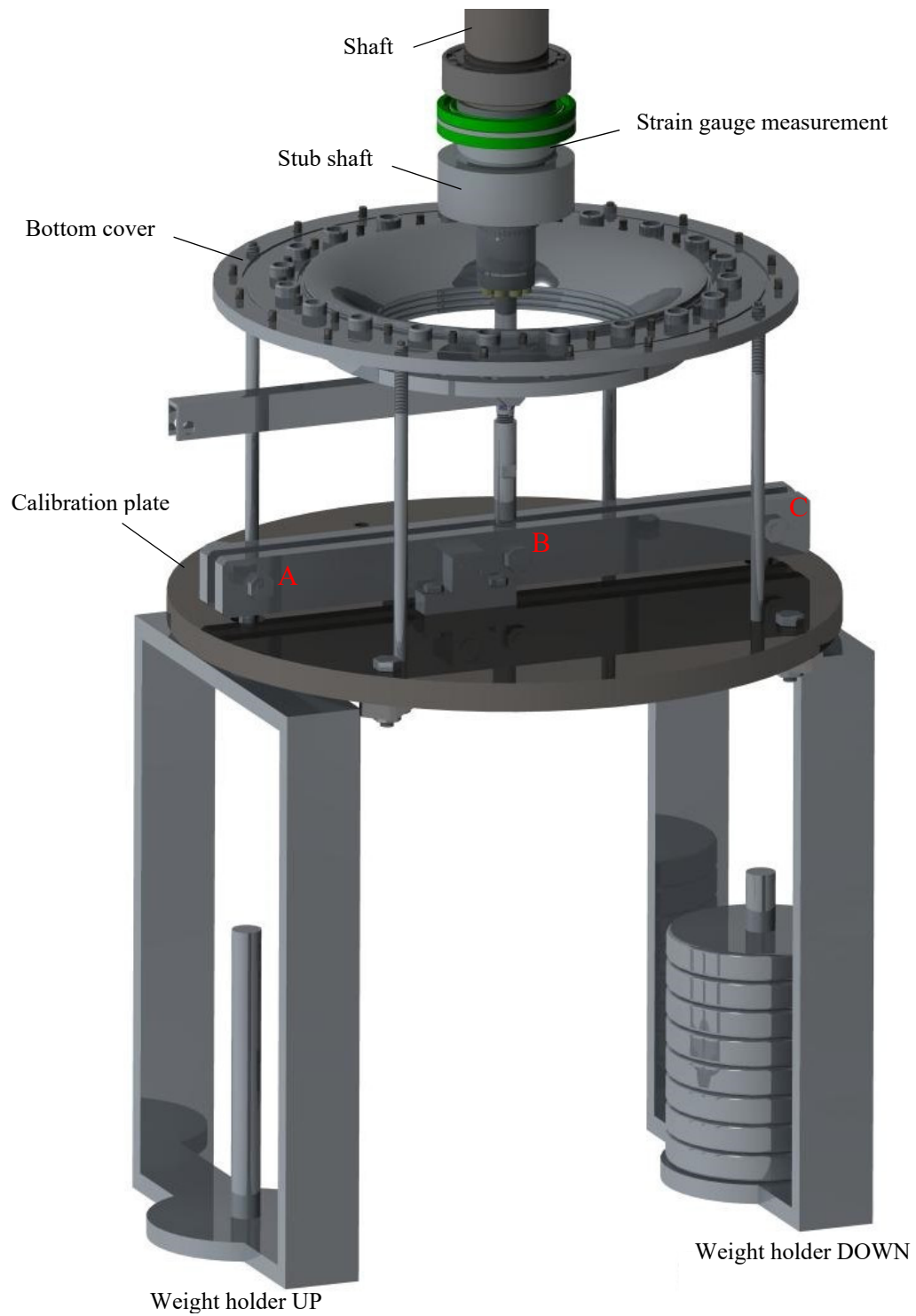


Figure 4-11: TTL Jig for Axial Load Calibration of Downward Force; 3D View

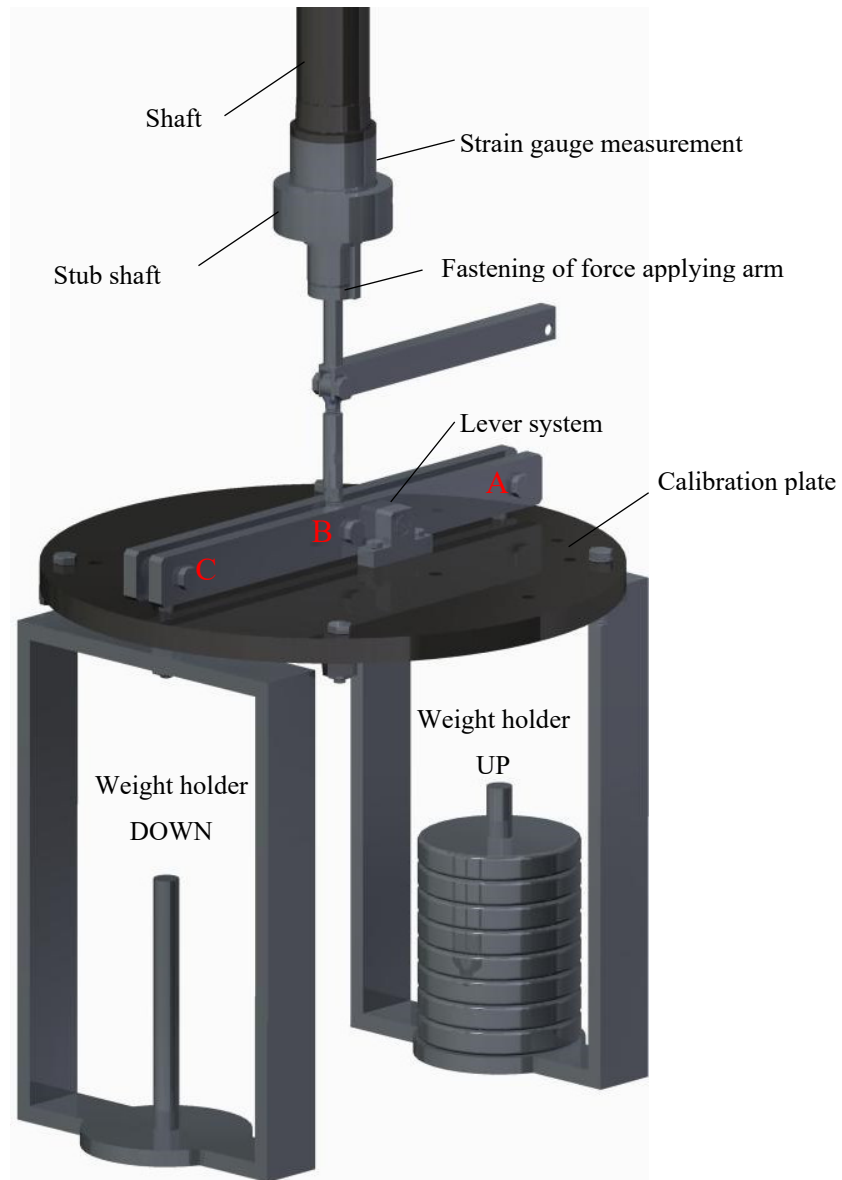


Figure 4-12: TTL Jig for Axial Load Calibration of Upward Force; 3D View

VI. References

- Calibration document for calibrated weights.
- Specification for the strain gauges.

Discussion:

The calibration procedure must be considered a draft that should be further developed by the TTL staff. Adding information for specific equipment and creating a step-by-step procedure of greater detail is recommended.

The strain gauges are calibrated during both on- and offload because mechanical hysteresis is a common error in measurements using strain gauges. The limits for the deviation between on- and offload data points for the same weights that are considered acceptable, or when the calibration should be discarded, must be decided at TTL.

Mounting the strain gauges directly above the bolts connecting the bipartite stub shaft should be avoided, as propagated material stress may influence the measurement. Alignment of the strain gauges in the direction of the principal axes is crucial to avoid errors.

Each weight used in the calibration should be calibrated by a certified instance, resulting in a calibration certificate which states measured weight with the accompanying uncertainty and deviation from claimed weight. The calibrated weights should be individually numbered and marked. The weight that is to be loaded onto *weight holder UP* to balance the lever arm for zero axial load transfer onto the shaft can be tailored to the required mass. The names of the weight holders in the calibration procedure can preferably be named otherwise to avoid confusion.

The lengths L_A , L_B and L_C must be measured with high accuracy, and the equations for axial load updated using the measured values. One way to make the measurement repeatable is creating a straight edge in the centre of the bolts in point A, B, C and D, against which the lengths between the points can be measured by a slide calliper. The attributable uncertainties involved in the measurements must be assessed.

The calibration jig must be protected from dust and other contaminants when stored. Deterioration in the roller bearings, in particular, will influence measurements results.

4.1.8. Generator Torque

At TTL, the generator torque T is to be measured by an HBM T40B torque flange as shown in Figure 4-13. It consists of two separate parts: the rotor and the stator. The rotor comprises the measuring body, with strain gauges installed, and signal transmission elements. The stator holds the connector plugs for speed signals and an optional rotational speed measuring system. With this installed, the rotational speed is measured magnetically by an AMR sensor and a magnetic ring which is welded to the flange (35).

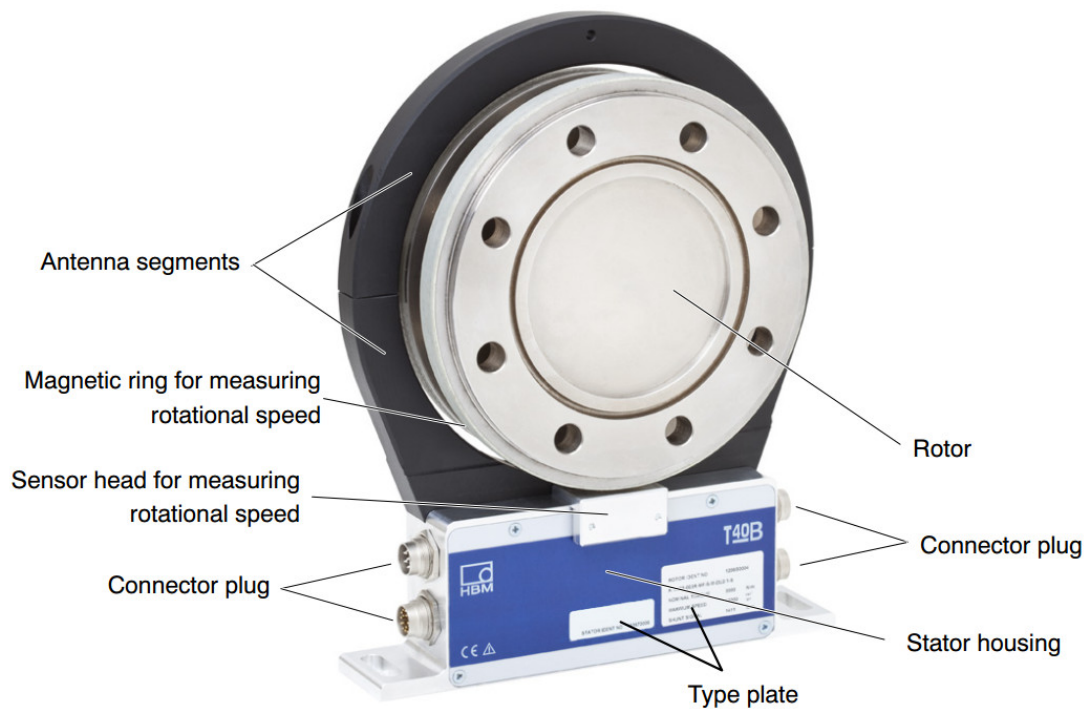


Figure 4-13: T40B Mechanical Construction (35)

Shaft Couplings

As the torque transducer is sensitive to shaft misalignments, the suggested design for generator torque measurement at TTL includes a disc coupling system to connect the shaft to the torque transducer. ROBA[®]-DS disc pack couplings of type 9110 is a backlash-free shaft coupling for HBM torque transducers. It has a double disc pack design and compensates for axial, parallel and angular shaft misalignments. The installation of this shaft coupling type with the aim to minimise the parasitic loads affecting the torque transducer provides optimum prerequisites for achieving exact and reliable torque measurement results. Several configurations are possible, but the “preferred variant” as shown with a red dotted line in Figure 4-14 is recommended as the shortest and most rigid design.

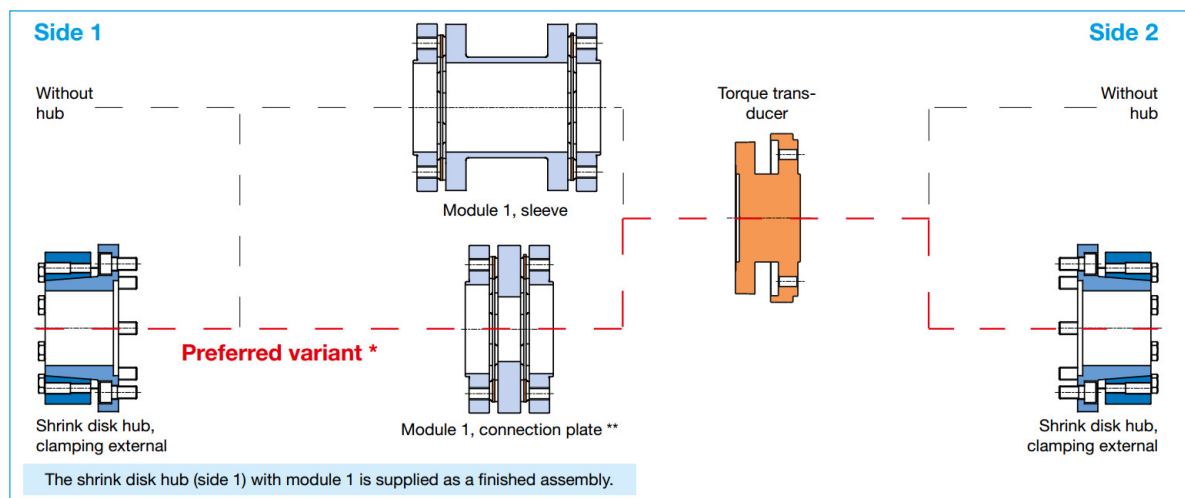


Figure 4-14: ROBA[®]-DS Shaft Coupling, “Preferred variant” (36)

The hubs with external clamping of the shrink disks are adapted to the generator shaft diameter on side 1 and the main shaft diameter $d=70\text{mm}$ on side 2, with hub bores within a H6 tolerance. For torque calibration, parts above the torque transducer is constrained from rotation. Methods of achieving this are locking on the bolts on side 1, or by a lock pin through a horizontal bore through the generator shaft. The couplings with the torque transducer is shown in Figure 4-15.

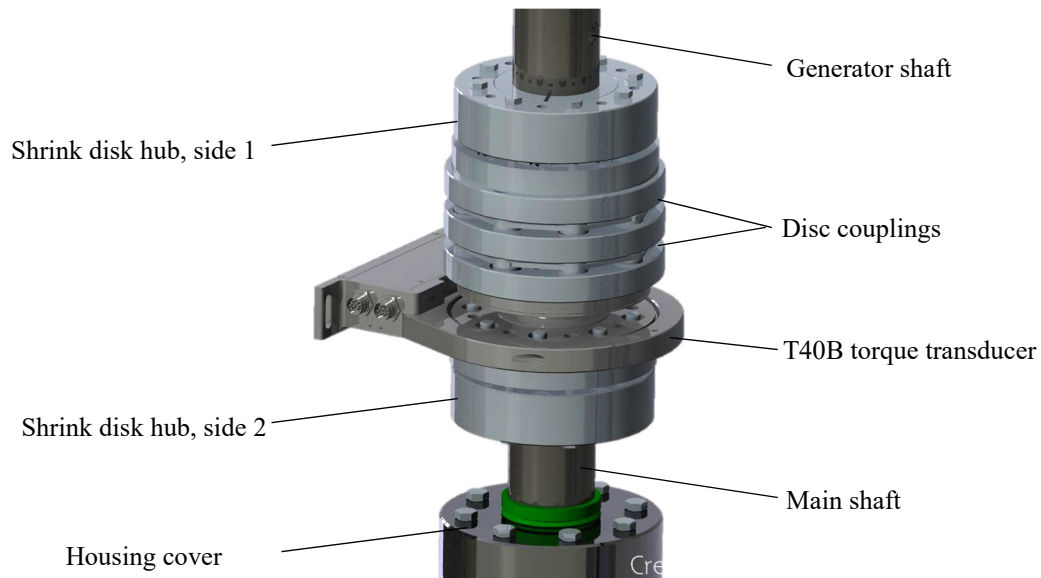


Figure 4-15: TTL Torque Transducer with Couplings

Discussion

The torque flange must be protected against dust, coarse dirt particles, oil, solvents and humidity. Other important precautions and information regarding maintenance, mechanical installation, electrical connection, run-out and concentric tolerances can be found in *Appendix D.1*.

The initial alignment of machinery is a critical factor for the reliability and performance of the coupling. Shafts are misaligned due to effects of heat and vibrations during operation, for this reason, shaft misalignments should occasionally be checked and corrected. Information regarding permitted axial displacement, radial and axial misalignment, tightening torques and operational instructions for the couplings are found in *Appendix D.2*.

4.1.9. Friction/Mechanical Torque

The mechanical torque imposed on the runner, T_m , is measured by strain gauges mounted on the area of maximum torque occurrence on the top stub shaft. This region of the stub shaft has a smaller cross-sectional area and influences from bolts or seals are minimised. The strain gauges are mounted at a 45° angle to the central axis of the shaft on the inside surface of the stub shaft top part, as shown in Figure 4-16.

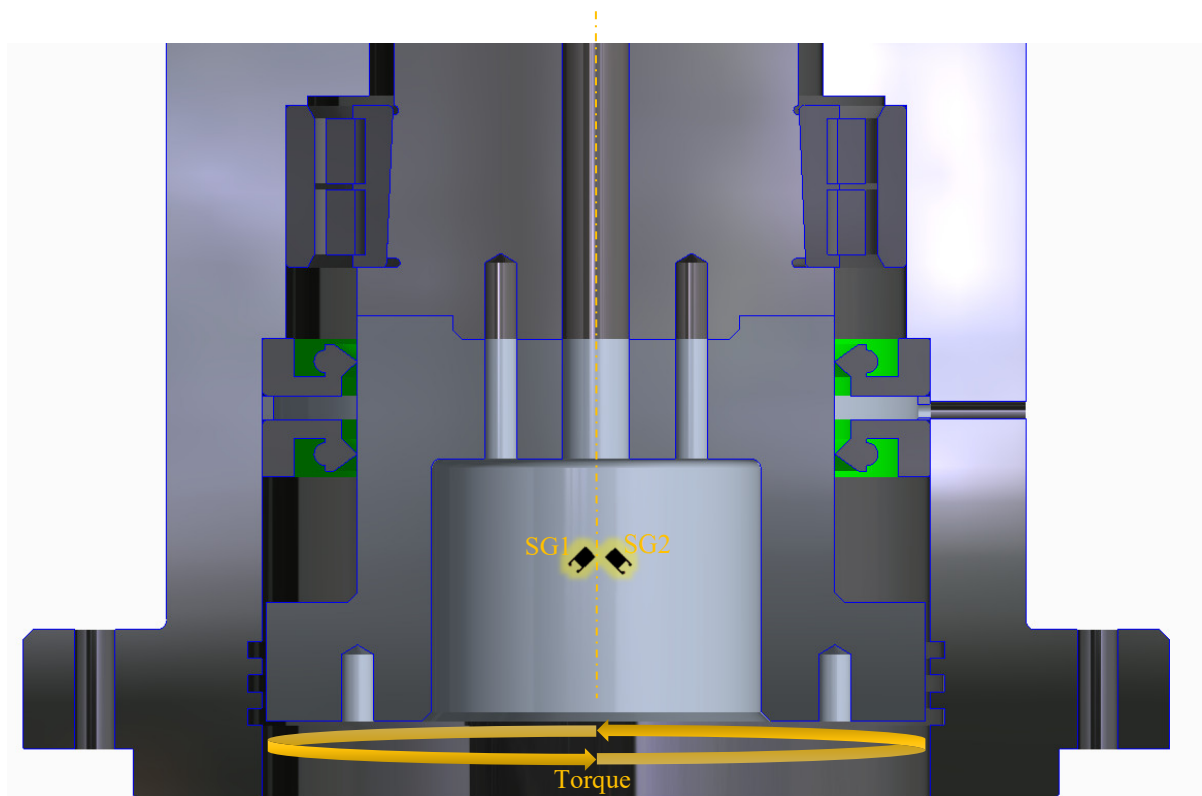


Figure 4-16: TTL Mechanical Torque at TTL

Two more strain gauges, SG3 and SG4, are mounted similarly revolved 180° around the shaft centre line, as shown in Figure 3-11.

HBM XY4 are V-shaped strain gauges with 2 measuring grids arranged at an angle of about 45° to the SG axis, as shown in Figure 4-16.

A mirror-imaged pair of the HBM XY4 connected in full bridge circuit is suited for measuring the mechanical torque at the TTL Francis turbine test rig.



Figure 4-16: HBM XY4 Strain Gauge (37)

Both the generator torque and the mechanical torque are calibrated by calibrated weighing masses on a calibrated lever arm. A weight holder with a wire connected to an arm over a pulley applies torque to the stub shaft. The shaft is locked from rotation above the torque transducer, such that the torsion propagates through the material for the strain gauges and the torque transducer to measure. The measured values are different due to the friction torque in the seals and bearings arrangement. The friction torque T_{Lm} is defined by the difference between the mechanical torque and the shaft torque: $T_{Lm} = T_m - T$. The setup is further described through the preliminary proposal for calibration procedure that follows.

4.1.9.1. Torque Measuring System and Calibration

I. General

The following subchapters present a procedure for calibration of the torque measuring system at the Francis Turbine Test Rig at The Testing Laboratory.

One set of values for the variables in Table 4.2 are obtained each of the torque measurements; that is generator torque and mechanical torque. The procedure describes the mechanical torque, but same calibration procedure applies to generator torque.

Table 4.2: Definitions and Abbreviations for Torque Measurement

Symbol	Description	Unit
T	Generator torque	<i>Nm</i>
T_m	Mechanical torque	<i>Nm</i>
m	Mass of weights	<i>kg</i>
m.v.	Measured value	<i>V</i>
a	Slope in calibration equation	<i>Nm/V</i>
b	Intersection constant in calibration equation	<i>Nm</i>
g	Gravity	<i>m/s²</i>
l_{arm}	Length of torque arm	<i>m</i>

Gravity g is 9.79506m/s^2 .

The length of the torque arm l_{arm} is 0.35m .

II. The System

a. Description

The measuring system for mechanical torque consists of strain gauges installed on the stub shaft. Through an external amplifier, the output signal from the strain gauge system is transformed into a 0-10V signal that varies linearly with the torque/weights applied and sent to the data acquisition unit for post-processing.

The measuring system for generator torque consists of a torque flange installed above the bearing block arrangement. Through an external amplifier, the output signal from the transducer is transformed into a 0-10V signal that varies linearly with the torque/weights applied and sent to the data acquisition unit for post-processing.

The torque for calibration is applied by placing weights in a weight holder that is connected to a wire, which is led over a pulley and attached to a torque arm in the other end. The torque arm is connected to the stub shaft and has a known length from the centre of the shaft.

b. Equipment Used in Measuring

- Strain gauges
- Measuring amplifiers
- Telemetry system
- Torque transducer
 - HBM T40B
- Data acquisition unit
 - National Instruments data acquisition unit
 - LabView for computation and presentation of data
 - External power supply
- Calibrated weights
- Calibration jig

III. Calibration

a. Preparations

1. Unfasten and detach the draft tube, runner and lower part of the two-part stub shaft.
2. Make sure the display for visualisation of the measured volt signal is present on the data acquisition system.
3. Record the volt signal with no torque applied. This is the zero point.
4. Connect the equipment necessary to apply torque:
 - a. Reattach the lower part of the stub shaft to the other stub shaft part where the strain gauges are mounted.
 - b. Fasten the connecting arm to the exposed stub shaft.
 - c. Fasten the calibration jig with plate, support and pulley holder to the bottom cover.
 - d. Restrain the coupling above the torque flange, making sure the torque arm is suspended such that the wire will be normal to the torque arm and in line with the pulley.

b. Calibration

1. Record the volt signal.

Attach the wire to the weight holder on one side, over the pulley, and to the torque arm on the other side. Setup with or without the axial force calibration equipment is shown from various angles in Figure 4-18, Figure 4-19 and Figure 4-20.

Record the voltage again.
2. Load on the weights one by one and record the total weight (W) and corresponding measured volt signal (m.v.) for each weight in the weight holder. The volt signal should be stable before the reading is taken.

A minimum of 10 points are needed to find a satisfying calibration equation and the whole measuring range (0-2900Nm or 0-850 kg) has to be covered.
3. Load off the weights one by one and record the volt signals for each weight again.
4. Repeat 1 to 3 to obtain a minimum of three sets of data.

IV. Computations

The torque (T) as a known mass (m) is added to the weight holder is calculated by:

$$T_m = m \cdot g \cdot l_{arm} \quad \text{Equation 4.1}$$

Gravity (g) and length (l_{arm}) is already known.

The strain gauge circuit gives an output signal in Volts that varies linearly with the torque/weights applied. For each load applied, the average voltage values from the data sets should be averaged. The calibration equations are linear equations for T and T_m respectively.

$$T_m = a \cdot (m \cdot v.) + b \quad \text{Equation 4.2}$$

And the parameters a and b are found in the calibration.

V. Figures

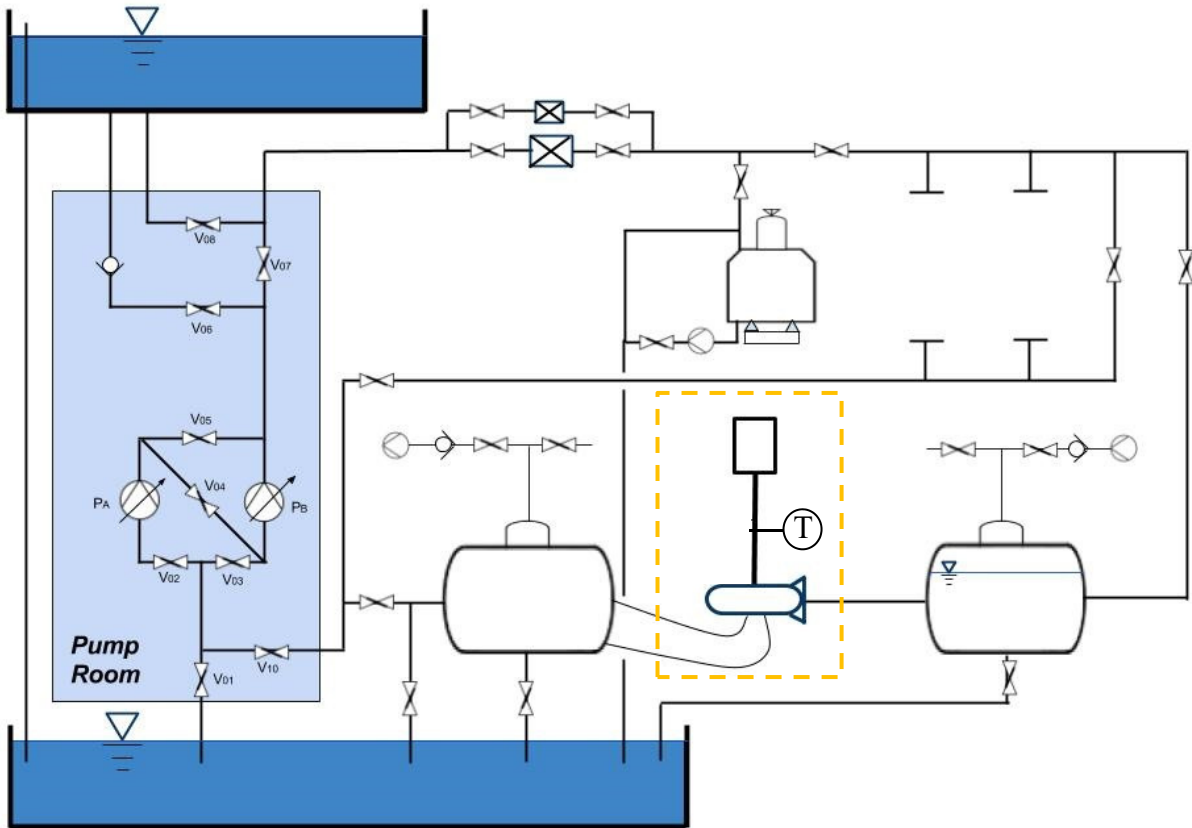


Figure 4-17: TTL Torque Arrangement



Figure 4-18: TTL Torque Calibration Jig Overview



Figure 4-19: TTL Torque Calibration Jig Attached to Bottom Cover

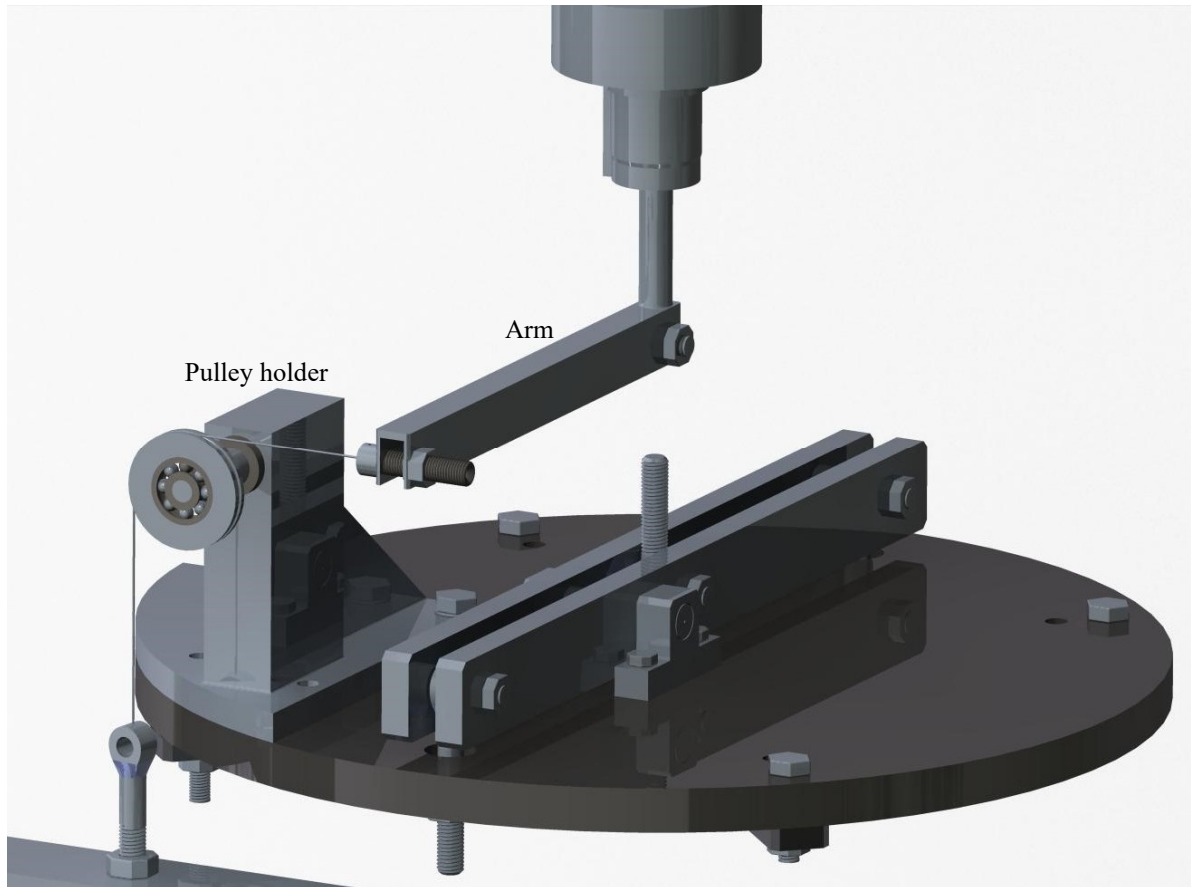


Figure 4-20: TTL Torque Calibration Jig with Axial Lever Arm

VI. References

- Calibration document for calibrated weights.
- Specification for strain gauges.
- Specification for torque transducer HBM T40B.

Discussion

The points that were discussed regarding the axial load calibration also apply to the torque measurement. Analogous to the calliper-measurement of the lever arm for axial load, the torque arm needs precise measurement and a way of ensuring that the torque is applied at a right angle. In addition, there are some other issues with the torque calibration setup that is worth addressing.

The principle behind applying torque as designed is good, but different designs for supporting the pulley in the torque calibration should be assessed. The proposed solution is an attempt to facilitate the use of the same jig for calibration of torque as for axial load. The addition of the pulley with support such as designed lead to uneven forces acting on the calibration plate and a strength analysis would likely show a twisting of the plate. Diagonal bracing could help counteract this, but an alternative method of supporting the pulley may yield further advances. If the arm can be increased, the weights necessary for the calibration reduces to $m = \frac{292kg}{l_{arm}}$.

4.1.10. Uncertainty

A full evaluation of the uncertainty in measurements at TTL is beyond the scope of this report. An analysis of the uncertainties at the VKL Francis test rig was done by Storli (23), and can, along with *IEC60193*, serve as guidance for a future uncertainty analysis at TTL. The most expected uncertainty sources in torque and axial loads measurements at the Francis test rig at TTL are presented in the following subchapters.

4.1.10.1. Uncertainty Sources, Axial Load Measurement at TTL

Table 4.4 presents the systematic uncertainties involved in the measurement of axial load. The uncertainties are dependent of the operating point.

Table 4.3: Systematic Uncertainties in Axial Load Measurement

Symbol	Description	Unit
$(f_{m_A})_s$	Relative systematic uncertainty in the weights used in calibration of the axial load. The combination of calibration weights at each calibration point will have a systematic uncertainty. When performing measurements, the uncertainty for the weights corresponding to the measured axial load should be used.	%
$(f_{regression_A})_s$	Relative systematic uncertainty in the regression process to find a calibration curve for the axial load. This is computed from the values registered when calibrating the strain. The value to be used is for the test point axial load.	%
$(f_{arm_{A+}})_s$ $(f_{arm_{A-}})_s$	Relative systematic uncertainty in the measurement of the axial load arm length (in the positive/negative direction), due to uncertainties in the measuring devices.	%

The relative systematic uncertainty in the measurement of axial load is defined as

$$(f_A)_s = \pm \sqrt{(f_{m_A})_s^2 + (f_{regression_A})_s^2 + (f_{arm_A})_s^2} \quad \text{Equation 4.3}$$

The absolute systematic uncertainty in the measurement of axial load is

$$(e_A)_s = (f_A)_s \cdot A \quad \text{Equation 4.4}$$

4.1.10.2. *Uncertainty Sources, Torque Measurement at TTL*

Table 4.4 presents the systematic uncertainties involved in the measurement of torque. The uncertainties are dependent of the operating point and are applicable both to the generator torque T and the mechanical torque T_m .

Table 4.4: Systematic Uncertainties in Torque Measurement

Symbol	Description	Unit
$(f_{m_T})_s$ $(f_{m_{T_m}})_s$	Relative systematic uncertainty in the weights used in calibration of torque. The combination of calibration weights at each calibration point will have a systematic uncertainty. When performing measurements, the uncertainty for the weights corresponding to the measured torque should be used.	%
$(f_{regression_T})_s$ $(f_{regression_{T_m}})_s$	Relative systematic uncertainty in the regression process to find a torque calibration curve. This is computed from the values registered when calibrating the torque transducer (for generator torque T) and the strain gauges (for mechanical torque T_m), and the value to be used is for the test point torque.	%
$(f_{arm_T})_s$ $= (f_{arm_{T_m}})_s$	Relative systematic uncertainty in the measurement of the torque arm length, due to uncertainties in the measuring devices.	%
$(e_T)_s$ $(e_{T_m})_s$	Absolute systematic uncertainty in the torque measurement.	Nm
T T_m	The measured generator torque. The measured mechanical torque.	Nm
$(f_T)_s$ $(f_{T_m})_s$	Relative systematic uncertainty in the torque measurement.	%

The relative systematic uncertainty in the measurement of torque is defined as

$$(f_T)_s = \pm \sqrt{(f_{m_T})_s^2 + (f_{regression_T})_s^2 + (f_{arm_T})_s^2} \quad \text{Equation 4.5}$$

$$(f_{T_m})_s = \pm \sqrt{(f_{m_{T_m}})_s^2 + (f_{regression_{T_m}})_s^2 + (f_{arm_{T_m}})_s^2} \quad \text{Equation 4.6}$$

The absolute systematic uncertainty in the measurement of torque is

$$(e_T)_s = (f_T)_s \cdot T \quad \text{Equation 4.7}$$

$$(e_{T_m})_s = (f_{T_m})_s \cdot T_m \quad \text{Equation 4.8}$$

The friction torque uncertainties are derived from the combination of uncertainties in generator torque and mechanical torque measurement:

$$(f_{T_{Lm}})_s = \pm \frac{\sqrt{(e_T)_s^2 + (e_{T_m})_s^2}}{T_m - T} \quad \text{Equation 4.9}$$

Possible error sources, creep, mechanical hysteresis and interference effects on a strain gauge measuring point, are handled in detail in HBM and Karl Hoffmann's *An Introduction to Stress Analysis and Transducer Design using Strain Gauges* (15).

4.2. Components at TTL

The suggested design for the main components at the Francis turbine test rig at TTL are presented in the following chapter. Some points should be kept in mind while viewing the 3D-illustrations:

- Simplifications are made regarding the representation of pumps, valves and other parts.
- The illustrations do not show all rigs and objects in the Turbine Testing Laboratory.
- It is emphasised that the work is only a suggestion and that better solutions might exist for the Francis rig at TTL. Design features include many small details that must be verified before any detail drawings are sent for manufacture of any part.
- The bolt types including diameter, length, thread and counterbore/countersunk holes should be viewed as illustrative, as strength analysis has not been performed.

An attempt is made to show the design through illustrations in the subchapters, but due to the many details and the time-demanding process of rendering and setting up views, far from all features are shown. A better understanding of the parts and connections between them can be obtained by viewing and manoeuvring the 3D-models that are handed in along with this report. Subchapters under three may also be used as a reference for the background and requirements behind the design.

4.2.1. Guide Vane Regulating Mechanism and Head Covers

The newly designed top cover and the existing bottom cover are shown with existing GV covers and bushings in Figure 4-21.

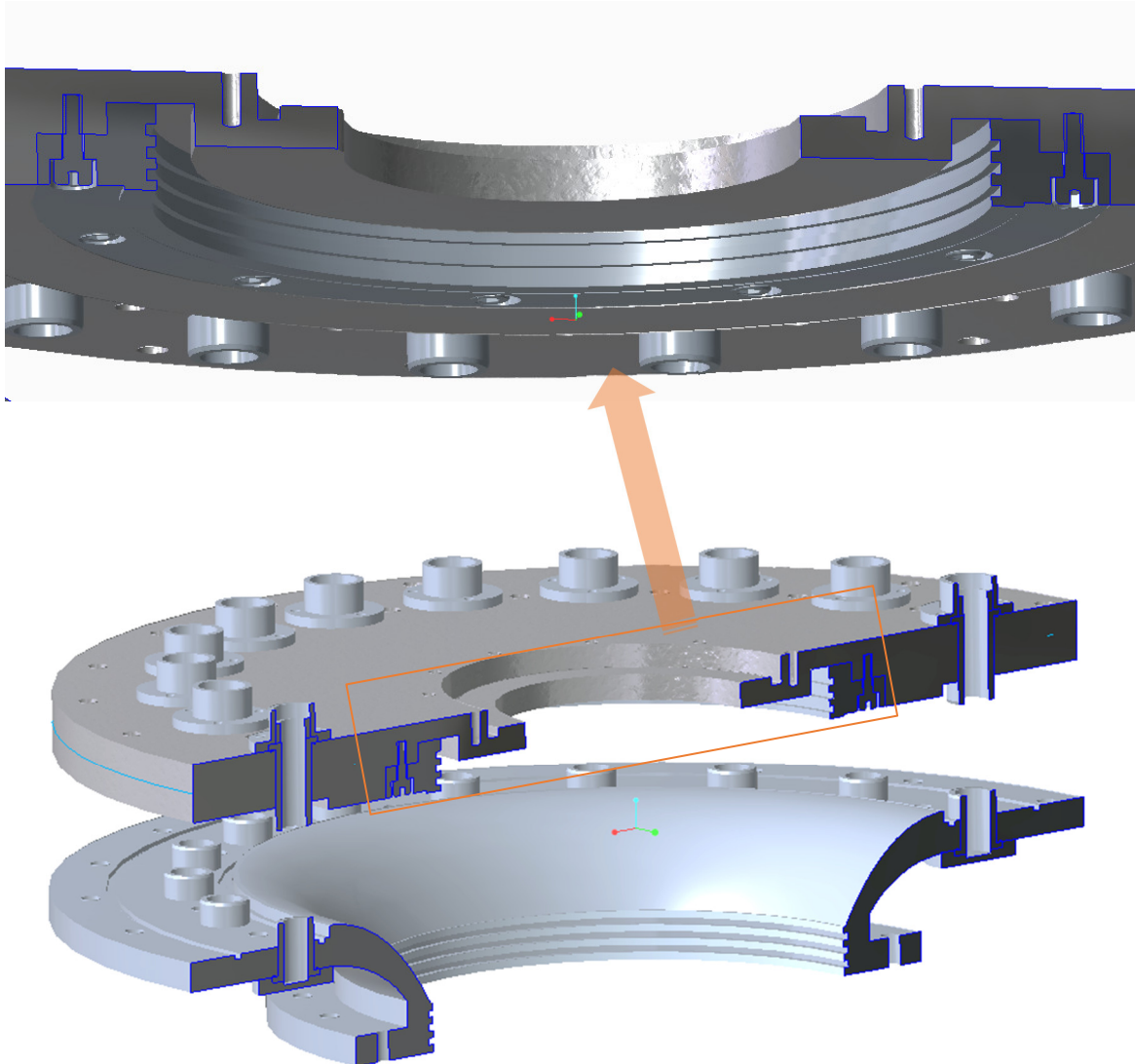


Figure 4-21: TTL Head Covers with Guide Vane Bushings and Covers

A separate part of the top cover with labyrinth seal will be manufactured to a different hardness. By this design, this part will give if accidental contact is made with the hub; hence protecting the hub. It is attached to the top cover from beneath to avoid sealing needs on top side.

Figure 4-22 illustrates the setup around the runner.

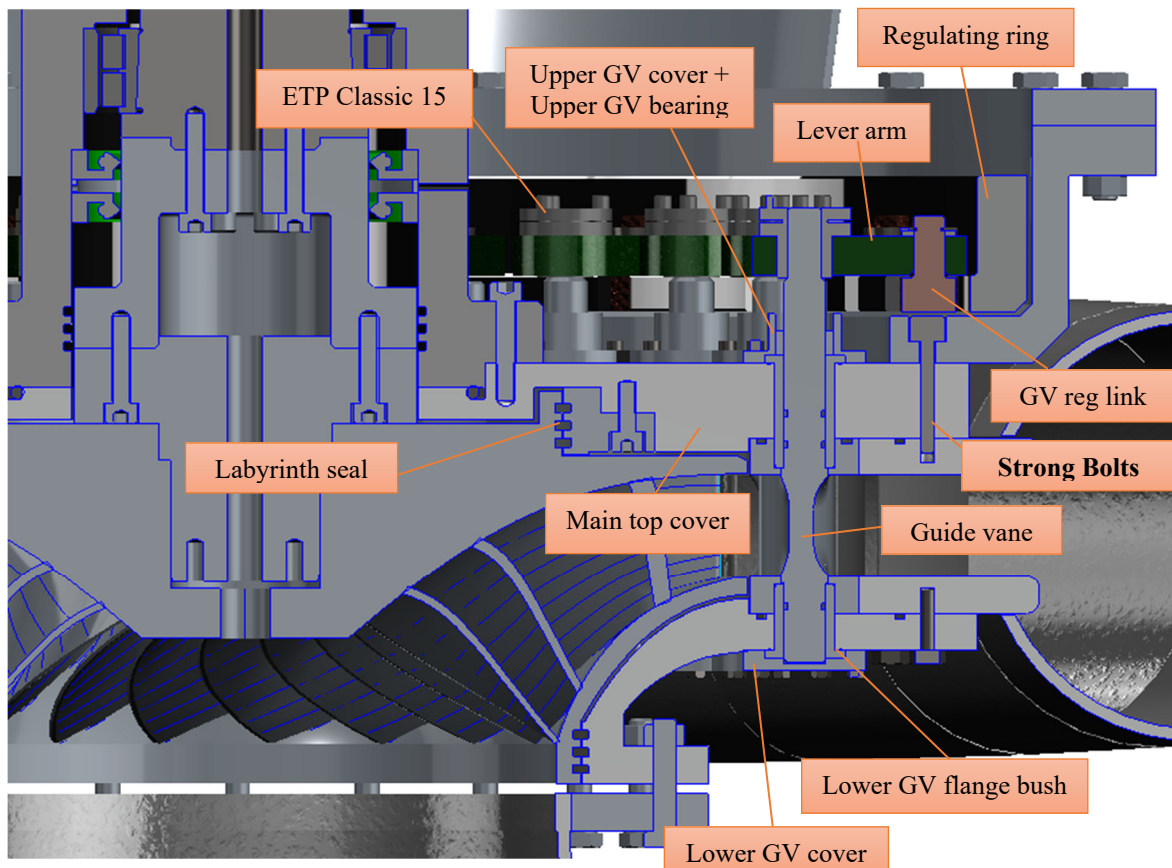


Figure 4-22: TTL GV Arrangement and Head Covers around Runner

The top cover is adapted to utilising the existing guide vanes.

The regulating ring is mounted on the spiral casing side of the guide vanes. A linear actuator pushes the regulating ring to revolve, with that also rotating the guide vanes through the lever arm that connects them. Nylon separates the regulating ring from the surfaces against which it slides.

The guide vane control system (without the linear actuator system) is shown in Figure 4-23.

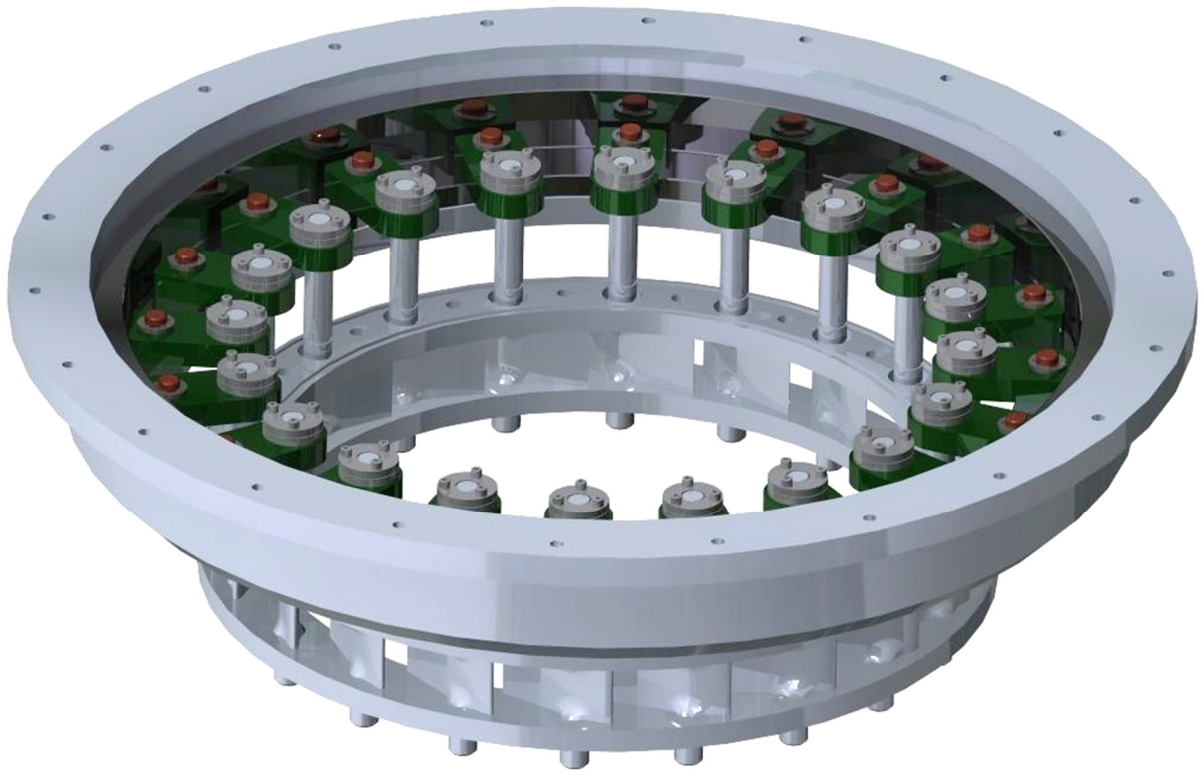


Figure 4-23: TTL Guide Vane System; 3D View

The suspension cone is attached to the outer diameter on topside of Figure 4-23, as shown in Figure 4-24.



Figure 4-24: TTL Suspension Cone; 3D View

Discussion

The necessary equipment on the shaft above the torque transducer, along with the shaft connection to the generator influences the necessary height for the placement of generator and generator support frame. The height and consequently the angles of the suspension cone depends on these factors for attachment to the generator support frame and needs adapting. The strength of all connections for supporting the turbine must be assessed thoroughly.

4.2.2. Runner, Spiral Casing and Stay Vanes

The following parts are implemented into the model without modification:

The hub, shroud and runner blades are shown in Figure 4-25.



Figure 4-25: TTL Runner; 3D View

The 20 spiral casing sections and the stay ring with the 20 stay vanes are shown in Figure 4-26.



Figure 4-26: TTL Spiral Casing with Stay Ring and Stay Vanes; 3D View

4.2.3. Bearing-Shaft-Housing System

4.2.3.1. Bearing Arrangement

Angular Contact Ball Bearings

Mounted just below the housing cover is a matched set of sealed super-precision angular contact ball bearings from SKF with designation *7015 CD/P4A*. Two single row bearings arranged back-to-back support combined radial loads and axial loads in both directions, while simultaneously providing accurate positioning of the shaft.

The recommended diameter tolerances for machining of the bearing seats on the shaft and the housing gathered from the product data (38), are shown in Figure 4-28.

A lock nut is used to locate the angular contact ball bearings onto the shaft. To prevent unintentional loosening, the lock nut is secured by a washer that engages a keyway in the shaft. An *MB15* lock nut and a *KM15* washer from SKF has been ordered and sent to TTL. The setup is shown in Figure 4-27 (The bearings are sealed, so the balls are not seen in reality).

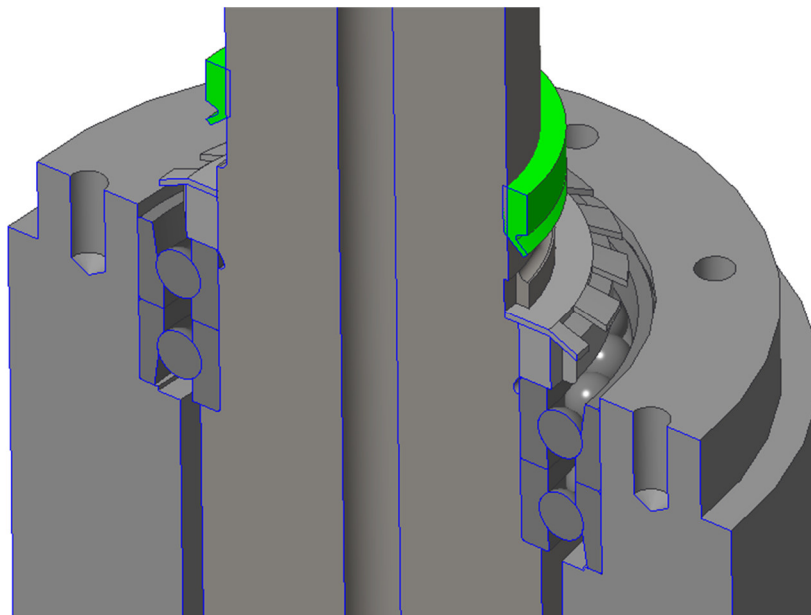


Figure 4-27: TTL Angular Contact Ball Bearings with Lock Nut and Washer

Cylindrical Roller Bearings

High-precision cylindrical roller bearings with designation *NN3017-AS-K-M-SP* support radial forces from the shaft closer to the runner. The sealed double-row, non-locating bearings allow the inner and outer ring to be axially displaced relative to each other.

The roller bearings have a 1:12 tapered bore. Recommendations for machining of the tapered shaft is illustrated in Figure 4-28.

The ball and roller bearings are distanced by 500mm and have both been ordered and sent to TTL.

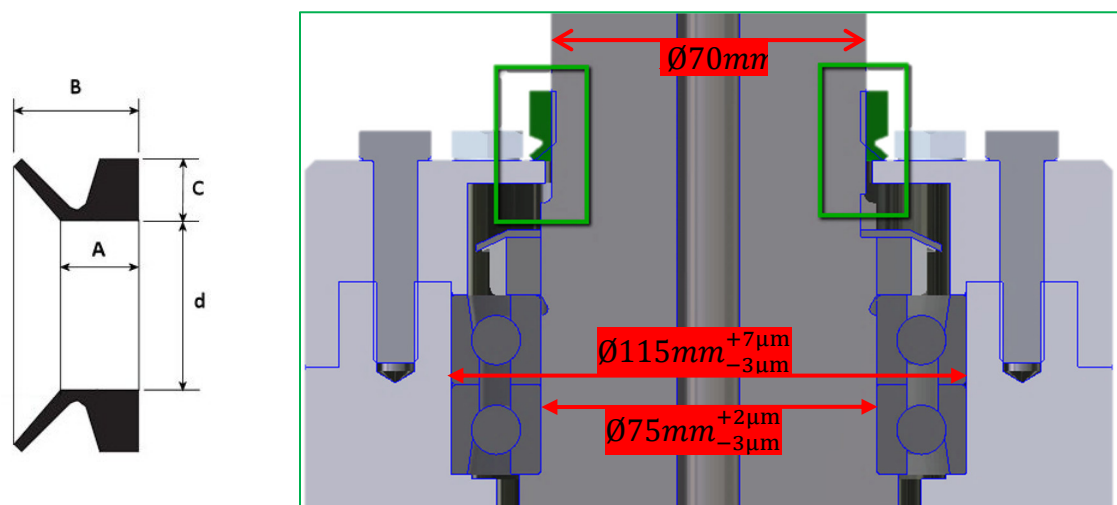
Discussion

A sensor that monitors the temperatures in the housing and which the bearings are subject to must be considered to prevent overheating if the turbine is to be run at high rotational speeds for longer periods.

The bearings are supplied with an integral seal fitted on both sides and should by design contain the lubricant for life and be maintenance-free. Installing a sensor that registers an eventual lubricant leakage is a safety measure that can be evaluated.

4.2.3.2. Seals

An elastic V-ring is installed with an interference fit on the shaft above the housing cover. The V-ring seal rotates with the shaft, while its outward directed sealing lip seals against the housing cover; preventing contaminants from entering the housing. A nitrile rubber V-ring seal of designation V-70A as shown in Figure 3-2 has been ordered and sent to TTL. (The tolerances for the bearing seats on the shaft and housing are also shown).



Shaft Size	d	C	A	B	Mounted Width
68-73	63	6	6.8	11	9 ± 1.2

Figure 4-28: TTL V-ring Seal

For sealing between the shaft and housing below the roller bearings, radial shaft seals of designation 100-140-13 BA has been ordered and sent to TTL. The seal has a nominal outside diameter of 140mm. The housing bore is machined to an ISO H8 tolerance ((32) table 9, p. 75). The shaft of $d=100\text{mm}$ at the sealing lip position has an ISO h11 counterface tolerance ((32) table 6, p. 71).

The red square in Figure 4-29 maps the thrust block region that is shown in Figure 4-30, where setup with the two radial shaft seals is shown. (+Tolerances for the shaft and housing in conjunction with the bearings and seals are also shown).

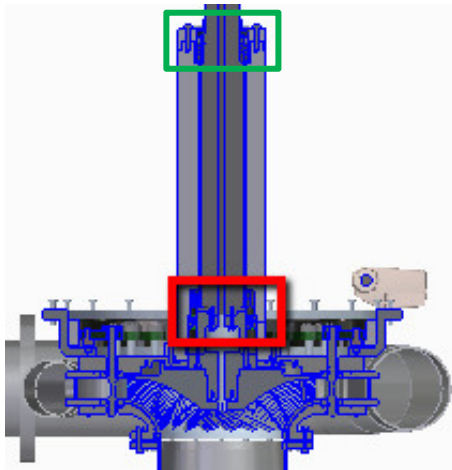


Figure 4-29: TTL Seal Placement Overview

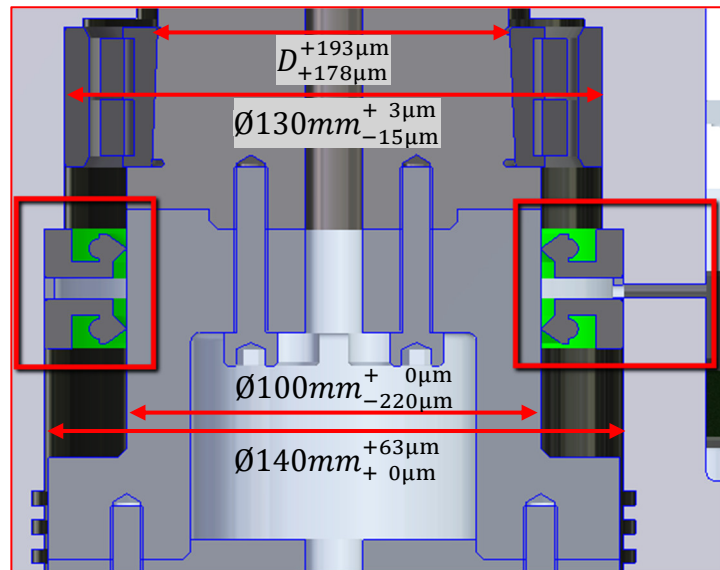


Figure 4-30: TTL Radial Shaft Seals

Discussion

When installing a V-ring as designed with no axial support, it is imperative to make sure that the shaft is dry and free from grease or oil (39). A thin film of grease lubricates the lip or, for minimum friction, the counterface can be coated with a low-friction agent. The V-ring must be installed with a uniform stretch around the shaft.

The radial shaft seal installed closest to the roller bearings is a safety measure, preventing eventual bearing grease leakages from entering the water. The lower seal, oppositely directed and separated by a spacing washer, will stop water from reaching the bearings. Eventual leakages passing the seals are monitored by a hole through the spacing washer and the outer housing. The hole through the outer housing can preferably be sloped downward and must be aligned with the hole in the spacing washer.

For the shaft seals to seal efficiently over a long time as well as to reduce the friction and tear to the sealing lip and the shaft, dry running should be avoided by applying a proper lubricant. The lubricant also dissipates heat generated by the seal. An initial greasing prior to installation may be sufficient, but there is a risk of lubricant starvation in the back-to-back arrangement in the TTL design. Two sets of seals are sent to TTL. After installation, the state of the seals should

be assessed after some time. If the seals deteriorate quickly, alternative methods of lubricating the seal lips should be assessed. Using the monitoring hole as a lubrication hole to fill the space between the seals with grease is possible, but will at the same time eliminate the possibility to monitor eventual leakages through the seal, and the risk of grease reaching the water arises.

Detailed information about seals and installation guidelines can be found in SKF's *Industrial Shaft Seal Catalogue* (32). Coaxial deviations will lead to an uneven distribution of force on the sealing lip and limit the sealing effect. Maximum coaxial deviation for the radial shaft seals at 1500rpm is $\approx 0.26\text{mm}$. A too high eccentricity of the shaft may render the sealing lip unable to follow the shaft surface, hence enabling the medium to escape through the sealing gap. Maximum permissible runout at 1500rpm is $\approx 0.23\text{mm}$ ((32) Diagram 4, p. 62).

4.2.3.3. Shaft and Housing

The bearing block facilitates the measurement of both axial load and torque by strain gauges. For centring and alignment, the main shaft and housing are designed with steps of diameter changes, and the bearing seats are distanced by 500mm. A hollow shaft centre allows for signal-transmitting wires to be led through the shaft.

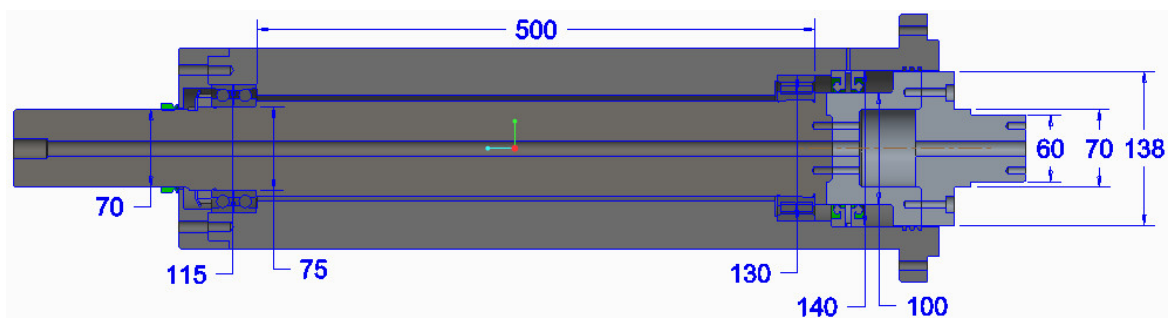


Figure 4-31: TTL Bearing-Shaft-Housing System

The arrangement from stub shaft to housing cover is shown in Figure 4-32.

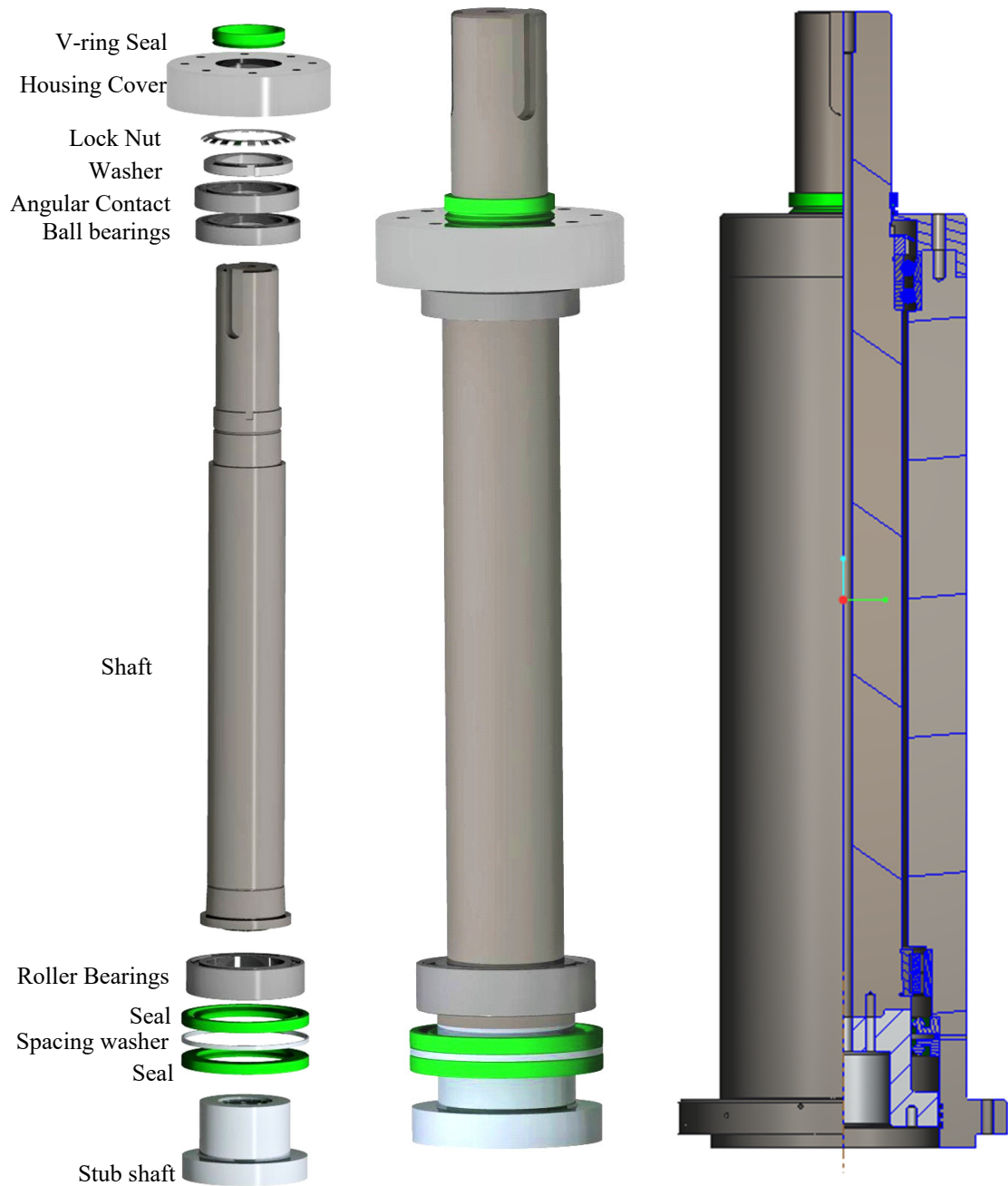


Figure 4-32: TTL Bearing Block Assembly

A split stub shaft has been designed and is shown in Figure 4-33. The two parts of the stub shaft are connected on the outer diameter, while the top part is connected to the shaft. The SG section has a thinner cross-sectional area to facilitate the measurement of material stress by strain gauges. Radial shaft seals are placed above the measuring sections. The lower part is adjusted to fit in the already existing hub with a bolted connection.

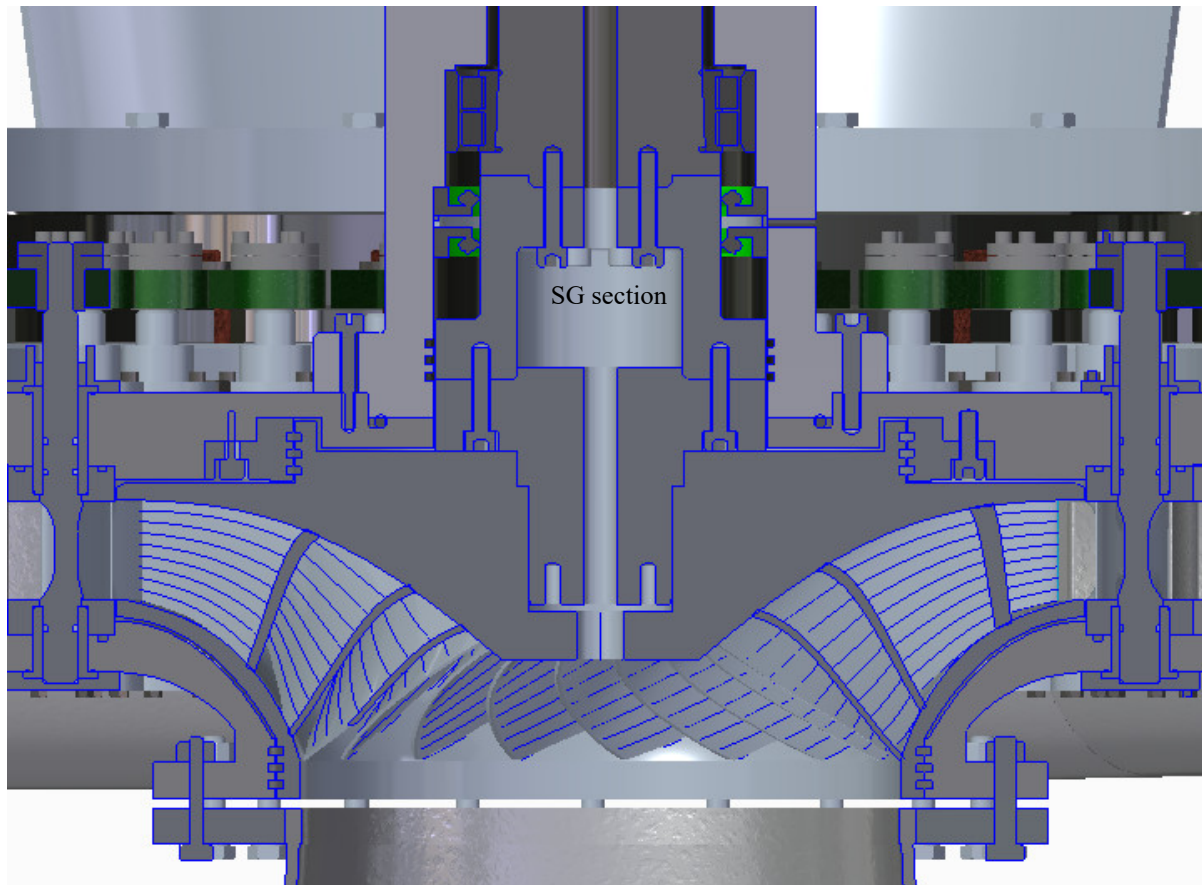


Figure 4-33: TTL Stub Shaft

The lower bearing is located by a press fit as indicated by the tolerances in Figure 4-30. Recommendations for the shaft and housing tolerances against the ball bearings can be seen from Figure 4-28.

Water leakages are opposed by an O-ring of 183.52mm diameter and 5.33mm thickness placed between the housing and the top cover, and a labyrinth seal between the housing and stub shaft.

Discussion

An alternative method of connecting the lower part of the stub shaft to the hub is by a bolt that engages threads in the centre of the stub shaft, as the design used at VKL shown in Figure 4-33.

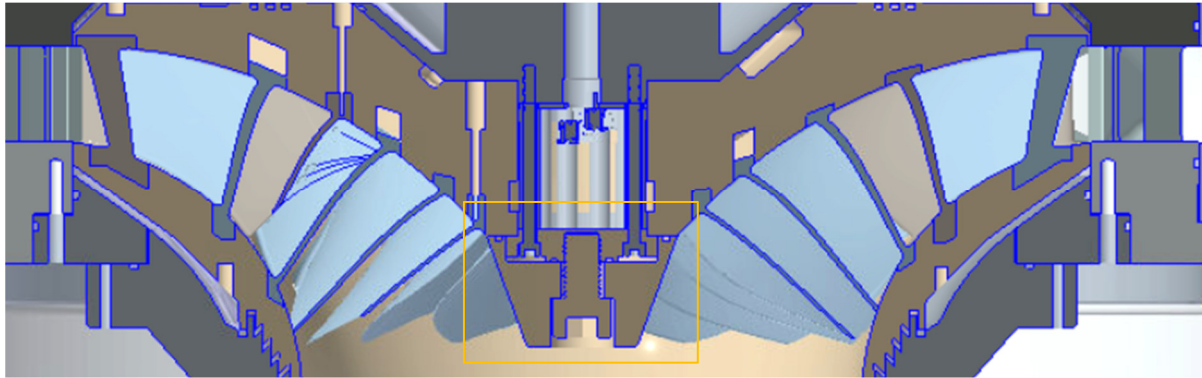


Figure 4-34: VKL Hub to Stub Connection

The same connection type would apply to the connection for the calibration of axial force and torque. If this design is chosen, the bolt cover must be designed as to hinder the water from going upward when the turbine is in operation. As mentioned in subchapter 4.1.7, a prerequisite for placing telemetry system and other equipment in the centre cavity of the stub shaft is that dryness is guaranteed. The labyrinth seal between housing could preferably be placed lower for this reason. The addition of an O-ring placed in the connection of the stub shaft parts will try to obstruct the water from reaching the cavity from the sides. High-precision machining is required between the connecting areas of the stub shaft. The tolerances are less critical in the non-contact areas along the shaft.

If the quotations for machining of the shaft are beyond the TTL budget, adding an adapter sleeve on the inside of the roller bearing can be considered. This would eliminate the need for costly machining of the tapered shaft seat.

4.2.4. High- and Low-Pressure Tank

The high-pressure tank is shown in Figure 4-35, with a volume $V \cong 15 \text{ m}^3$. On top of the tank is a dome where a pipe with a pressure gauge and a venting valve is connected. By the dome is the inlet from the main pipe system. The pipe coming out towards the right connected to the Francis turbine inlet.

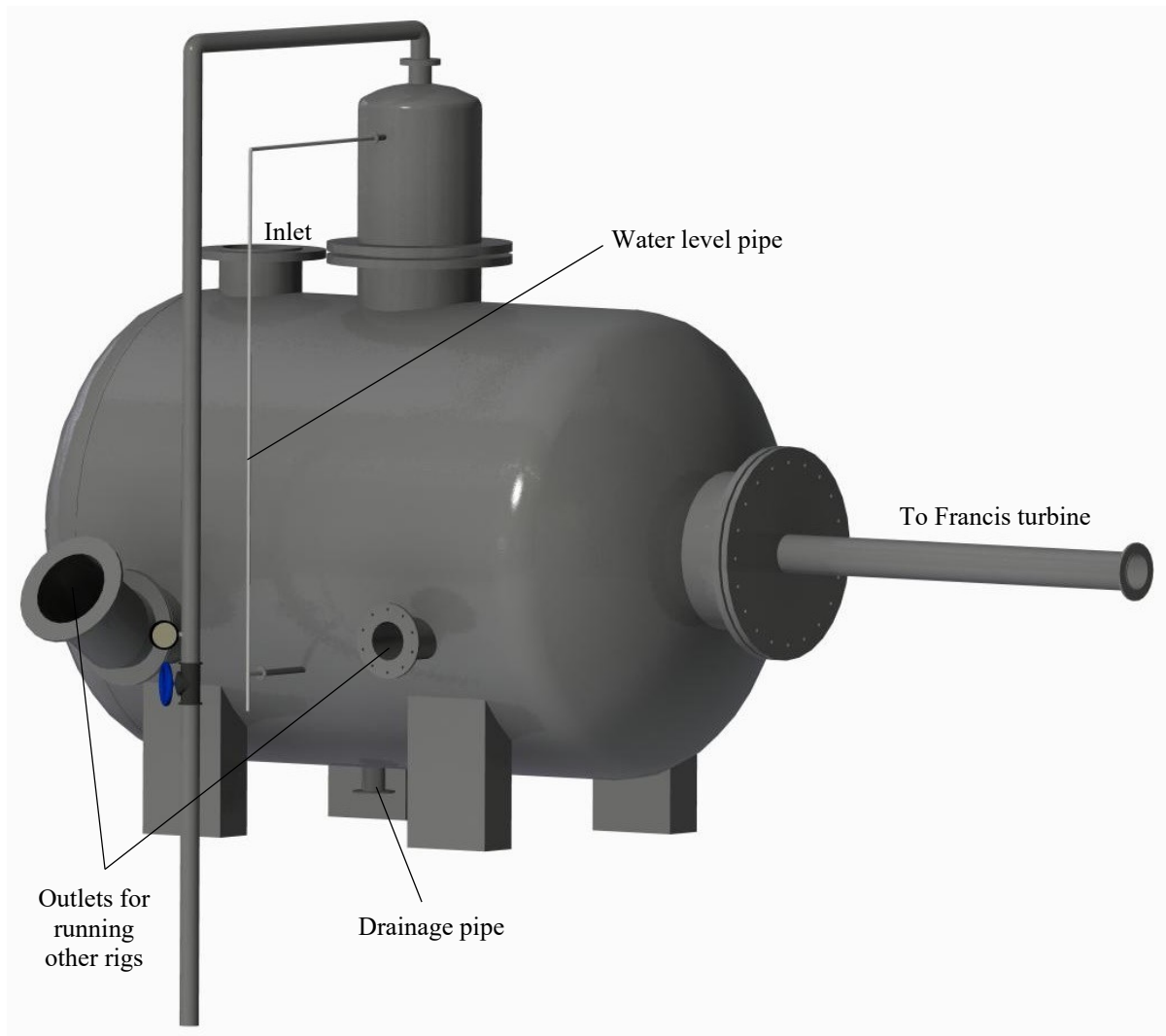


Figure 4-35: TTL High-Pressure Tank; 3D View

There must be means of releasing air into the tank when needed.

Downstream of the Francis turbine, the suggested low-pressure tank at TTL has the same shape as the low-pressure tank at the Waterpower Laboratory. In the low-pressure tank, there is a water-to-air surface. To obtain the desired pressure in the tank, air is evacuated by the use of a vacuum pump connected to the dome that sits on top of the tank.

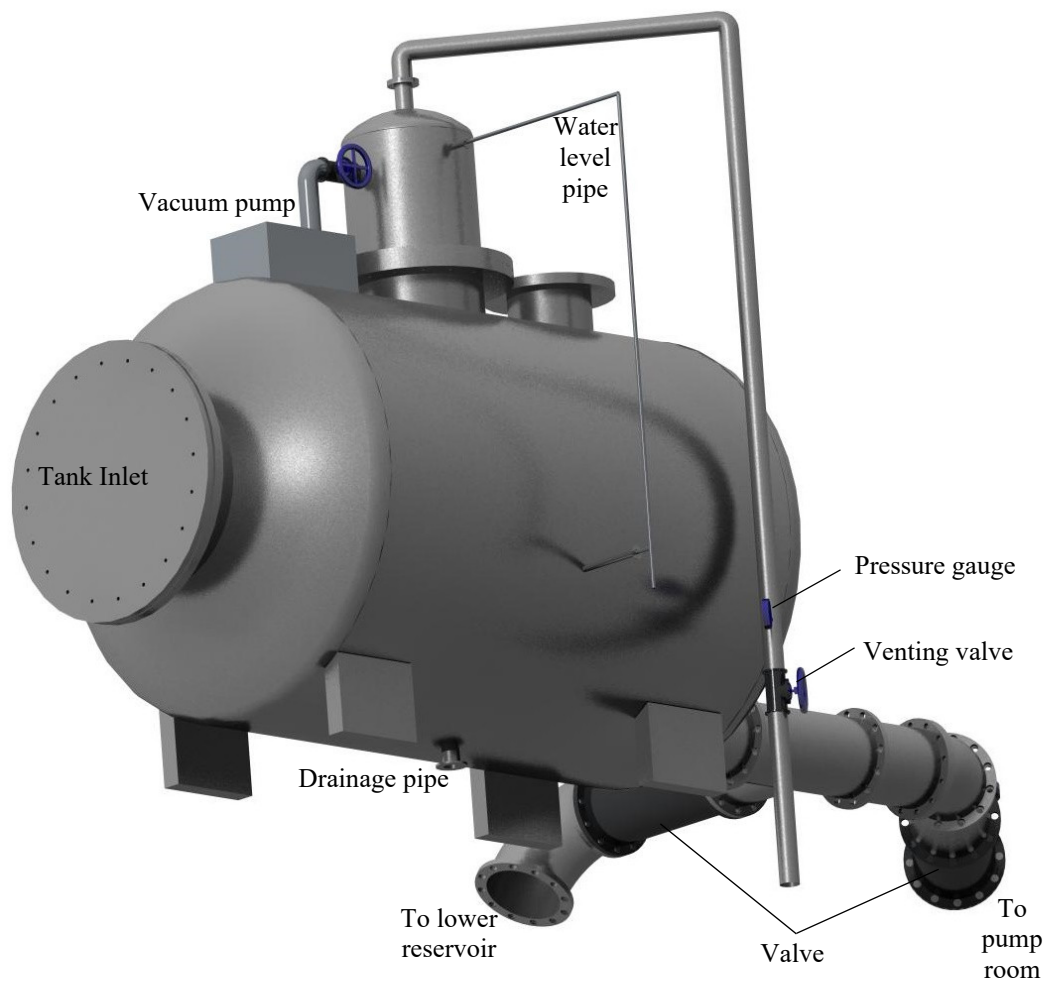


Figure 4-36: TTL Low-pressure Tank; 3D View

A pipe with a venting valve and a pressure gauge is also connected to the dome. There is an upper port on the low-pressure tank for inlet purpose. This allows the tank to be operated as a high-pressure tank if needed. For both pressure tanks, a safety valve that is set to blow if the tank pressure builds dangerously close to the rated maximum tank pressure is necessary. A suggested setting is 10-20 % below max. pressure, which should be tested for function. The safety valves are not shown in the 3D-models. Additionally, a check valve should be installed between the pump and the shut-off valve prior to the dome on the low-pressure tank.

A front-, side-, and top view of the low-pressure tank is shown in Figure 4-37. The low-pressure tank has a volume $V \cong 10.5 \text{ m}^3$.

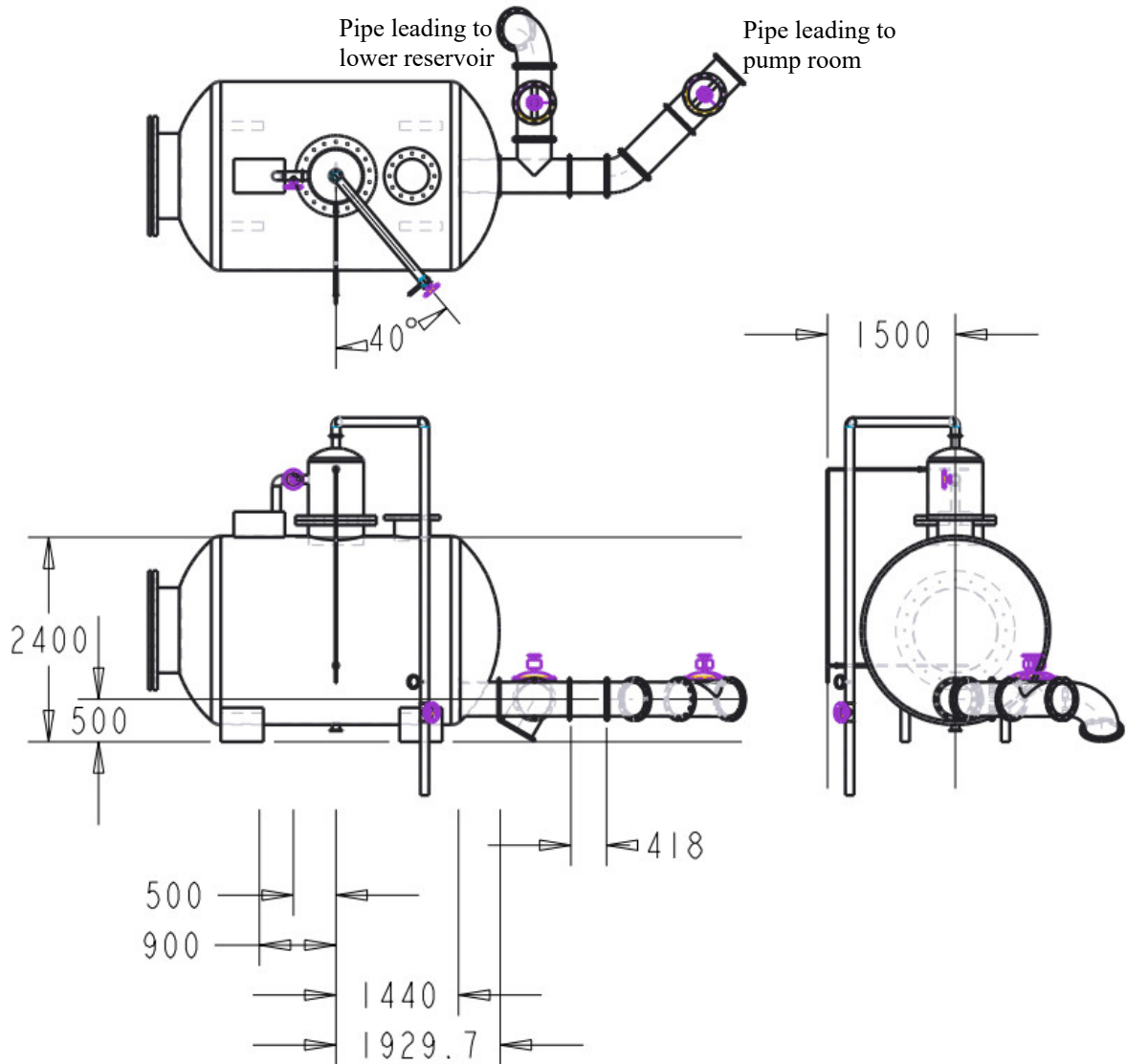


Figure 4-37: TTL Low-pressure Tank; Front-, Side- and Top View

The pipe coming out of the low-pressure tank towards the right as seen from the front and top directs the flow to the lower reservoir when running in open loop, and to the pump room when running in closed loop.

4.2.5. Components Combined

The components in the Francis turbine test rig at TTL are shown in various combined views from Figure 4-38 to Figure 4-45.

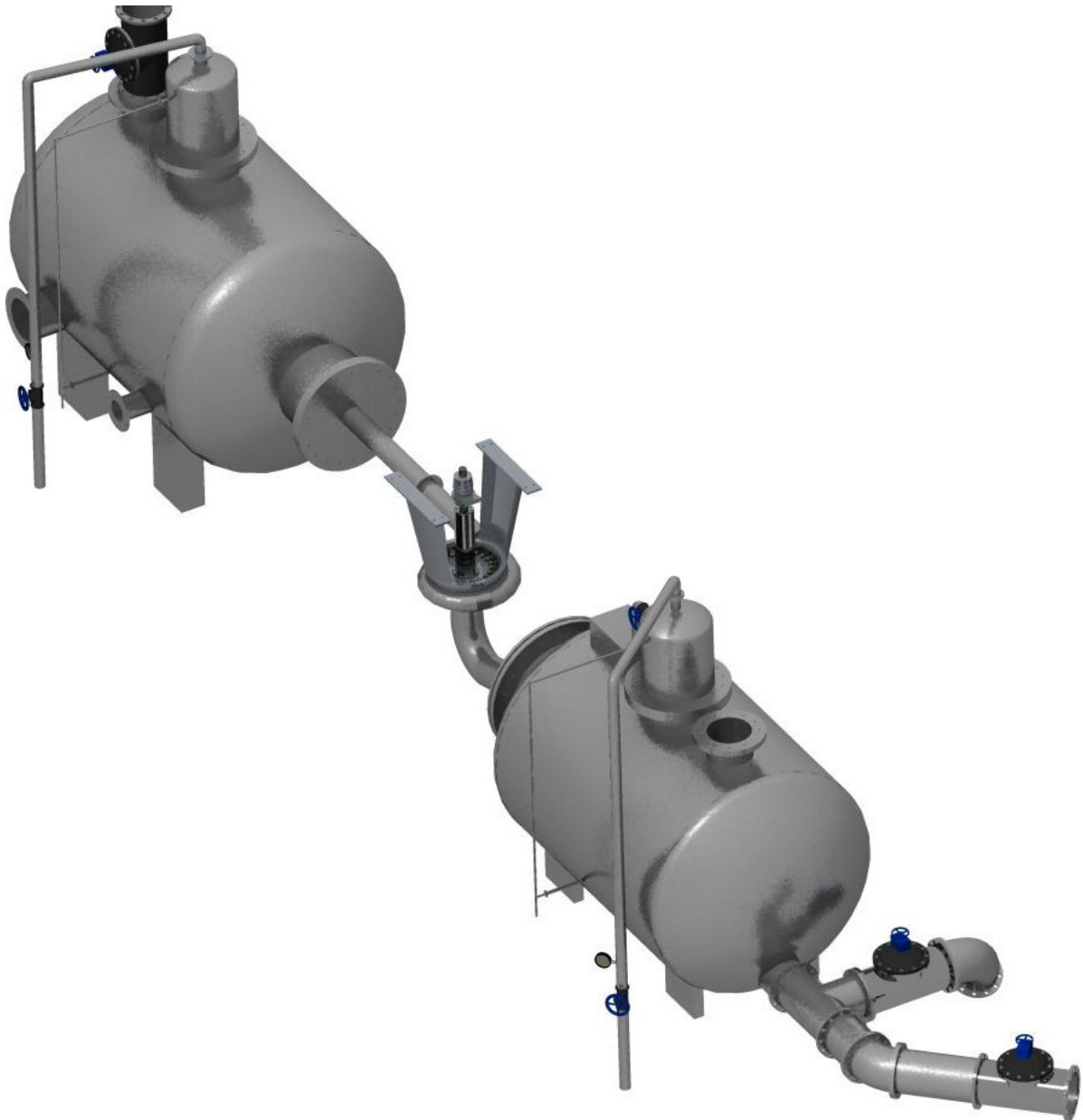


Figure 4-38: TTL Francis Turbine Test Rig; 3D View

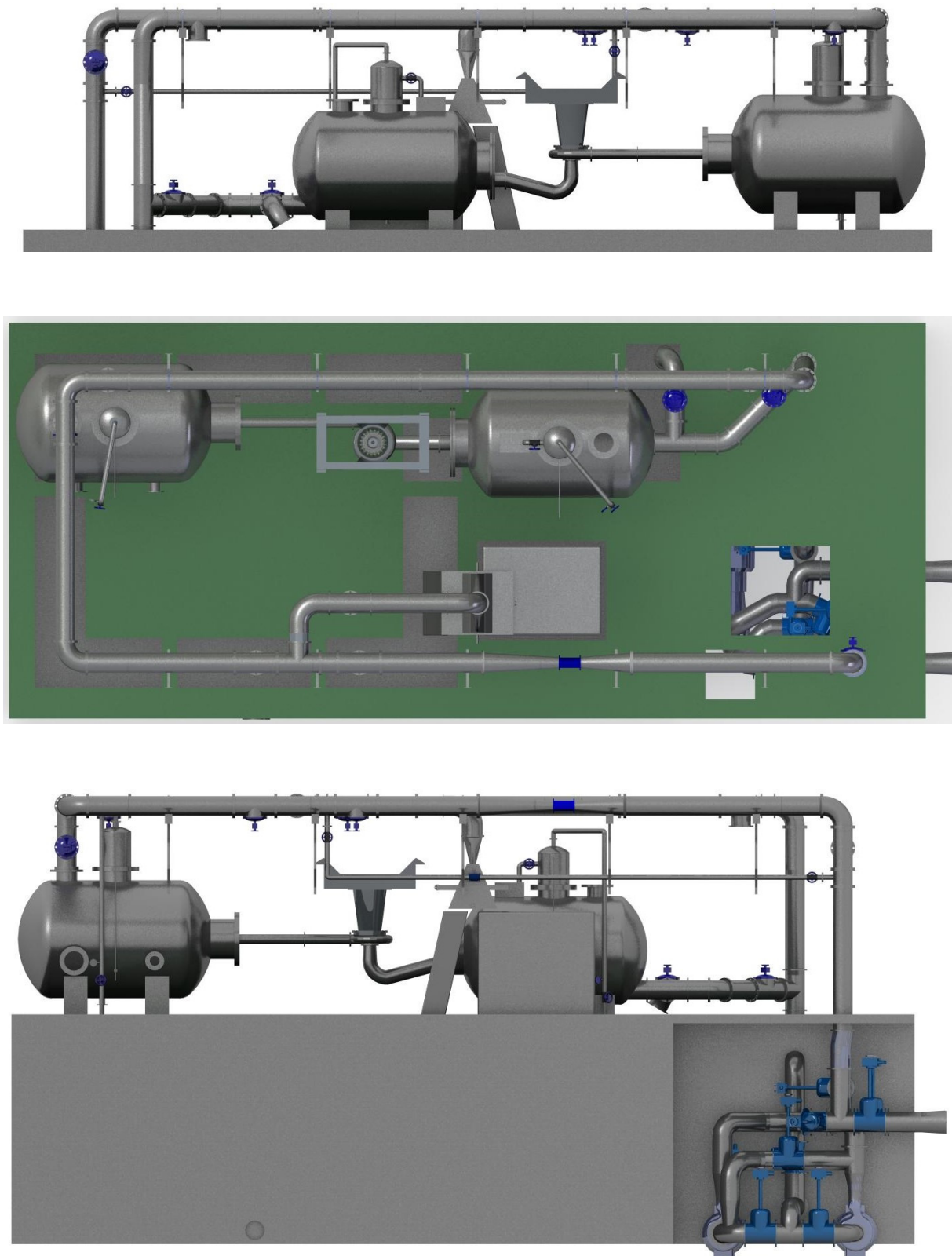


Figure 4-39: TTL Back, Top and Front View

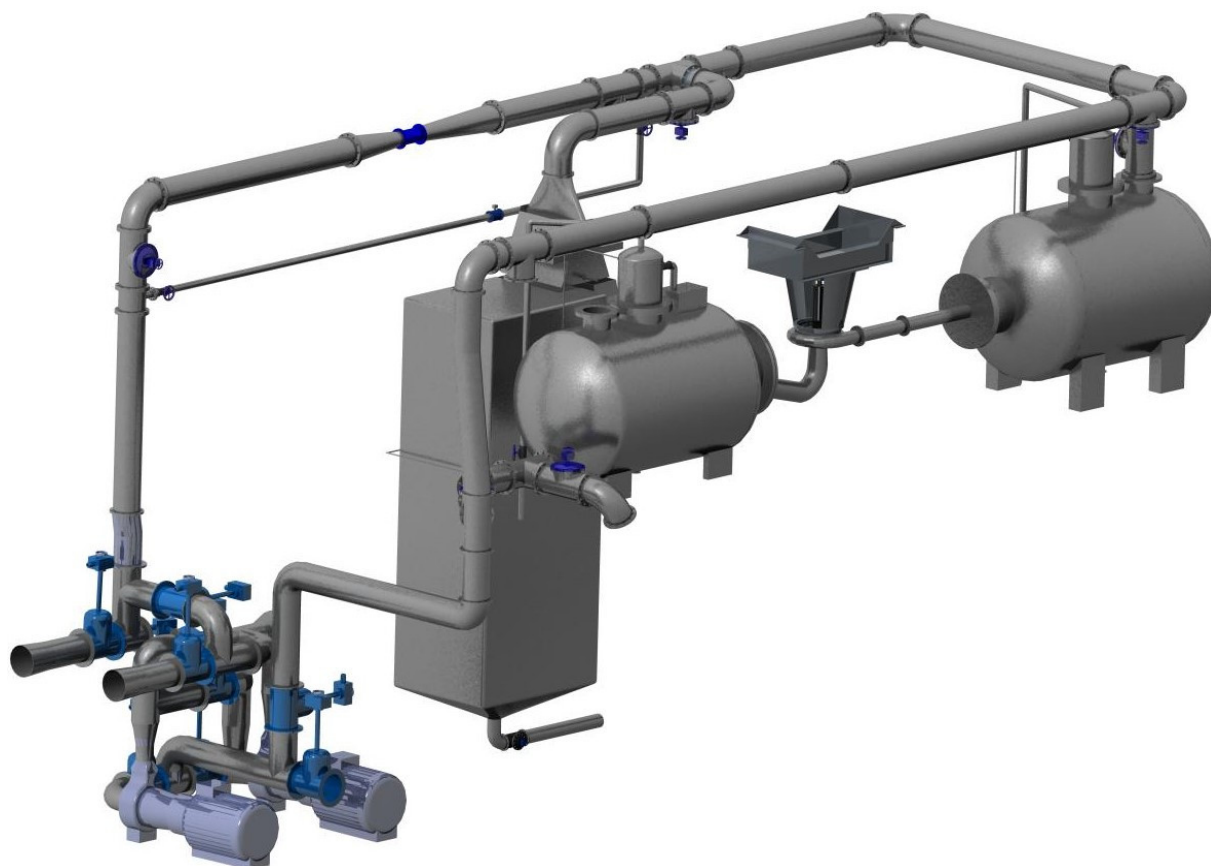


Figure 4-40: TTL Overview Without Lab Building, 3D View

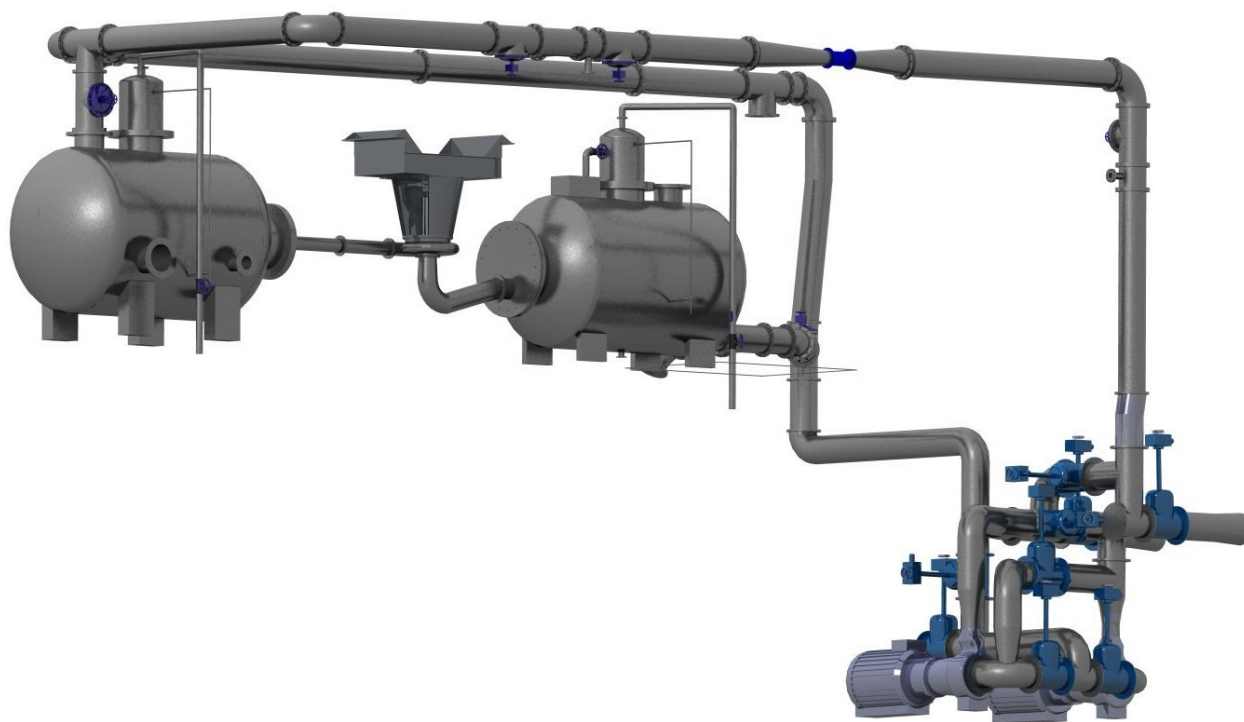


Figure 4-41: TTL Loop Overview without Weighing Facility, 3D View



Figure 4-42: TTL Axial Force Calibration; 3D View

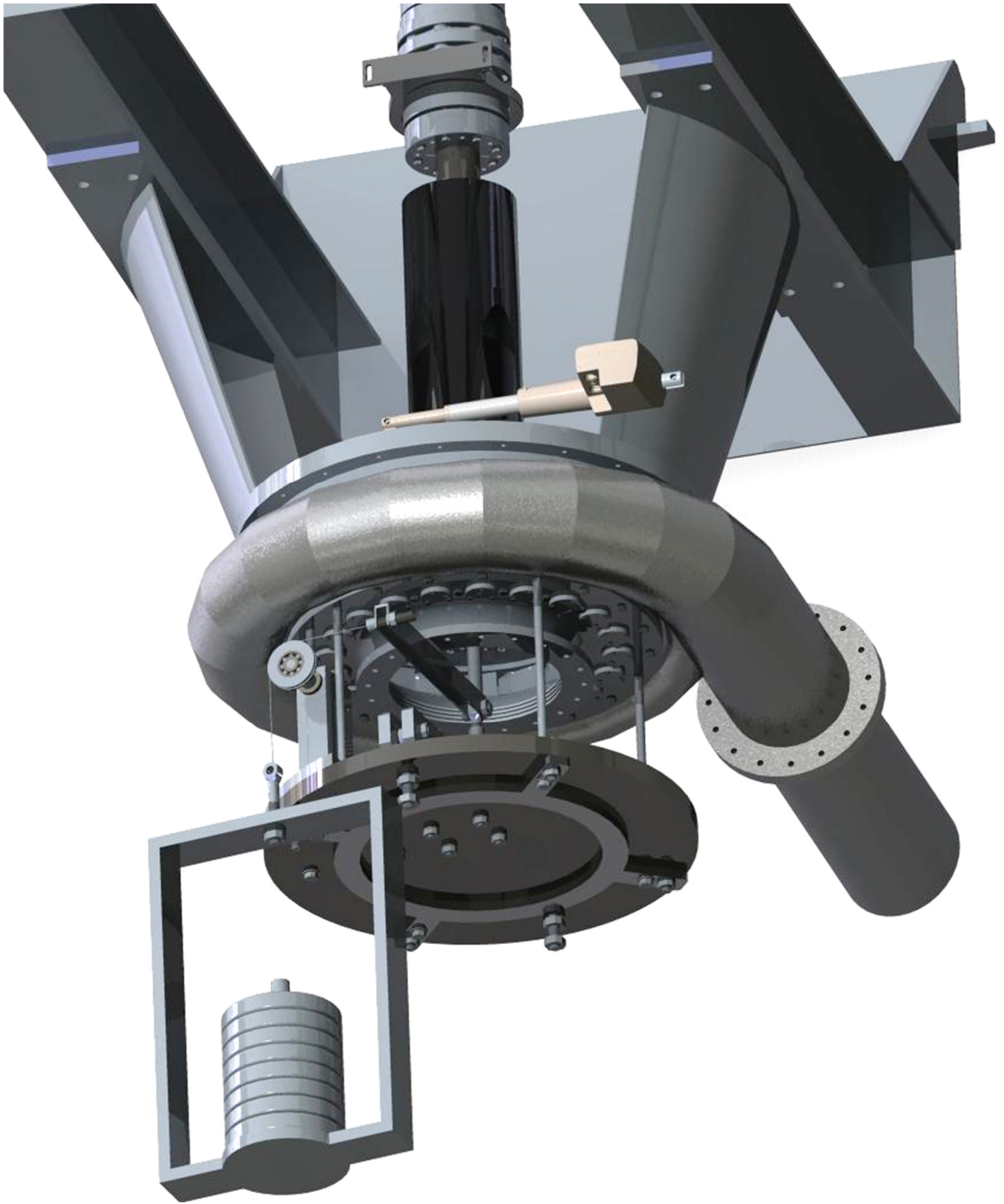


Figure 4-43: TTL Torque Calibration; 3D View

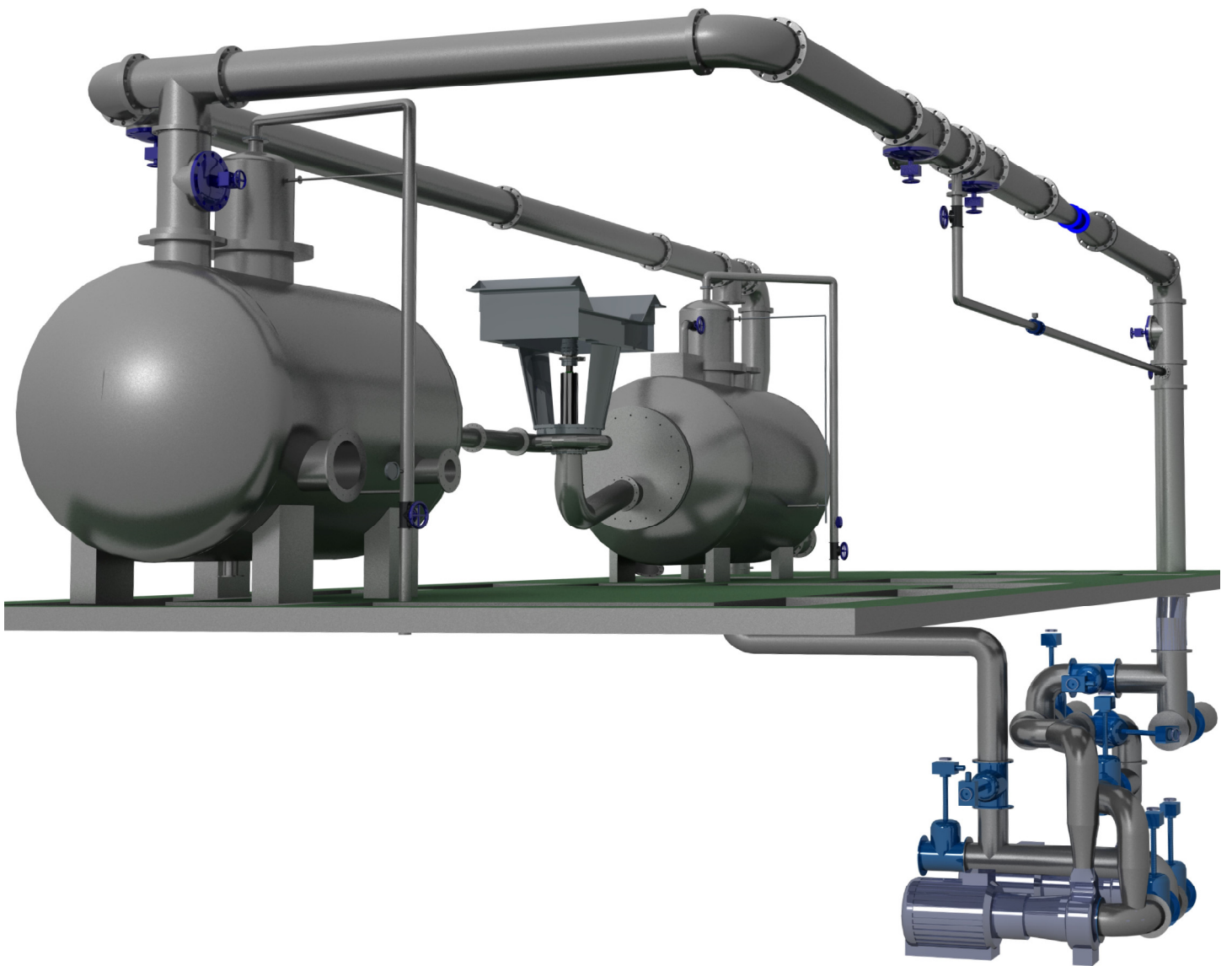


Figure 4-44: TTL Francis Rig; 3D View

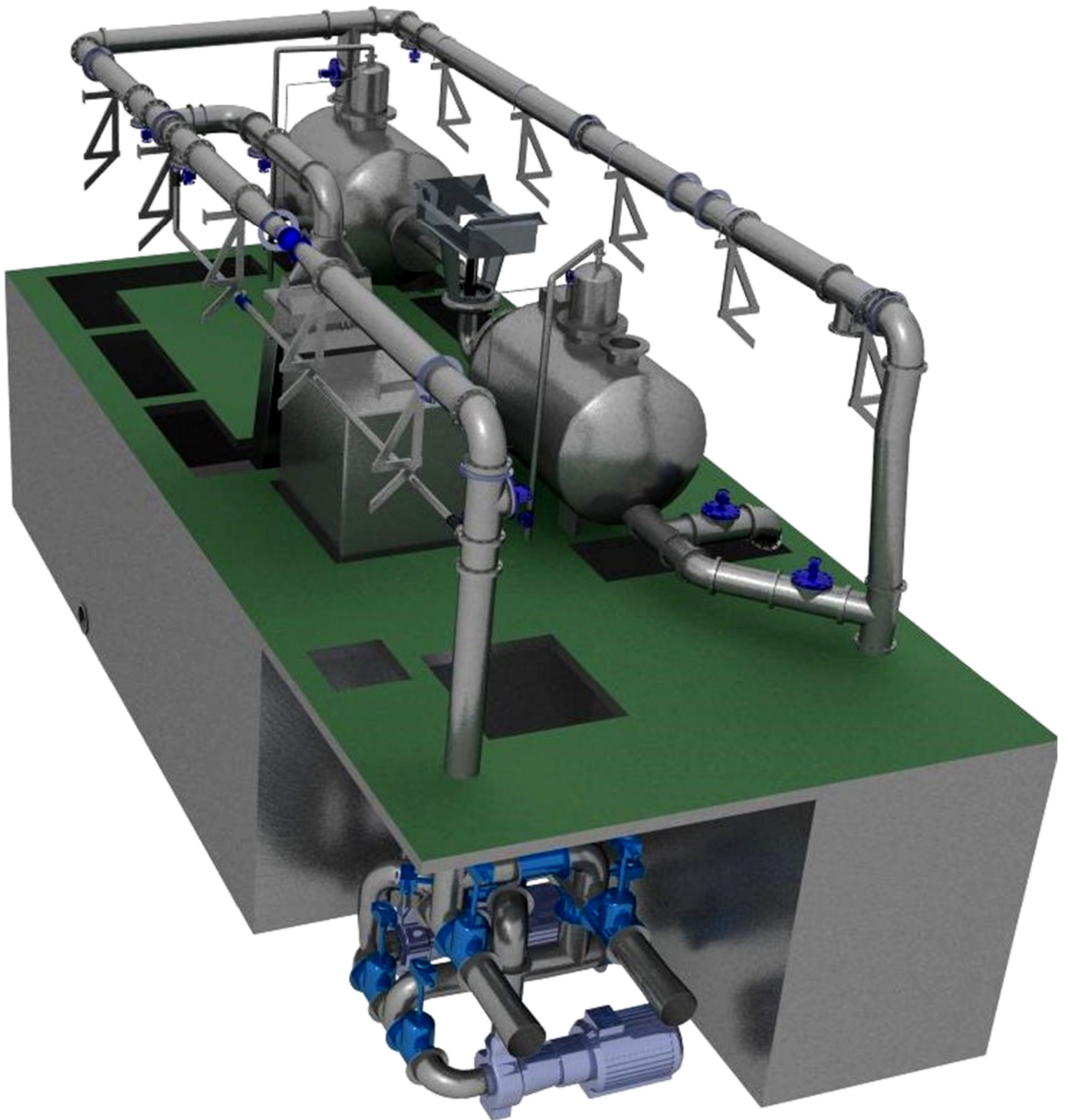


Figure 4-45: Turbine Testing Laboratory; 3D View

5. Conclusion

The Turbine Testing Laboratory (TTL) at Kathmandu University (KU) has been developed with the purpose of aiding in future developments and improvements of hydraulic machinery necessary for the Nepali market and throughout the Himalaya region. A major step towards this goal is the establishment of a Francis turbine test rig in accordance with the International standard *IEC60193* (1).

Experience from the Francis turbine test rig at NTNU's Waterpower Laboratory (VKL) has been utilised for the design of a complete system for efficiency measurement of Francis turbines at TTL. The documents and procedures for the VKL test rig have been investigated thoroughly along with the *IEC60193* requirements upon which the design is based. Operation of the rig and calibration of the instruments have provided practical background for the TTL design.

The piping and instrumentation diagram in Figure 4-1 sums up the measurements for efficiency tests of Francis turbine at TTL. Measuring methods in compliance with *IEC60193* (1) are presented in subchapters under 4.1. A temperature probe measures the temperature. The generator torque is measured by a torque flange that in addition has an integrated rotational speed measurement. Pressure taps give input to differential pressure transducers that are calibrated by deadweight manometers for the pressure measurements. The volume flow rate is measured by an electromagnetic flowmeter that is calibrated by a weighing tank system as illustrated in Figure 4-7. Strain gauges mounted on a customised stub shaft measure the axial force in both directions and the mechanical torque. Calibration procedures are suggested in subchapter 4.1.7.1 for the axial and 4.1.9.1 for the mechanical torque measuring system.

3D-drawings of the main components in the Francis turbine test rig, including an axial load measuring system and bearing block are featured in figures throughout chapter 4.

The work presented in this thesis is done in relation to the NORAD-funded research program *Energize Nepal*, aiming to facilitate Nepal in utilising the vast hydropower resources. It is emphasised that the work is only a suggestions and that better solutions might exist for the Francis turbine test rig at the Turbine Testing Laboratory.

6. Further Work

In addition to the tasks discussed in each subchapter under 4. The following points suggest some of the tasks that may be done in the stages towards full operability of the Turbine Testing Laboratory.

3D-drawings

- Improving the 3D-model of TTL. Adding the pipe configuration to and from the upper reservoir.
- Adding the linear actuator system for guide vane regulation.
- Adjusting the placement of components in the Francis turbine rig, taking the laboratory installations and floor openings into consideration.
- Designing the draft tube in detail.
- Designing the calibration facility for the flow measurement in detail, including placement, type of calibrated weight with method for on- and offloading, and assuring the structural strength of the calibration tank.
- Performing strength analysis of critical parts that are subject to high loads, with special focus on bolted connections and on the equipment used in calibrations. In particular, different methods of supporting the pulley that is used for the torque calibration should be assessed.

Through the strength analysis, material thickness for parts can be optimised.

Calibration, Instruments and Documentation

- Developing calibration procedures for all measuring instruments.
- Testing strain gauges on a simple setup, connecting different circuits and applying a variation of loads to gain understanding of the function
- A thorough analysis of all uncertainties involved in the measurements needs to be done.
- After the lever arms intended for use in the calibrations have been manufactured, they must be accurately measured.

- Quotations for specific instruments and components that are needed for the rig should be acquired. Detailed design including technical drawings of the customised parts will improve the accuracy of the quotations and the predictability of the costs. Locally produced parts should be preferred without compromise on quality. As Nepalese hydropower industry is less developed, the quality of products that are offered needs to be evaluated and tested.
- Developing test procedures for runaway speed, pressure pulsation, cavitation.
- Designing and installing a system for acquiring and processing data from the measuring instruments.
- Assessing which adjustments should be made in connection to the lab in order to ensure that the water is of sufficient quality.
- Establishing an efficient way of knowledge and data exchange between VKL/TTL staff/students. Making sure the relevant documents and updated information is easily accessible for students involved in the collaborations between KU and NTNU in the future.
- Making a plan for the connection to the electrical grid, including preparing the lab for power outages.
- Making an inventory list for existing parts, ordered parts and needed parts. Establishing procedures for how newly acquired parts should be registered, where they are placed and how they should be stored.
- Creating a step-by-step procedure for mounting, including checklists for runout, clearances, alignment and other critical installation requirements. Maintenance intervals for rig components should also be decided.
- Establishing a pressurized “clean room” for storage of sensitive instruments like the deadweight manometer.

Appendices

Appendix A: Piping & Instrumentation Diagrams, TTL

- A.1. P&ID for the Francis Turbine Test Rig at TTL, KU
- A.2. P&ID, Closed Loop Configuration, Pump B in Single Mode
- A.3. P&ID, Open Loop Configuration with Both Reservoirs, Pumps in Series Mode

Appendix B: Measurement Procedures for the Francis Rig, VKL

Measurement Procedures for the Francis Turbine Test Rig at the Waterpower Laboratory are attached digitally as Appendix B.

Appendix C: Calibration Procedures for the Francis Rig, VKL

Calibration Procedures for the Francis Turbine Test Rig at the Waterpower Laboratory are attached digitally as Appendix C.

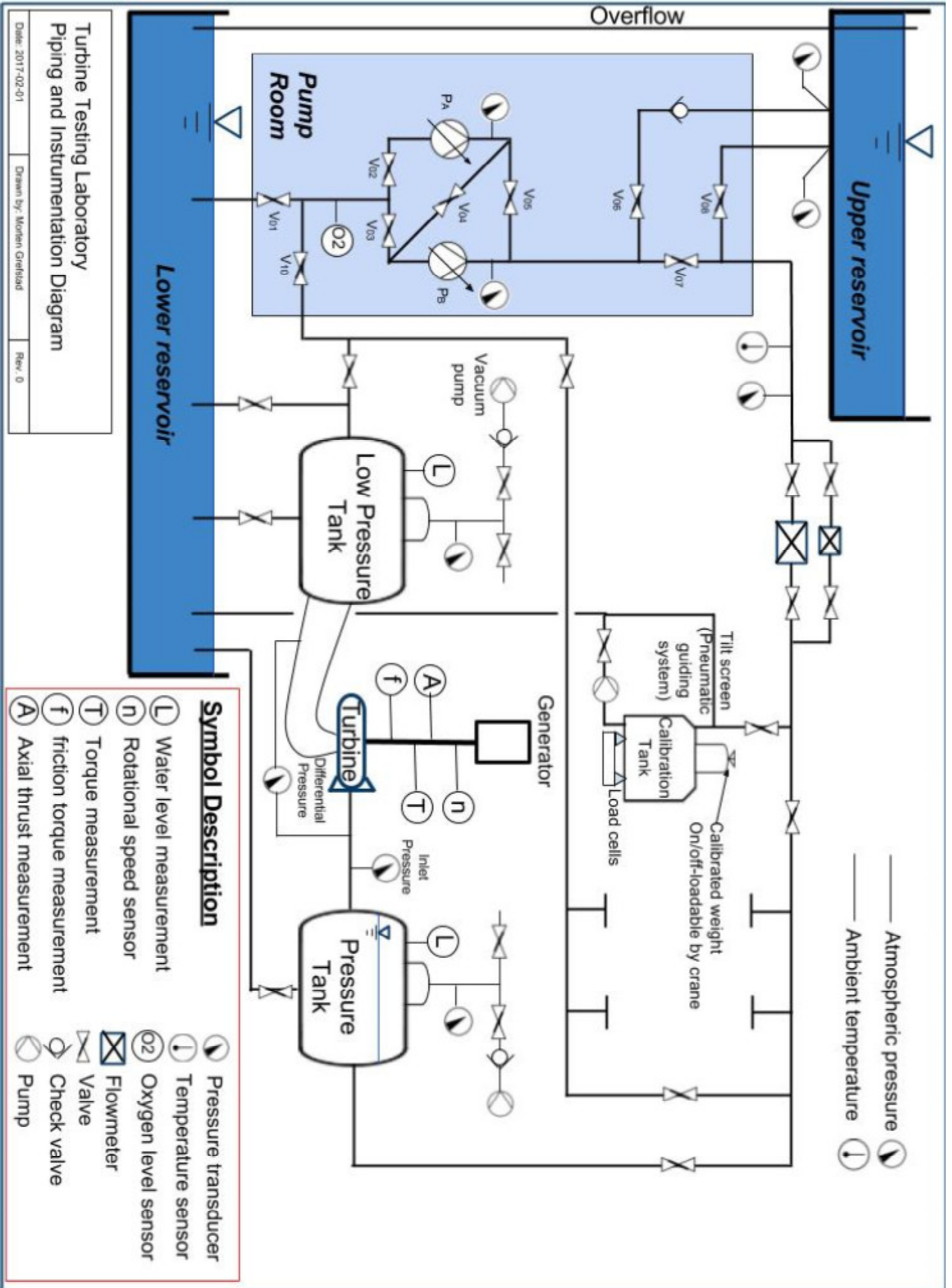
Appendix D: Product Data Sheets

Product data sheets are attached digitally as Appendix D.

- D.1. HBM T40B Torque Flange Mounting Instructions
- D.2. ROBA®-DS Coupling Installation Instructions to T40B

Appendix E: CRHT-VII, Paper no. CRHT17-12

The paper “Development of a Francis Turbine Test Rig at Kathmandu University” submitted for the *International Symposium on Current Research in Hydraulic Turbines*, April 04, 2017, is attached digitally as Appendix E.

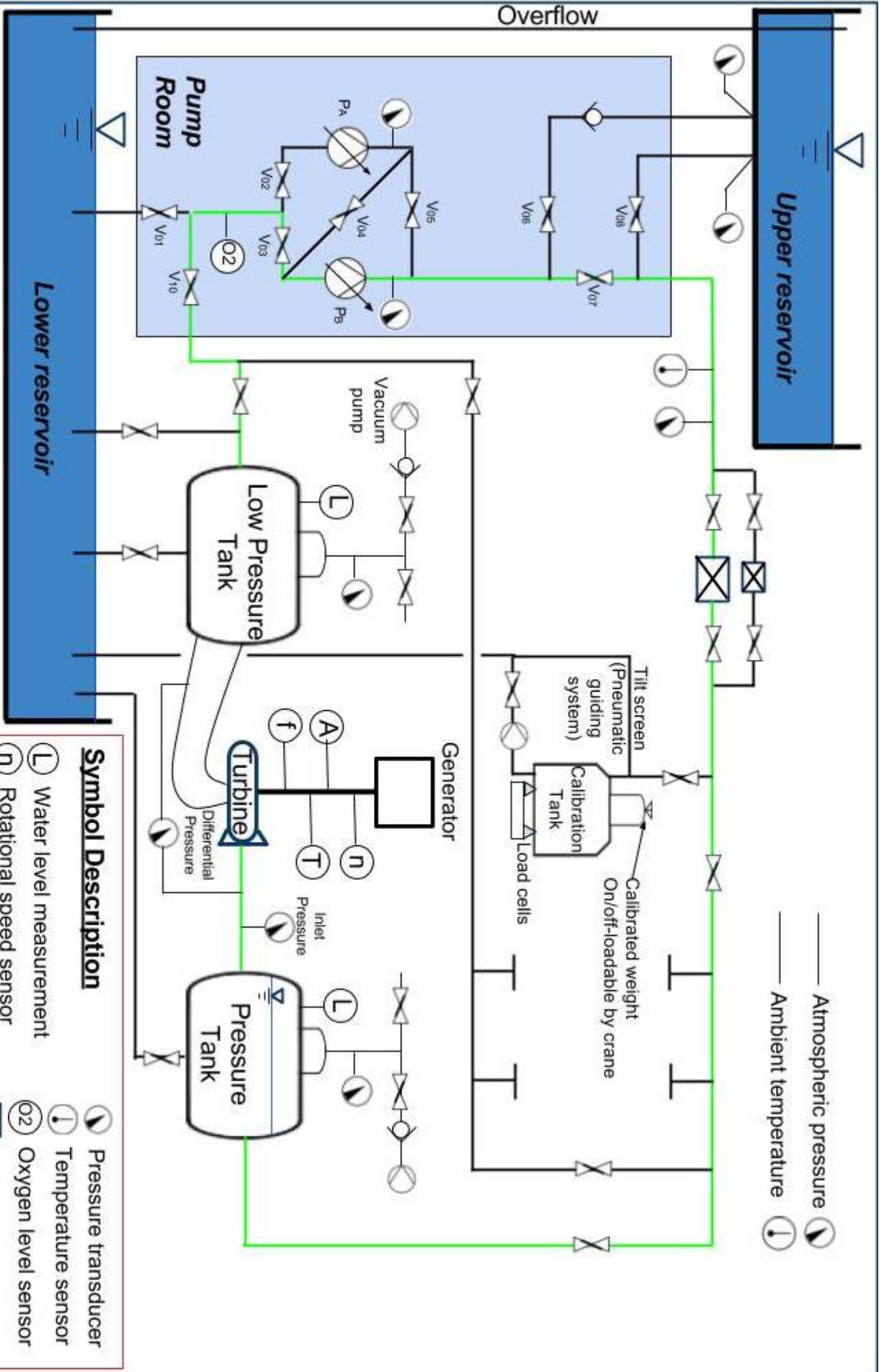


Turbine Testing Laboratory
Piping and Instrumentation Diagram

Date: 2017-02-01

Drawn by: Morten Grefstad

Rev. 0



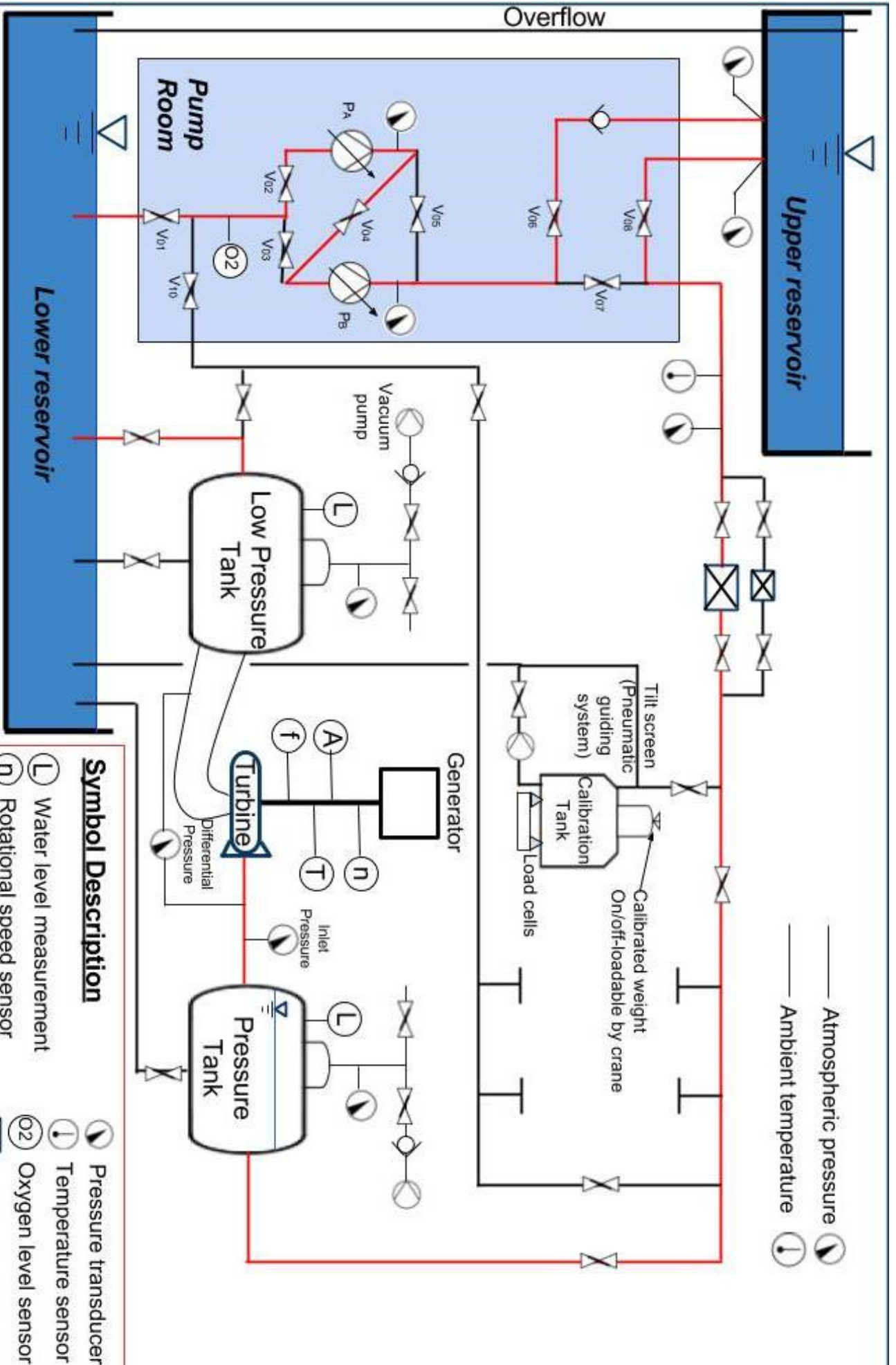
Atmospheric pressure
 Ambient temperature

Symbol Description

- Water level measurement
- Rotational speed sensor
- Torque measurement
- friction torque measurement
- Axial thrust measurement
- Pressure transducer
- Temperature sensor
- Oxygen level sensor
- Flowmeter
- Valve
- Check valve
- Pump

Turbine Testing Laboratory
Piping and Instrumentation Diagram
 Example of closed loop configuration, pump B running in single mode

Date: 2017-02-01
 Drawn by: Morden Giesiad
 Rev. 0



Turbine Testing Laboratory
 Piping and Instrumentation Diagram
 Example of open loop configuration with upper reservoir, pumps in series

Date: 2017-02-01

Drawn by: Morten Grefstad

Rev. 0

Symbol Description

- ⬇️ Pressure transducer
- ⬇️ Temperature sensor
- ⓪2 Oxygen level sensor
- ⓪ Water level measurement
- Ⓝ Rotational speed sensor
- Ⓣ Torque measurement
- ⓕ friction torque measurement
- ⓐ Axial thrust measurement
- ⬇️ Pressure transducer
- ⬇️ Temperature sensor
- ⓪2 Oxygen level sensor
- ⓪ Flowmeter
- Ⓝ Valve
- ⓐ Check valve
- ⓐ Pump

Bibliography

1. **International Electrotechnical Commission.** *Hydraulic turbines, storage pumps and pump-turbines - Model Acceptance tests.* 1999. IEC 60193.
2. **Government of Nepal - Office of the Investment Board.** Hydropower Sector Overview. *IBN.* [Online] <http://ibn.gov.np/hydropower>.
3. **The International Hydropower Association.** *2017 Hydropower Status Report.* 2017.
4. **Halwai, Bidhan Rajkarnikar.** *Design of a Francis turbine test rig.* s.l. : Norwegian University of Science and Technology, 2012.
5. **Kayastha, Aatma Ram and Gurung, Nikel.** *Simplified Francis Test Rig Drawings.* s.l. : Turbine Testing Laboratory, 2013.
6. **Seierstad, Johanne.** *Design system for primary calibration of flow.* s.l. : Norwegian University of Science and Technology, 2013.
7. **Rasmussen, Inger Johanne.** *Design of a Francis Model Test Rig at Kathmandu University.* s.l. : Norwegian University of Science and Technology, 2014.
8. **Selmurzaev, Magomed.** *Design of the measurement setup for the friction torque and axial load on the Francis turbine test rig.* s.l. : Norwegian University of Science and Technology, 2016.
9. **Kjerschow, Andreas.** *Development of a Francis Turbine Test Rig at Kathmandu University.* s.l. : Norwegian University of Science and Technology, 2017.
10. **Dahlhaug, Ole Gunnar.** *Vannkraftsamarbeidet mellom NTNU og Kathmandu University.* *NTNU Techzone.* [Online] <http://www.ntnutechzone.no/wp-content/uploads/2015/12/TT.png>.
11. **Kathmandu University.** *Turbine Testing Laboratory. Kathmandu University.* [Online] <http://www.ku.edu.np/ttl/>.

12. **Brandåstrø, Bård.** *The Waterpower Laboratory at NTNU - A brief Introduction to the Laboratory.* s.l. : Vannkraftlaboratoriet NTNU, 2002.
13. **ETERNOO MACHINERY CO., LTD.** Francis Turbines. [Online] <http://www.eternoohydro.com/d/pic/products/turbines/francis-turbines/3.jpg>.
14. **Hoffmann, Karl.** *Applying the Wheatstone Bridge Circuit.* s.l. : HBM.
15. —. *An Introduction to Stress Analysis and Transducer Design Using Strain Gauges.* s.l. : HBM, 2012.
16. **National Instruments.** *Engineer's Guide to Accurate Sensor Measurements.* 2016.
17. **Dahlhaug, Ole Gunnar, et al.** *Tokke model test 2006-2007 - NTNU reference runner.* Trondheim : NTNU - Waterpower Laboratory, 2007. VKL 2007/1.
18. **Brandåstrø, Bård.** *Presentation of the Waterpower Laboratory.* s.l. : Vannkraftlaboratoriet NTNU, 2005.
19. *Experimental and Numerical Studies for a High Head Francis Turbine at Several Operating Points.* **Trivedi, Chirag, et al.** 11, s.l. : Journal of Fluids Engineering, 2013, Vol. 135. 0098-2202.
20. *Measurement of liquid flow in closed conduits -- Weighing method.* s.l. : International Organization for Standardization, 2014. ISO 4185.
21. **Rexnord.** Thomas Flexible Disc Coupling Catalog. *Rexnord Tech Docs.* [Online] 2016. https://www.rexnord.com/ContentItems/TechLibrary/Documents/2000_Thomas-Flexible-Disc-Couplings_Catalog-pdf.aspx.
22. **Weissbrodt, Klaus.** Couplings and Mounting Parts for Torque Applications — Your Selection Guide. *HBM.* [Online] <https://www.hbm.com/en/3167/couplings-and-mounting-parts-for-torque-applications/>.
23. **Storli, Pål-Tore Selbo.** *Modelltest av Francis turbin i Vannkraftlaboratoriet ved NTNU.* 2006.

24. Thapa, Biraj Singh. *RE: Drawings Of The Turbine Testing Lab At KU*. [E-mail] 2017.
25. Kjølle, A. *Mechanical Equipment*. 2001.
26. SKF. *Bearing Basics (GRB001)*. [Online engineering course] 2015.
27. Harnoy, A. *Bearing Design in Machinery: Engineering Tribology and Lubrication*. s.l. : New Jersey Institute of Technology, 2003.
28. SKF. *Sealed single row angular contact ball bearings*. 2013.
29. —. *Angular contact ball bearings (GRB003)*. [Online engineering course] 2015.
30. NSK. *NSK Academy - Bearing Types - Cylindrical Roller Bearings*. [Online engineering course] 2017.
31. SKF. Single row cylindrical roller bearings. [Online] <http://www.skf.com/in/products/bearings-units-housings/roller-bearings/cylindrical-roller-bearings/single-row-cylindrical-roller-bearings/index.html>.
32. Industrial shaft seals. SKF. [Online] 2013. http://www.skf.com/binary/83-129139/Industrial-shaft-seals---10919_2-EN.pdf.
33. Koirala, Ravi. *Low Pressure Tank*. s.l. : Turbine Testing Laboratory, 2016.
34. Kjølle, Arne. *Hydraulisk Måleteknikk*. Trondheim : s.n., 2003.
35. HBM. *T40B Mounting Instructions*. 2002.
36. mayr. *Shaft Couplings ROBA-DS configurator for torque transducer*. [Online] 2016. http://www.mayr.com/synchronisation/documentations/p_9110_v01_en_04_02_2016.pdf.
37. HBM. *Strain Gauges Catalogue*. 2017.
38. SKF. *Angular contact ball- bearings, super precision*. SKF. [Online] 2017. <http://www.skf.com/sg/products/bearings-units-housings/super-precision-bearings/angular-contact-ball-bearings/acbb-skf-high-and-super-precision/index.html?designation=7015%20CD>.

39. —. Installing V-rings. *SKF*. [Online] <http://www.skf.com/uk/products/seals/industrial-seals/power-transmission-seals/v-ring-seals/all-rubber-v-rings/installing-v-rings/index.html>.
40. Coordinates for Turbine Testing Lab, Dhulikhel, Nepal. *Mapcoordinates*. [Online] 2017. <http://www.mapcoordinates.net/en>.